

POLITECNICO DI TORINO

Collegio di Ingegneria Chimica e dei Materiali

Master of Science Course in Ingegneria Chimica e dei Processi Sostenibili

Master of Science Thesis

**Environmental and Process Implications of Lignin-Based
Rigid Polyurethane Foams for Thermal Insulation:
a Comparative Life Cycle Assessment**



Tutor

Prof.ssa Almudena Ochoa Mendoza (UPM)

Prof Giuseppe Pipitone

Candidato

Lorenzo Garrione

Dicembre 2024

INTRODUCTION	8
1. Thermal insulation	11
1.1 Historical evolution of thermal insulation	11
1.2 Classification of thermal insulation	12
1.3 Properties of materials for thermal insulation	12
1.4 Heat transfer principles	14
1.4.1 Conduction	14
1.4.2 Convection	18
1.4.3 Radiation	20
1.5 Heat transfer mechanism through walls	24
1.6 Energy efficiency	25
1.7 Importance and functioning of thermal insulation panels	26
2. Polyurethane foam thermal insulation panels	29
2.1 Polyurethane foams	31
3. Lignin-based rigid polyurethane foam thermal insulation panels	36
3.1 Lignin as a renewable raw material for biopolyols	37
3.2 Rigid polyurethane foam partially bio-based with lignin	38
3.2.1 Bio-based rigid polyurethane foam using lignin by direct replacement	39
3.2.2 Bio-based rigid polyurethane foam using chemically modified lignin	40
3.3 Comparative analysis of thermal insulation properties between bio-based and fossil-based rigid polyurethane foams	40
4. Scale-up of lab-scale Kraft lignin chemical modification processes	44
4.1 Hydrolytic depolymerization of Kraft lignin catalyzed by NaOH	44
4.2 Oxypropylation of depolymerized Kraft lignin	46
5. Life cycle assessment (LCA)	49
5.1 SimaPro: software overview	50
5.2 Goal and scope definition	56
5.2.1 Goal	57
5.2.2 Scope	57
5.2.3 Functional unit	58
5.2.4 Allocation methods	58
5.2.5 System boundaries	58
5.2.6 Data quality and categories	64
5.2.7 Critical review process	65
5.3 Life cycle inventory (LCI)	65
5.4 Life cycle impact assessment (LCIA)	75
5.4.1 Kraft lignin extraction process	78
5.4.2 Hydrolytic depolymerization of Kraft lignin catalyzed by NaOH	79
5.4.3 Oxypropylation of depolymerized Kraft lignin	81
5.4.4 Comparative impact assessment of the four rigid polyurethane foam scenarios	82
5.5 Interpretation	83
6. Conclusions	87

Nomenclature

α	Thermal diffusivity, m^2/s
α_r	Absorbance, dimensionless
ϵ_r	Emissivity, dimensionless
ϵ	Energy carried by an electromagnetic wave or a photon, J
ρ	Density, kg/m^3
ρ_r	Reflectance, dimensionless
λ	Wavelength, m
η	Wavenumber, m^{-1}
σ	Stefan-Boltzmann constant, $\text{W}/(\text{m}^2 \cdot \text{K}^4)$
τ_r	Transmittance, dimensionless
ν	Frequency, Hz
ω	Angular frequency, rad/s
A	Area, m^2
c	Speed of light, m/s
c_0	Speed of light in a vacuum, m/s
c_p	Specific heat (constant pressure), $\text{J}/(\text{K} \cdot \text{kg})$
h	Convective heat transfer coefficient, $\text{W}/(\text{m}^2 \cdot \text{K})$
h_p	Planck constant, J·s
j_q	Heat flux per unit area, W/m^2
k	Thermal conductivity, $\text{W}/(\text{m} \cdot \text{K})$
k_B	Boltzmann constant, J/K
K_t	Translational kinetic energy, J
N	Number of molecules, dimensionless
Q	Amount of thermal energy, J
q	Thermal energy per unit time, W
R	Thermal resistance, K/W
T	Temperature, K
t	Time, s
u	Velocity, m/s

Figure index

Figure 1: Annual global temperature anomalies compared to the 20th-century average, extracted from [2]	8
Figure 2: Distribution of global GHG emissions in 2022, with data taken from EDGAR - Emissions Database for Global Atmospheric Research [6]	9
Figure 3: Relationship between density and thermal conductivity of a corn stalk insulation block, extracted from [16]	17
Figure 4: Variation of thermal conductivity with density for various insulating materials, sourced from [17]	18
Figure 5: Velocity and Thermal Boundary Layers, extracted from [19]	19
Figure 6: The electromagnetic radiation spectrum, showing the thermal radiation zone in yellow, extracted from [22]	21
Figure 7: Absorption, reflection, and transmission through a slab, extracted from [21]	22
Figure 8: Heat transfer to, through, and from a wall, sourced from [9]	24
Figure 9: Improvement in Global Primary Energy Intensity, Annual Change in the Net Zero Emissions Scenario, 2000-2030, extracted from [26]	26
Figure 10: Variable thickness of thermal insulation and its effect on comfort rating, extracted from [29]	27
Figure 11: Thermal insulation materials market in 2010, extracted from [31]	29
Figure 12: Chemical structures of polyols used for PU synthesis, extracted from [34]	30
Figure 13: Chemical structures of isocyanates used for PU synthesis, extracted from [34]	30
Figure 14: Insulation thickness of different materials with equivalent thermal resistance, extracted from [37]	31
Figure 15: General data on blowing agents, extracted from [35]	33
Figure 16: Change in thermal conductivity over time at an average temperature of 10°C for rigid PU foam panels blown with R11, produced by different methods (a, b, c, d, e), extracted from [35]	35
Figure 17: Sustainable Development Goals related to bio-based polyurethane foams	36
Figure 18: Examples of typical structures in the chemical formula of lignin, extracted from [46]	38
Figure 19: Ansys Granta EduPack logo	40
Figure 20: Search for rigid polyurethane foam in Ansys Granta EduPack	41
Figure 21: Process flow diagram of the hydrolytic depolymerization of lignin	45
Figure 22: Process flow diagram of the oxypropylation of depolymerized lignin	47
Figure 23: Process flow diagram of the acetone and OxyDKL separation in Aspen Plus®	48
Figure 24: Life Cycle Assessment Framework - Phases of an LCA (ISO, 1997a)	50
Figure 25: SimaPro® text logo	50

Figure 26: SimaPro 9.6.0.1 version libraries	51
Figure 27: Ecoinvent (and Agri-footprint) distinguishes unit and system processes, extracted from [60]	52
Figure 28: Life cycle impact assessment methods	53
Figure 29: Overview of the impact categories that are covered in the ReCiPe2016 methodology and their relation to the areas of protection, extracted from [61]	54
Figure 30: Cradle-to-gate system boundaries (MDI), extracted from [64]	59
Figure 31: Cradle-to-gate system boundaries (short chain polyols), extracted from [65]	60
Figure 32: Traditional rigid polyurethane foam system boundaries	61
Figure 33: System boundaries for the life cycle inventory of kraft lignin, extracted from [69]	62
Figure 34: System boundaries for the life cycle inventory of DKL	63
Figure 35: System boundaries for the life cycle inventories of chemical modification processes	64
Figure 36: Sankey diagram, global warming potential of electricity production and voltage transformation	66
Figure 37: oxypropylation reaction schemes, extracted from [84]	72
Figure 38: oxypropylated depolymerized lignin	73
Figure 39: Causal chain from greenhouse gas emissions to human health damage and relative loss of species in terrestrial and freshwater ecosystems [61]	77
Figure 40: hydrolytic depolymerization sensitivity analysis results, as CO ₂ eq percentage change	80
Figure 41: oxypropylation sensitivity analysis results, as CO ₂ eq percentage change	82
Figure 42: Sankey diagram of climate change impact relative to 1 kg fossil PUR	84
Figure 43: climate change per kg of polyols in 1 kg of PUR, with the studied allocation methods	85
Figure 44: climate change % of bio-based polyols vs. fossil-based polyols	86
Figure 45: Results of the present work, compared with literature data	87

Table index

Table 1: Physical, mechanical and thermal properties of different rigid polyurethane foams	43
Table 2: Main operating parameters of the scaled-up hydrolytic depolymerization process flows	46
Table 3: Main operating parameters of the scaled-up oxypropylation process flows	48
Table 4: ReCiPe2016 Categories and indicators at the midpoint level	55
Table 5: Life cycle inventory of the Electricity, medium voltage {EU} dataset	67
Table 6: Life cycle inventory of the Electricity, medium voltage {RER} from wind dataset	68
Table 7: Life cycle inventory of the Electricity, medium voltage {RER} from hydropower dataset	68
Table 8: Life cycle inventory of the Polyether polyols, short chain dataset	69
Table 9: Life cycle inventory of the Methylene diphenyl diisocyanate (MDI) dataset	69
Table 10: Life cycle inventory of 1 kg of untransformed dry Kraft Lignin, based on Bernier et al.'s work	70
Table 11: Life cycle inventory of 0.193 kg of depolymerized Kraft Lignin	71
Table 12: Life cycle inventory of 0.43 kg of oxypropylated depolymerized Kraft Lignin	73
Table 13: Life cycle inventory of 1 kg of fossil based rigid polyurethane foam	76
Table 14: Life cycle inventory of 1 kg of KL PUR	76
Table 15: Life cycle inventory of 1 kg of DKL PUR	77
Table 16: Life cycle inventory of 1 kg of OxyDKL PUR	77
Table 17: Comparison of the results obtained for 1 kg untransformed dry Kraft lignin powder	79
Table 18: Comparison of the results obtained for 0.193 kg DKL	80
Table 19: Comparison of the results obtained for 0.193 kg DKL	82
Table 20: Comparison of the results obtained for 1 kg of rigid polyurethane foam in four scenarios	84
Table 21: Climate change impact per amount of polyols in 1 kg of PUR	86

Introduction: Thermal insulation of buildings

In the year 2023, the average surface temperature of the Earth was the warmest on record. Every month from June to December set a global record, with July being the hottest month ever recorded [1]. Overall, the Earth was about 1.2°C warmer in 2023 than the 20th-century average, when the mean temperature was 13.9°C [2].

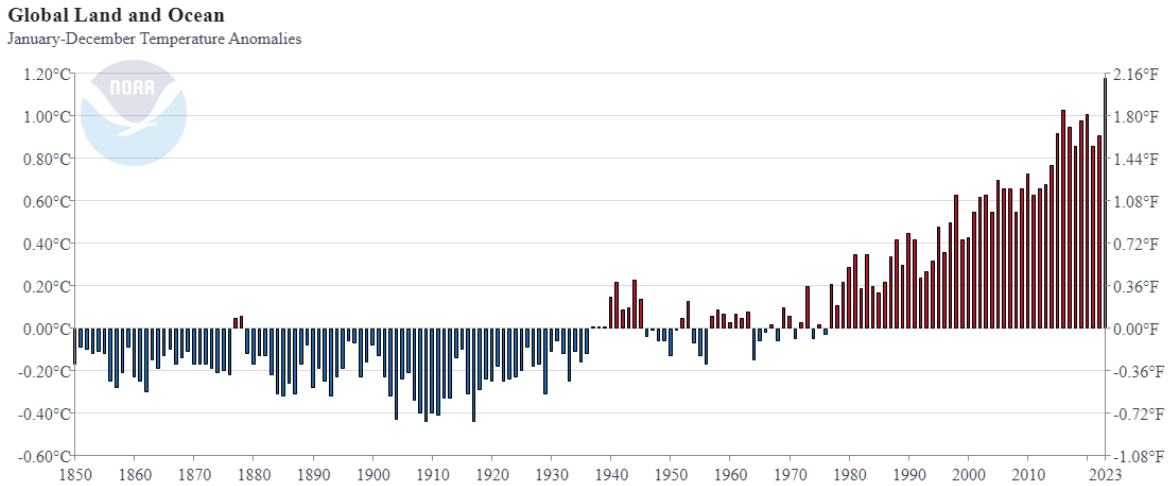


Figure 1: Annual global temperature anomalies compared to the 20th-century average, extracted from [2]

In Figure 1, a general increase in the global average temperature can be observed since the last decades of the 20th century, mainly attributable to global warming. This refers to changes in the surface air temperature caused by the greenhouse effect induced by the emission of greenhouse gases (GHGs) into the atmosphere [3]. These gases allow the entry of solar radiation from the sun while hindering the exit of infrared radiation emitted from the Earth's surface (characterized by a wavelength of approximately 15 microns, which is longer than the wavelength of the incoming radiation). This results in an increase in the temperature of the celestial body involved in the phenomenon. The natural greenhouse effect, caused by the typical concentration of CO₂ and other gases in the atmosphere, keeps the Earth's temperature warmer, which is the reason that sustains life on the planet. In fact, greenhouse gases are crucial for maintaining our planet at a suitable temperature for life because, without the natural greenhouse effect, the heat emitted by the Earth would pass outward from the Earth's surface into space, and the Earth would have an average temperature of approximately -20°C [5].

Many greenhouse gases occur naturally in the atmosphere, but human activity contributes to their accumulation. As a result, the greenhouse effect in the atmosphere intensifies and alters the climate of our planet. From the last decades of the 20th century until 2019, global greenhouse gas emissions had followed an increasing trend. Consequently, atmospheric concentrations of greenhouse gases rose substantially, enhancing the natural greenhouse effect. However, due to the COVID-19 pandemic, global emissions decreased by 3.7% in 2020 compared to 2019 levels, interrupting a continuous upward trend of over ten years. Nevertheless, global GHG emissions resumed growth just after the pandemic peak, reaching 53.8 Gt CO₂.eq in 2022, which represents a 2.3% increase compared to 2019 and a 1.4% increase from 2021 [6]. Figure 2 shows the distribution of the main greenhouse gases within the total emissions.

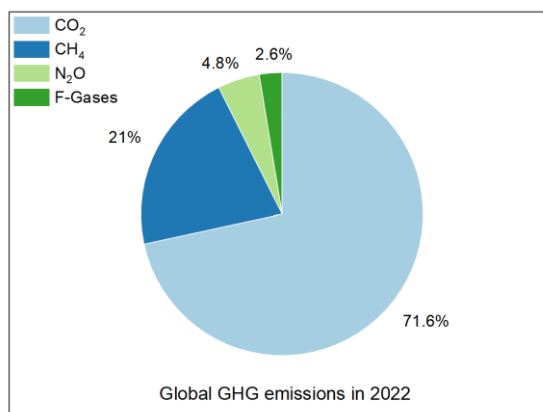


Figure 2: Distribution of global GHG emissions in 2022, with data taken from EDGAR - Emissions Database for Global Atmospheric Research [6]

In Europe in 2022, greenhouse gas emissions generated by the economic activities of EU resident units in particular amounted to 3.6 Gt CO₂-eq [7]. The activities with the highest GHG emissions were the manufacturing and supply of electricity, gas, steam, and air conditioning, contributing 745 million tons of CO₂-eq, which represents 21% of the total greenhouse gases emitted. These were followed by households (718 million tons of CO₂-eq; 20%), which are emitters of greenhouse gases related to transportation, heating, and other purposes [7].

One way to reduce the impact of energy supply is to increase the energy efficiency of homes and buildings.

Thermal insulation is defined as the combination of insulating materials and construction techniques whose installation reduces heat transfer between two spaces (between the interior and exterior of a house, or between spaces within the same house), minimizing heat transfer through mechanisms such as conduction, convection, and radiation [11].

Thermal insulation is therefore used in buildings to slow the transfer of heat from a hot side to a cold side, as heat always moves towards a cooler area. Therefore, thermal insulation should be used where heat is needed or on shaded facades. In winter, for example, it prevents excessive heat loss from the building to the outside. In summer, the same insulation resists the rapid transfer of heat from the outside to the inside of the building. In summary, insulation aims to keep heat where it is desired.

Today, building without thermal insulation incurs additional costs for energy-efficient systems to control climate and temperature. Thermal insulation is presented as a critical necessity, offering unmatched energy efficiency, reduced environmental impact, and increased comfort for both residential and commercial spaces.

Proper installation of thermal insulation in walls, roofs, and floors means lower investment in cooling, heating, and air climate control systems to maintain a comfortable ambient temperature. In summary, building with thermal insulation implies lower energy consumption to maintain buildings over their lifetime, significantly contributing to environmental preservation.

As energy costs rise and concerns about climate change grow, improving energy efficiency in buildings becomes a priority to reduce greenhouse gas emissions and mitigate the impacts of climate change. By enhancing thermal insulation, buildings can reduce their carbon footprint by decreasing the need for heating and cooling, which often relies on fossil fuel-based energy sources.

For this reason, many European countries have regulations requiring the use of thermal insulation in new constructions and renovations to improve energy efficiency and reduce greenhouse gas emissions. These regulations align with the goal of reducing emissions by at least 55% by 2030 compared to 1990 levels and achieving climate neutrality in Europe by 2050, as outlined by the European Union's Green Deal [8].

In Spain, national codes and regulations promote the use of thermal insulation in new buildings and renovations to improve energy efficiency and reduce greenhouse gas emissions, aligning with the European Union's environmental objectives. The Technical Building Code (CTE) provides the regulatory framework for the basic quality requirements that buildings must meet regarding safety and habitability, as established in Law 38/1999 of November 5, on the Regulation of Building (LOE). This includes basic requirements for "structural safety," "fire safety," "safety in use," "hygiene, health, and environmental protection," "protection against noise," and "energy savings and thermal insulation" [40]. The CTE also serves as a tool for the transposition of European directives. For example, Directive 2010/31/EU of the European Parliament and Council, dated May 19, 2010, on the energy performance of buildings, has been partially transposed into Spanish law through modifications to the Basic Document DB-HE by Orders FOM/1635/2013 of September 10 and FOM/588/2017 of June 15 [40]. Insulation requirements are specified in the Basic Document DB-HE Energy Savings of the Technical Building Code, in DB-HE1 "Conditions for Energy Demand Control," applicable to both new buildings and interventions in existing buildings. The document sets limit values for parameters such as thermal transmittance and the overall heat transfer coefficient through the thermal envelope. Additionally, applying the insulation values from DB HE1 2019 in new residential buildings, insulation thicknesses vary depending on the climatic zone, compactness, and the choice of construction elements.

Thermal insulation panels are among the most common tools for achieving this goal. However, further improvements in design and materials can yield even better results.

The present work focuses on the synthesis of rigid polyurethane foam, commonly used in thermal insulation panels. The implementation of an abundant biomass, i.e. lignin, is studied through different processes and allocation methods, which are ultimately compared in terms of environmental sustainability. After an initial focus on thermal insulation itself, four scenarios are analysed and studied in detail:

- Scenario 1: traditional synthesis of rigid polyurethane foam, derived from fossil-based polyols and methylene diphenyl diisocyanate (MDI);
- Scenario 2: synthesis of rigid polyurethane foam, where 30wt.% of fossil-based polyols are replaced by softwood Kraft lignin (MDI content remains unchanged);
- Scenario 3: synthesis of rigid polyurethane foam, where 50wt.% of fossil-based polyols are replaced by hydrolytically depolymerized softwood Kraft lignin (MDI content remains unchanged);
- Scenario 4: synthesis of rigid polyurethane foam, where 100wt.% of fossil-based polyols are replaced by hydrolytically depolymerized and oxypropylated softwood Kraft lignin (MDI content remains unchanged);

CHAPTER 1: THERMAL INSULATION

1.1 Historical evolution of thermal insulation

Thermal insulation has always been deeply connected with humankind comfort. In fact, from caves to highly insulated houses, humans have always demonstrated a need for protection against the elements. The true origins of the science of thermal insulation are still difficult to pinpoint. Nevertheless, Pliny the Elder, a prominent first-century author and naturalist, mentioned the use of cork as an insulating material for roofs, an example that thermal insulation has very ancient roots. This is also evidenced by the fact that the early inhabitants of Spain covered their stone houses with cork bark, while the natives of North Africa used cork mixed with clay for the walls of their homes [9].

The first Spanish mission houses in the western United States, built during the 17th and 18th centuries where temperatures reached between 49 and 60 °C, were relatively cool due to their several-meter-thick clay and straw walls. Similarly, throughout various periods of history, the indigenous peoples of the Pacific Islands constructed huts made of dried seagrass, which provided a good degree of thermal resistance due to its hollow fibers [10].

Mineral fiber, another important insulating material, was first used by ancient Hawaiians to cover their huts. The fibers came from volcanic deposits where escaping steam had broken the molten lava into fluffy fibers. Another widely used insulating material is fiberglass, whose origins date back to ancient Egypt [10]. By the late 19th century, wood shavings emerged as a very popular insulating product due to the wide availability of raw materials and their low cost. Often treated with lime or other chemicals to increase resistance to water absorption, fire, and fungal growth, they played a significant role in insulation practices.

However, it was not until the 1920s that there was a significant increase in public awareness of the value of thermal insulation. Actually, insulation was not as necessary before 1920 as it is now due to the materials and construction methods used at that time. Materials were heavier, including door and window frames, providing adequate weather resistance. The growing popularity and use of lighter construction materials increased the need for insulating products. The gradual introduction of air conditioning systems into home design also contributed to a greater need for thermal insulation [10]. While in the 1920s fiberboard was advertised as the most economical insulation of its time, the popularity of batts also began to rise. Aluminum and copper were also applied to batts as reflective foil. The production of fiberglass began in the mid-1930s. During World War II, the use of insulation in buildings became mandatory to conserve metal needed for heating and air conditioning equipment and to save fuel. This likely also contributed to increased public awareness of the applications of insulation in residences [10]. The emergence of plastic foams (polystyrene, polyurethane) represented a huge revolution in the insulation materials market in the 1940s and 1950s. From this point onward, synthetic insulating materials (plastic foams, mineral wool) surpassed natural materials [31].

1.2 Classification of thermal insulation

Thermal insulation in homes can be divided into two types, depending on whether they require energy consumption: active and passive [11].

Passive insulation systems do not require any external energy input to function and include building orientation, construction techniques that promote cross-ventilation, and the use of thermal insulation materials in facades or floors.

Active thermal insulation systems, on the other hand, involve the use of heating systems, cooling equipment, or humidifiers, among others. An example is a layer of concrete on the exterior wall of buildings that contains a coil directly connected to a heat exchanger. The refrigerant circulating in this system has a lower temperature than the internal air and a higher temperature than the external air in winter. As a result, it is possible to reduce the thermal flow through this wall during the cold season. The energy efficiency of active thermal insulation and the potential to improve thermal comfort both in winter and summer depends on how effectively the temperature in the active insulation layer can be raised or lowered compared to conventional wall construction [12].

The present work will analyze a type of passive thermal insulation, based on the selected materials used as insulators and the design of panels to enhance insulation.

Panels used in thermal insulation can serve as either mass insulation or reflective insulation [9], depending on their composition, design, and intended application. Mass insulating panels rely on a defined thickness of material to provide heat resistance, whereas reflective insulating panels depend solely on the surface characteristics, i.e., the emittance.

1.3 Properties of materials for thermal insulation

The analysis of fundamental variables in thermal insulation is crucial for designing and implementing effective solutions to regulate heat flow. Understanding factors such as thermal conductivity (k), thermal resistance (R), thermal transmittance (U), the water vapor diffusion resistance factor (μ), specific heat (c_p), and the density of the insulating material (ρ) allows for the optimization of the overall effectiveness of the thermal insulation system. The meaning and importance of these parameters are briefly summarized below.

- Thermal Conductivity (k): This is a constant for any given material and describes its ability to transfer thermal energy from one point to another when there is a temperature gradient. It is numerically equal to the amount of heat that flows per unit of time through a unit area of a surface with unit thickness and a unit temperature difference between its faces.
- Thermal Resistance (R): This is a measure of a material's ability to resist the flow of heat through it. It is calculated by dividing the thickness of the material by the product of the material's thermal conductivity and its cross-sectional area. In simple terms, thermal resistance indicates how difficult it is for heat to flow through a material or structure.
- Thermal Transmittance (U): This measures how heat flows through a material, considering a temperature difference on each side. It represents the amount of energy that passes every second through one square meter of a material for each one-degree Celsius difference between the two

faces. Since U measures the heat flow, the lower its value, the slower the material is at transferring heat in and out of a building, for example [10]. There is a relationship between U and R :

$$U = \frac{1}{R}$$

- Water Vapor Diffusion Resistance Factor (μ): This measures a material's resistance to allowing water vapor to pass through, taking into account its thickness. It is a material property, dimensionless and temperature dependent. The higher the μ value, the better the insulating material is at limiting the ingress of water vapor over time. This is important because moisture accumulation within an insulation system can compromise its effectiveness and cause issues such as mold growth, material degradation, and an increase in the overall thermal conductivity of the system.
- Density (ρ): The density of the material can significantly affect both thermal conductivity and thermal resistance. Denser materials tend to have higher thermal conductivity, as a greater mass per unit volume facilitates heat transfer through the material.
- Specific heat (c_p): The specific heat of a material can influence its ability to store and release heat. A high specific heat value, for example, indicates that the material requires more energy to raise its temperature, which affects its capacity to retain and slowly release heat over time.

1.4 Heat transfer principles

Thermal energy is a form of energy associated with the temperature of a substance. It arises from the random movement of atoms and molecules within a material. Atoms and molecules are constantly in motion, even in solids, where they vibrate in fixed positions. In liquids and gases, they move more freely, colliding with each other and bouncing off surfaces. The kinetic theory of gases helps explain thermal energy. It states that the average kinetic energy of ideal gas molecules is directly proportional to the temperature of the gas. Therefore, as the temperature increases, the average speed of the molecules increases, leading to greater kinetic energy and, consequently, greater thermal energy. In [1.1], T represents the temperature of the gas, K_t is the translational kinetic energy, k_b is the Boltzmann constant, and N is the number of molecules.

$$T = \frac{2}{3} \frac{K_t}{Nk_B} \quad [1.1]$$

In solids, thermal energy is primarily associated with the vibrational movement of atoms and molecules within the material's lattice structure. Although in solids, kinetic energy manifests through vibrational motion rather than translational motion as in gases, the underlying principle remains unchanged. Thus, in solids, an increase in temperature leads to higher average kinetic energy, with greater vibrational amplitudes of atoms and molecules resulting in increased thermal energy.

This increase in thermal energy affects various properties of solids, such as expansion, thermal conductivity, and specific heat capacity. It's the transfer of thermal energy what is commonly known as heat.

To understand how insulation works, it helps to comprehend the three mechanisms of heat transfer: conduction, convection, and radiation. In typical situations, all three modes of heat transfer occur simultaneously. The purpose of thermal insulation is to reduce these mechanisms, for example, by creating a thermal barrier for conduction or causing the lower-temperature surface to reflect rather than absorb thermal radiation.

1.4.1 Conduction

When heat is transferred by conduction, it moves from one part of a body to another part of the same body, or from one body to another body in contact with it. Molecules or particles that vibrate more rapidly transfer some of their energy to molecules that move more slowly. In this way, energy is transferred during the collision process from one part of the body to another without any change in the exact position of the body parts.

Therefore, conduction is the transfer of heat through stationary matter by physical contact. The result of this process is to increase the average energy and, consequently, the temperature of the areas in contact with the heat source as thermal equilibrium is reached [9].

Conduction is more significant in solids because the relatively close and fixed spatial relationships between atoms help transfer energy between them through vibration. In non-metallic solids, there are no free particles, but the molecules are elastically bound to each other by bonding forces. The transfer of heat in such cases can be considered a transfer of vibrational energy from one particle to

the next. In metallic solids, the free conduction electrons in their own electron cloud also contribute to thermal conductivity. However, understanding this principle, fluids, liquids, and gases are less conductive than solids due to the greater interatomic distances, especially in gases, where there will consequently be fewer collisions between atoms [13].

The mathematical theory of heat conduction in solids is primarily attributed to Jean Baptiste Joseph Fourier (1768 - 1830). It has been experimentally discovered that the rate at which heat is transferred from a hot portion to a cooler one depends on several conditions. Consider, within a body, two parallel planes with an area A and a distance x between them, each having a constant temperature, T_1 in one case and T_2 in the other. Then the heat will flow from the hotter of these isothermal surfaces to the cooler one, and the amount Q that will be conducted over time will be given by:

$$Q = k \frac{T_1 - T_2}{x} At \quad [1.2]$$

Or:

$$q = \frac{dQ}{dt} = k \frac{T_1 - T_2}{x} A \quad [1.3]$$

Where k is the thermal conductivity.

$(T_2 - T_1)/x$ or dT/dx is one of the three components of a temperature gradient.

Therefore, equation [1.3] can be written as [1.4] or [1.5], with the latter representing the thermal energy flux per unit time through a unit area of a surface [14].

$$q = -kA \frac{\partial T}{\partial x} \quad [1.4]$$

$$j_q = -k \frac{\partial T}{\partial x} \quad [1.5]$$

The most general form of [1.5] considers three dimensions.

$$j_q = -k \nabla T \quad [1.6]$$

The temperature in a solid object is assumed to be a finite and continuous function of x , y , z , and time. Taking this into account, the heat flux in a body is expressed by a linear and homogeneous partial differential equation known as the Fourier equation.

$$\frac{\partial T}{\partial t} = \alpha \nabla^2 T \quad [1.7]$$

Where α is the thermal diffusivity, relating the thermal conductivity of the material to other characteristics such as its density and specific heat capacity.

However, in the general case, where the thermal conductivity varies from one point to another, the corresponding equation is:

$$\frac{\partial T}{\partial t} = \frac{1}{c_p \rho} \left[\frac{\partial}{\partial x} \left(k \frac{\partial T}{\partial x} \right) + \frac{\partial}{\partial y} \left(k \frac{\partial T}{\partial y} \right) + \frac{\partial}{\partial z} \left(k \frac{\partial T}{\partial z} \right) \right] \quad [1.8]$$

The solution to virtually all heat conduction problems involves determining the temperature profile. The temperature function must not only solve the general differential equation but also satisfy certain boundary condition equations characteristic of each particular problem, such as initial conditions or boundary conditions.

In numerous systems involving flow, whether of heat or electricity, it has been observed that the amount of flow is inversely proportional to the resistances applied to the system.

$$Flow \propto \frac{potential}{resistance} \quad [1.9]$$

Therefore, the heat flow through a wall, as previously mentioned, occurs due to a temperature difference between the hot and cold faces. According to equation [1.3], the term $\frac{x}{kA}$ acts as a resistance to heat flow.

$$R = \frac{x}{kA} \quad [1.10]$$

Conductance is the inverse of the resistance to heat flow, so equation [1.9] can be expressed using [1.11].

$$Flow \propto conductance \cdot potential \quad [1.11]$$

When thermal conductivity k is low, it means that the material is a poor conductor of heat. In the case of equation [1.10], thermal resistance R will be higher for a given thickness x and area A . Therefore, materials with low thermal conductivity tend to exhibit higher thermal resistance and are often used as thermal insulators precisely because they effectively impede heat transfer.

The thermal conductivities of different solids at ordinary temperatures vary by about 20,000 times. Among common materials, metals have the highest thermal conductivity due to the movement of electrons in their electron cloud, as previously mentioned, with silver having the highest thermal conductivity ($k = 418 \text{ W}/(\text{m}\cdot\text{K})$), followed by copper ($k = 167.36 \text{ W}/(\text{m}\cdot\text{K})$).

On the other hand, materials with the lowest thermal conductivity are considered thermal insulators. Notable examples include various types of rocks with thermal conductivities around $2 \text{ W}/(\text{m}\cdot\text{K})$, and silica aerogel, which has a thermal conductivity of $0.021 \text{ W}/(\text{m}\cdot\text{K})$, slightly lower than that of still air. Many building insulators have thermal conductivity values around $0.04 \text{ W}/(\text{m}\cdot\text{K})$ [14].

The thermal conductivity of non-metallic substances generally increases with temperature (although there are many exceptions, such as most rocks). However, the thermal diffusivity of these substances (as described by equation [1.7]) does not increase in the same manner. Although thermal diffusivity is proportional to thermal conductivity, other material-specific factors also come into play in this parameter.

$$\alpha = \frac{k}{\rho c_p} \quad [1.12]$$

Specific heat generally increases with temperature in most cases, while the change in density is small [14]. Density itself can affect the thermal conductivity of materials, which is particularly important in insulation. For most insulating materials, thermal conductivity decreases as their density decreases. For the same insulating material with all other conditions being equal, this variation often follows a linear trend. Figure 3 illustrates an example of a material that exhibits this behavior.

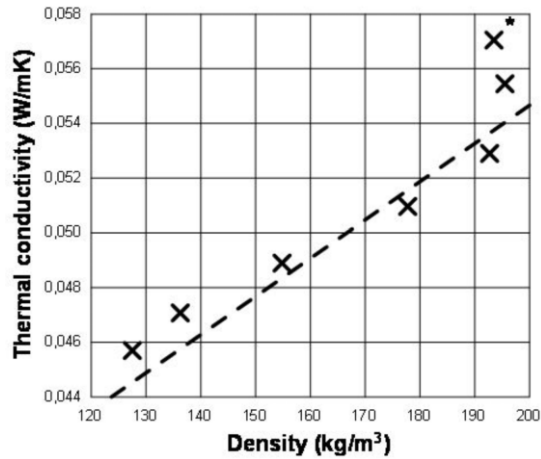


Figure 3: Relationship between density and thermal conductivity of a corn stalk insulation block, adapted from [16]

Certain types of materials exhibit what is known as an optimal density, meaning a density that yields the minimum heat transfer rate. Any increase or decrease from this optimal value will result in higher conductivity.

For instance, although the heat transfer rate through rock is high, the heat transfer rate through the same material in an aerated or porous condition (like rock wool) is significantly reduced because the density of the rock is also reduced. Conversely, if a material is expanded to the point where heat is transmitted through it by radiation or convection, the heat flow will increase. In other words, there is a limit to how porous a material can become before the heat flow starts to increase rather than decrease. Once the material reaches this threshold, further increases in porosity may result in increased heat flow due to heat transfer by radiation or convection in addition to conduction. Additionally, if the material is packed or compacted at a high density, its heat transfer rate increases as density increases [9].

Figure 4 illustrates the variation of thermal conductivity with density for various insulating materials, showing the presence of an optimal density. This is particularly evident in rock wool and banana fiber. For example, as shown in the figure, the optimal density for rock wool is around 70 kg/m³, where thermal conductivity reaches a minimum. However, at densities both lower and higher than this value, conductivity increases again. For banana fiber, the optimal density is slightly higher, around 75 kg/m³.

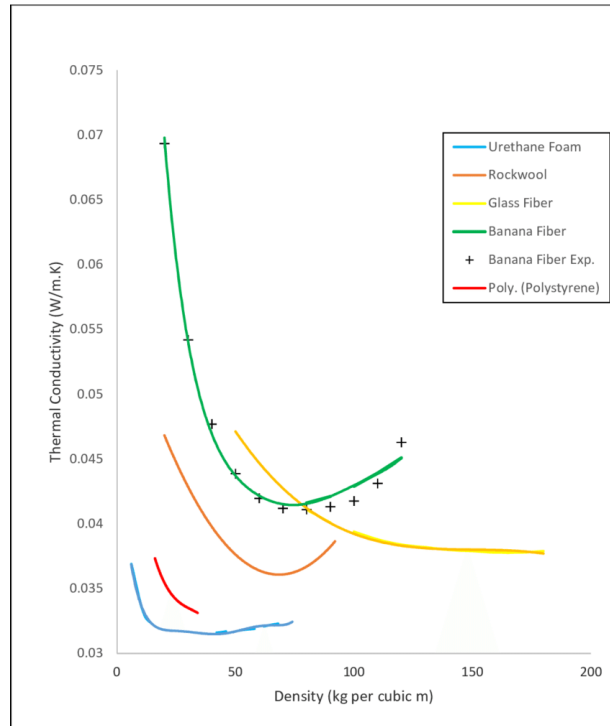


Figure 4: Variation of thermal conductivity with density for various insulating materials, sourced from [17]

Other factors, such as moisture and the arrangement and characteristics of fibers in a fibrous material, can have a greater effect on conductivity than density.

In summary, an ideal material for thermal insulation should have the following characteristics:

- Low moisture: since water conducts heat more rapidly than air [9];
- Low density: as previously discussed, or optimal density for materials that exhibit this property;
- High specific heat: can contribute to a material's insulating effectiveness, as it allows the material to absorb more thermal energy before heating up, thus slowing down heat transfer.

Typical thermal conductivity values for polyurethane foams range between 0.02 and 0.03 W/(m·K) [18].

1.4.2 Convection

Thermal convection is the transport of energy by conduction from a boundary surface and a moving fluid when the two are at different temperatures. Therefore, it consists of two mechanisms: on one hand, the transfer of energy due to random molecular motion (conduction), and on the other, energy is also transferred through the bulk movement of the fluid, associated with the fact that at any instant, a large number of molecules move collectively as aggregates. This movement, in the presence of a temperature gradient, contributes to heat transfer. Since the molecules in the aggregate retain their random motion, the total heat transfer is thus due to a superposition of:

- The transport of energy by the random motion of the molecules
- The bulk movement of the fluid

A consequence of the fluid-surface interaction is the development of a region in the fluid through which the velocity varies from zero at the surface to a finite value u_∞ associated with the flow, called the velocity boundary layer. Additionally, if the temperatures of the surface and the flow differ, there will be a region of the fluid through which the temperature varies from T_w at the wall to T_∞ in the outer

flow. This region is called the thermal boundary layer.

If $T_w > T_\infty$, heat transfer by convection will occur between the surface and the outer flow [19].

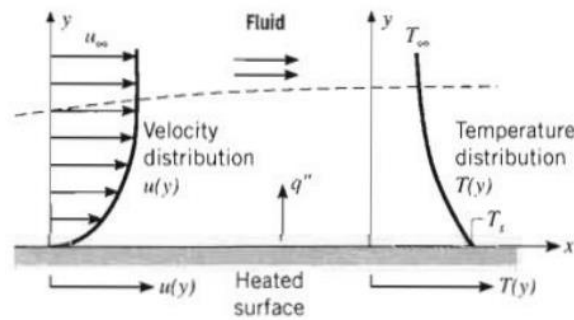


Figure 5: Velocity and Thermal Boundary Layers, extracted from [19]

The contribution due to random molecular motion (conduction) dominates near the surface where the fluid velocity is low. At the interface between the surface and the fluid, the fluid velocity is zero, and heat is transferred solely through this mechanism.

The mechanism of transfer by convection is complex and depends greatly on whether the flow is laminar or turbulent. The usual and simplified approach in convection is to express the rate of heat transfer as:

$$q = hA(T_w - T_\infty) \quad [1.13]$$

analogy with [1.5], in convection, [1.13] can also be written to refer to the flow of thermal energy per unit time through the unit area of a surface.

$$j_q = h(T_w - T_\infty) \quad [1.14]$$

In [1.13] and [1.14], also known as Newton's law of cooling, h is referred to as the convective heat transfer coefficient. T and T_w are, respectively, the total temperature of the fluid and the temperature of the wall. By analogy with the above, from equation [1.13], it is also possible to identify a thermal resistance to heat flow, equal to $\frac{1}{hA}$.

$$R = \frac{1}{hA} \quad [1.15]$$

The convective heat transfer coefficient depends on:

- The fluid
- The velocity of the fluid
- The flow channel
- The degree of development of the flow field

In building insulation, air is one of the primary fluids involved in heat transfer due to its presence in cavities, gaps, or layers within the building envelope. Therefore, in these applications, the convective heat transfer coefficient often refers to the heat transfer coefficient associated with air.

The thermal resistance due to convection given by [1.15] can be added to that arising from pure conduction, given by [1.10], to model the overall thermal resistance of a system.

$$R_{TOT} = \frac{x}{kA} + \frac{1}{hA} \quad [1.16]$$

When aiming to achieve a high level of thermal insulation, the goal is to maximize the resistance to heat flow through a material. Referring to equation [1.16], this is typically achieved by:

- Increasing the thickness x of the insulating material: Greater thickness means there is more material through which heat must travel, thereby increasing resistance to conduction.
- Reducing the thermal conductivity k of the material: Lower thermal conductivity means the material is less efficient at transferring heat.
- Decreasing the heat transfer coefficient h by convection: This can be achieved, for example, by using materials with a smooth surface that minimizes air turbulence or contact with other fluids, thereby reducing convection.
- Reducing the heat exchange area A : This might involve choosing a shape or design that reduces the contact area with the surrounding environment, thus limiting heat transfer by convection.

Convection can occur through two mechanisms:

- Forced convection: This occurs when the flow is induced by external means, such as a fan, a pump, or atmospheric winds. In forced convection, buoyancy forces are negligible. This is because forced convection systems are often designed to have relatively high flow velocities and turbulent flow conditions, and in such cases, the fluid flow momentum dominates over buoyancy forces.
- Natural convection: This occurs when the movement of the fluid is entirely due to buoyancy forces, generally confined to a layer near the heated or cooled surface. Buoyancy forces arise from density differences caused by temperature variations within the fluid.

Most building structures experience forced convection along exterior walls or roofs, while natural convection occurs within narrow air spaces and interior walls.

The heat transfer coefficient by convection in relation to air generally ranges from approximately 6 W/(m²·K) for natural convection to approximately 35 W/(m²·K) for forced convection with an air velocity of about 6 m/s.

1.4.3 Radiation

Thermal radiation is a form of heat transfer generated by any matter with a temperature above absolute zero. Thermal radiative energy can be viewed as consisting of electromagnetic waves (as predicted by electromagnetic wave theory) or as consisting of massless energy packets called photons (as predicted by quantum mechanics) [21]. No single perspective can fully describe all the radiative phenomena observed. Therefore, it is common to use both concepts interchangeably.

Generally, the radiative properties of liquids and solids (including tiny particles) and interfaces (surfaces) are more easily predicted using electromagnetic wave theory, while the radiative properties of gases are more conveniently obtained from quantum mechanics.

All materials continuously emit and absorb electromagnetic waves or photons as their molecular energy levels decrease or increase. The intensity and wavelengths of the emission depend on the temperature of the emitting material. For heat transfer applications, wavelengths between 10^{-7} m and 10^{-3} m (ultraviolet, visible, and infrared) are of greatest importance [21].

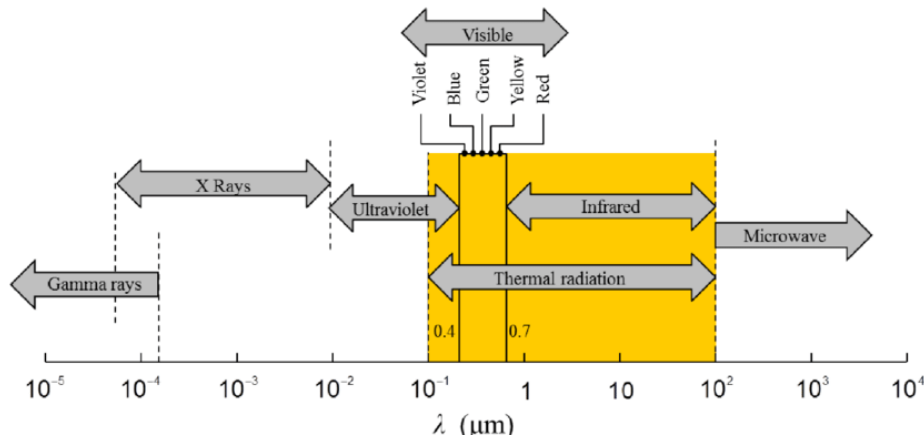


Figure 6: The electromagnetic radiation spectrum, showing the thermal radiation zone in yellow, extracted from [22]

Both conduction and convection require the presence of a medium for energy transfer; however, thermal radiation is transferred through electromagnetic waves, or photons, which can travel long distances without interacting with a medium.

Another distinguishing feature between conduction and convection, on one hand, and thermal radiation, on the other, is the difference in their temperature dependencies [21]. For most conduction applications, heat transfer rates are well described by [1.5], while convective heat flow can be determined by [1.14]. Thus, for most applications, conductive and convective heat transfer rates are linearly proportional to temperature differences. In contrast, radiative heat transfer rates are generally proportional to the fourth power (or higher) of the temperature differences.

$$j_q \propto T^4 - T_\infty^4 \quad [1.17]$$

Therefore, radiative heat transfer becomes more significant with increasing temperature levels and can become entirely dominant over conduction and convection at very high temperatures.

All electromagnetic waves or photons propagate at the speed of light through any medium. The speed of light depends on the medium through which it travels and can be related to the speed of light in a vacuum by:

$$c = \frac{c_0}{n} \quad [1.18]$$

In [1.18], n is the refractive index of the medium, and c_0 is equal to $2.998 \cdot 10^8$ m/s.

Each wave can be identified either by its frequency, wavelength, wave number, or angular frequency. All these quantities are related to each other through the following formulas:

$$v = \frac{\omega}{2\pi} = \frac{c}{\lambda} = c\eta \quad [1.19]$$

Additionally, each wave or photon carries an amount of energy, determined by quantum mechanics as:

$$\epsilon = h_p v \quad [1.20]$$

In [1.20] h_p is Planck's constant and $h_p = 6.626 \cdot 10^{-34}$ J·s.

When an electromagnetic wave travels through a medium (or vacuum) and strikes the surface of another medium (solid or liquid surface, particle, or bubble), the wave can be reflected (partially or fully), and any non-reflected part will penetrate into it. As it traverses the medium, the wave can be continuously attenuated. Based on the degree of attenuation, materials can be classified as:

- Opaque materials: If attenuation is complete and no penetrating radiation re-emerges.
- Transparent materials: If a wave passes through a medium without attenuation.
- Translucent material: When attenuation is partial, and part of the wave penetrates the material while another part is absorbed or reflected.

Whether a medium is transparent, translucent, or opaque depends on the material and its thickness (i.e., the distance the electromagnetic wave must travel through the medium) [21].

An ideal thermal insulation material for a house should ideally be opaque or translucent rather than transparent. An opaque material would be effective in blocking both radiant heat and light, helping to maintain the desired temperature inside buildings by preventing heat transfer through the insulation. Translucent materials, on the other hand, allow some light or heat to pass through but attenuate it to some extent. Thermal insulation panels made of polyurethane foam are generally considered opaque.

As discussed earlier, when thermal radiation strikes a medium of certain thickness, three main processes occur: part of the radiation is reflected away from the medium, a portion is absorbed within the layer, and the rest passes through the slab. Figure 7 illustrates these phenomena.

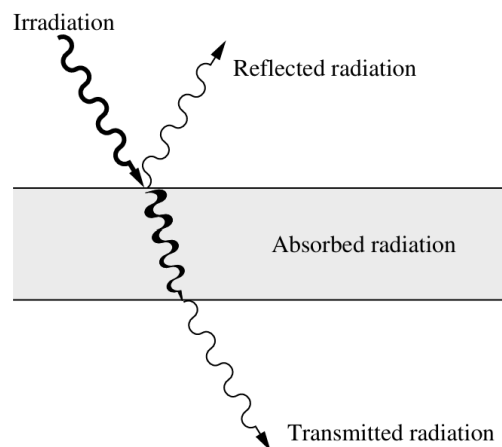


Figure 7: Absorption, reflection, and transmission through a slab, extracted from [21]

Based on this observation, the three fundamental radiative properties are defined as follows:

$$\text{Reflectance, } \rho_r \equiv \frac{\text{reflected radiation}}{\text{total incident radiation}}$$

$$\text{Absorptance, } \alpha_r \equiv \frac{\text{absorbed radiation}}{\text{total incident radiation}}$$

$$\text{Transmittance, } \tau_r \equiv \frac{\text{transmitted radiation}}{\text{total incident radiation}}$$

The three properties are dimensionless and can vary in magnitude between 0 and 1. Since all radiation must be either reflected, absorbed, or transmitted, the following relationship is established between these properties:

$$\rho_r + \alpha_r + \tau_r = 1 \quad [1.21]$$

If the medium is thick enough to be considered opaque, then $\tau_r = 0$ and [1.21] is modified to:

$$\rho_r + \alpha_r = 1 \quad [1.22]$$

All surfaces also emit thermal radiation (or, more precisely, radiant energy within the medium, part of which escapes from the surface). Since, at a given temperature, the maximum amount possible is emitted by a black surface, a fourth dimensionless property can be defined:

$$\text{Emissivity, } \epsilon_r \equiv \frac{\text{energy emitted by a surface}}{\text{energy emitted by a black surface at the same temperature}}$$

The emissivity can vary between 0 and 1, with a black surface having $\epsilon_r = 1$. All four properties can be functions of both temperature and wavelength (or frequency). Absorptance may vary for different directions of irradiation, while emissivity can vary with the directions of emission. Finally, the magnitudes of reflectance and transmittance may depend on both incoming and outgoing directions [21].

The energy emitted by a black surface at temperature T , per unit area, is determined by the Stefan-Boltzmann law. Therefore, for non-black bodies at the same temperature T , the Stefan-Boltzmann law is modified to include emissivity.

$$j_q = \sigma T^4 \quad [1.23]$$

$$j_q = \epsilon_r \sigma T^4 \quad [1.24]$$

The Stefan-Boltzmann constant σ is found to have the value $5.67 \times 10^{-8} \text{ W}/(\text{m}^2 \cdot \text{K}^4)$. The net rate of energy transfer from one blackbody at temperature T_1 to another blackbody at temperature T_2 is given by:

$$q_{12} = A_1 F_{12} \sigma (T_1^4 - T_2^4) = A_2 F_{21} \sigma (T_1^4 - T_2^4) \quad [1.25]$$

Areas A_1 and A_2 are typically chosen as the total areas of bodies 1 and 2, and F_{12} and F_{21} are dimensionless view factors. The view factor F_{12} , for example, represents the fraction of radiation leaving A_1 that is directly intercepted by A_2 [23]. The actual calculation of view factors is a complex problem and is often carried out using appropriate diagrams.

This equation can be useful for determining the solar energy received by the entire Earth each second, which amounts to $1.74 \times 10^{17} \text{ W}$. By dividing this quantity by the area of the circle representing the cross-sectional area of solar irradiation reaching the Earth, it is possible to determine the solar constant, i.e., the amount of radiant energy received by the Earth from the Sun per unit time and area of surface, measured at the top of the Earth's atmosphere, perpendicular to the solar rays [24]. The solar constant is therefore approximately $1,366 \text{ W}/\text{m}^2$. This parameter is very useful as it provides an indication of the amount of solar energy impacting buildings and structures daily.

1.5 Heat Transfer Mechanism Through Walls

Heat transfer through walls from the air on one side to the air on the other involves all three heat transfer processes explained. Figure 8 illustrates this mechanism.

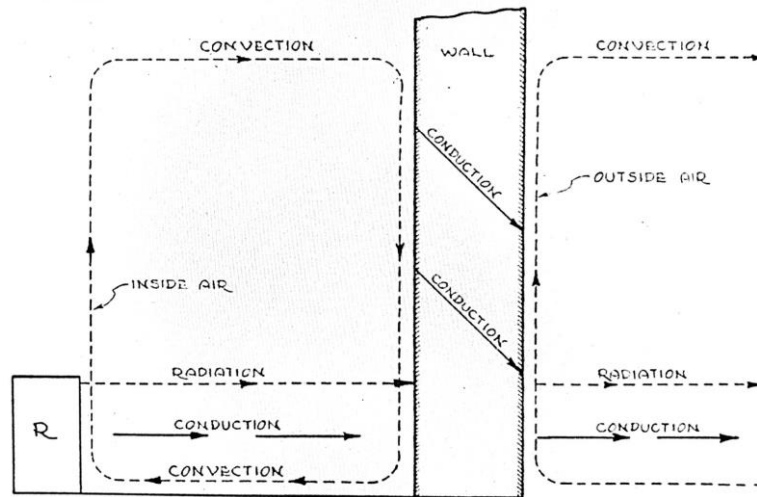


Figure 8: Heat transfer to, through, and from a wall, sourced from [9]

In this figure, R represents a hot body, such as a radiator or stove. Thus, heat is transferred from the surface of R to the inner surface of the wall (or ceiling) through radiation, convection, and conduction [9]. Heat passes by radiation in a straight line from the surface of the hot body R through the air without appreciably heating it, to the cooler receiving wall. The air in direct contact with the hot body R will absorb heat, expand, rise, and circulate through the process of convection, thus transferring its heat in turn to the cooler surfaces of the walls or ceiling. When this hot air encounters the cooler surfaces of the wall or ceiling, its temperature decreases, and the air falls to the floor, returning to the hot body R and resulting in a continuous circulation of air that completes the convection process. A small amount of heat is also transferred by conduction from one gas molecule to another in the direction of the cooler wall surface [9]. Then, the transfer of heat from the inner surface of the wall to the outer surface through the solid materials that make up the wall is done entirely by conduction.

Heat transfer from the outer wall surface to the outside air occurs in reverse order. The outer wall releases heat not only through natural convection due to the tendency of the warm air in contact with this wall surface to rise, but also through forced convection caused by the wind blowing over the outer surface. This outer surface also releases heat through the process of radiation to surrounding objects.

In the removal of heat from the outer surface, there may also be a small amount of conduction of heat through air particles, as in the case of heat transfer to the inner wall surface.

The principles of heat transfer described would similarly apply in reverse, with the Sun acting as the hot body radiating heat towards the outer surface of a wall, thereby initiating the heat transfer process through radiation, conduction, and convection.

From the above, it is evident that heat flow by conduction can vary from a small percentage in the case of air spaces to 100 percent in the case of solid materials, while radiant heat transfer can vary

from zero percent in the case of solid materials to 70 percent or more in the case of air spaces. Similarly, convection can vary from zero percent through solids to almost 100 percent in the case of surfaces exposed to forced convection [9]. Therefore, it is evident that the percentage of heat transferred by the three processes varies greatly and depends on the environmental conditions and materials involved.

1.6 Energy Efficiency

The concept of energy efficiency refers to achieving optimal results in any activity using the least possible amount of energy resources. It facilitates the reduction of energy consumption and the associated environmental impacts throughout the entire cycle of energy production and consumption. Additionally, it involves maintaining consistent operational efficiency through the implementation of responsible practices, sustainable management models, and investments in technological innovation [25]. It is evident, therefore, that energy efficiency entails a multitude of benefits, such as energy and cost savings, environmental preservation through responsible energy management and optimization of resource utilization.

In response to the global energy crisis, governments are revising energy efficiency targets and policies to reflect a greater sense of urgency in a focused effort to reduce dependence on high-priced fossil fuels, protect consumers from high energy bills, and reduce reliance on Russian gas in Europe. Efficiency is the most important measure to avoid energy demand in the Net Zero Emissions Scenario for 2050 and has been advancing in recent years. However, to move towards this scenario, the rate of improvement in global energy intensity must be much higher than historical rates [26].

Energy efficiency, electrification, digitalization, and material efficiency shape global energy intensity: the amount of energy needed to produce one unit of GDP, a key measure of the energy efficiency of the economy [26]. When discussing the amount of energy needed to produce a unit of GDP, it essentially measures how much energy is consumed to generate a certain level of economic activity. This relationship, often referred to as energy intensity, reflects the efficiency of energy use within an economy. For example, if the energy intensity of an economy is high, it means that a relatively large amount of energy is required to produce each unit of GDP. Conversely, if the energy intensity is low, it means that less energy is needed to produce the same level of economic output. Lower energy intensity suggests that the economy is operating more efficiently in terms of energy use. In practical terms, lower energy intensity often implies that businesses and industries are using energy more efficiently, employing technologies, processes, and practices that allow them to produce goods and services while consuming less energy. This can yield several benefits, including reduced energy costs, lower environmental impact, and better overall resource utilization.

The energy intensity of the global economy (a key measure of energy efficiency) improved by just over 2% in 2022. Higher energy costs, supply disruptions, and imminent shortages have sharpened the focus on improving efficiency, with consumers and governments taking steps to conserve and better manage energy. The global improvement in 2022 is roughly double the average of the previous five years and could indicate a shift after years of slowing progress in energy efficiency, especially during the Covid-19 pandemic. To move towards the NZE scenario, sustained improvement will be needed to increase the annual progress from the 2% achieved last year to around 4% annually between now and 2030 [26].

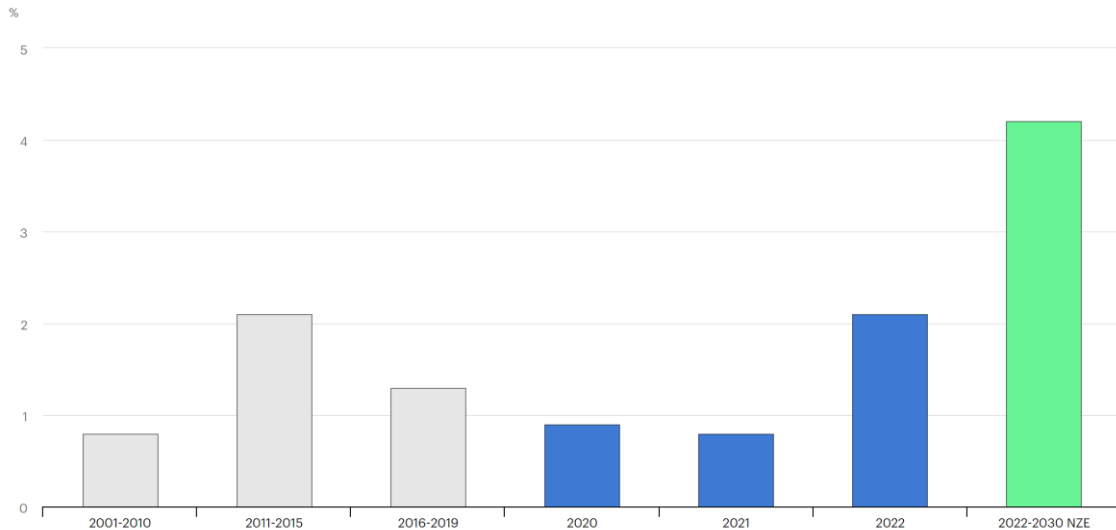


Figure 9: Improvement in Global Primary Energy Intensity, Annual Change in the Net Zero Emissions Scenario, 2000-2030, extracted from [26]

With this objective in mind, countries representing more than 70% of the world's energy consumption have introduced new or strengthened efficiency policies since the start of the current energy crisis. The European Union agreed on stricter standards to boost energy efficiency in March 2023. These standards almost double the annual energy savings rate that EU countries are required to achieve on average each year between 2024 and 2030, increasing from 0.8% per year previously to 1.49%. This increases the EU-wide energy savings target to 11.7% by 2030 relative to a 2020 baseline projection [26].

Buildings are the largest energy consumers in Europe: 42% of the energy consumed in the EU in 2021 was used in buildings, and more than 1/3 of the EU's energy-related GHG emissions come from buildings. Moreover, 85% of EU buildings were built before the year 2000, and among them, 75% have poor energy performance [27].

Therefore, the construction sector is crucial for achieving the EU's energy and climate goals. To boost the energy efficiency of buildings, the EU has established a legislative framework that includes the EU/2010/31 Energy Performance of Buildings Directive and the EU/2023/1791 Energy Efficiency Directive, both revised in 2023. Together, the directives promote policies that will help achieve a highly energy-efficient and decarbonized building stock by 2050, create a stable environment for investment decisions, and enable consumers and businesses to make more informed decisions to save energy and money.

In this framework, thermal insulation proves to be a fundamental component for improving energy efficiency.

1.7 Importance and Functioning of Thermal Insulation Panels

As already mentioned, panels used in thermal insulation can serve as either mass insulation or reflective insulation.

The effectiveness of mass insulation in reducing heat transfer is due to the material's low thermal

conductivity and virtually no heat transfer by convection and radiation [9]. These characteristics, in turn, are due to the material's subdivision or density. In the absence of insulation, an air gap between two bodies at different temperatures (one interior and one exterior, for example) would provide the most reasonable medium for ensuring maximum insulation efficiency due to its low thermal conductivity [28], as represented below by the "no insulation" section of the wall.

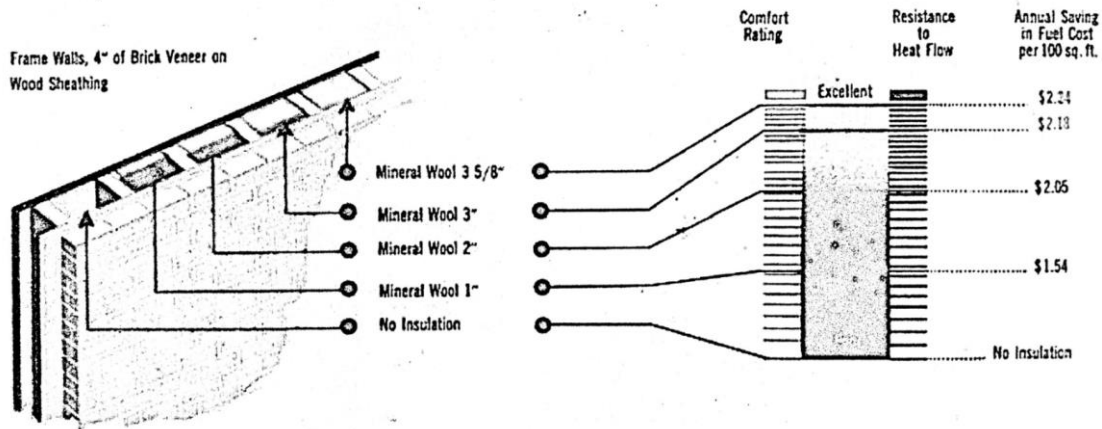


Figure 10: Variable thickness of thermal insulation and its effect on comfort rating, extracted from [29]

However, as mentioned earlier, when air is heated, it becomes less dense and tends to rise, allowing colder, denser air to descend and take its place. In this way, air circulation between the two surfaces is established, and the convection currents formed make the air act as a medium for transferring heat from the hotter surface to the cooler one. If the temperature difference is significant and there is no frictional resistance to air flow, air circulation will be rapid, and the heat transfer rate will be high. However, if the temperature difference is small or there is considerable resistance to air flow, the convective heat transfer rate will be low. Therefore, enclosing the air mattress in a sealed enclosure is the first step to preventing air currents.

A further step is to divide the enclosure into several smaller ones so that the overall temperature difference becomes the sum of several smaller temperature differences [28]. The air circulation speed in these smaller enclosures is significantly reduced compared to that in a single large one, due to the reduction in temperature difference that drives air movement. Further subdividing these smaller enclosures reduces the cause of air currents even more and increases frictional resistance to movement until, finally, when the subdivisions are so small that the mattress can have a cellular formation, the confined air becomes virtually stationary. This way, convective heat transfer is minimized.

Thermal insulation panels made from materials such as polyurethane foam, expanded polystyrene, or similar substances often incorporate this principle. These materials typically have a cellular structure with numerous small air pockets or pores inside. This cellular structure helps confine the air and reduce convective heat transfer within the material.

The material forming the boundaries of the air cells must be very thin and have low thermal conductivity to effectively contribute to the insulation. This same subdivision of the air mattress also minimizes heat transfer due to radiation, as the closer two temperatures T_1 and T_2 are, the smaller the quantity $T_1^4 - T_2^4$ will be at a given mean temperature [28].

Thermal transmission through the subdivided air mattress will never be as low as the thermal conductivity of air due to the inevitable presence of solid material needed to form the subdivisions. Moreover, molecular theory explains why these insulating materials have a lower rate of heat conduction compared to dense and hard materials like steel, concrete, and glass [9]. If the molecules of a material are more tightly packed, as in the case of steel, any vibration or movement of the molecules easily transmits from one part of the substance to another. On the other hand, with lighter and porous materials, commonly used in thermal insulation panels, any movement of molecules due to heat applied to one side does not easily transmit to the other side through impact with adjacent molecules, because the molecules are less compact.

This work will focus on rigid board insulation, normally classified as a type of mass insulation rather than reflective insulation. Rigid board insulation is made from dense, resilient sheets of certain types of foam, with polyurethane, polystyrene, and polyisocyanurate being the most commonly used. Due to their chemical structure, these types of foams are defined as closed-cell.

CHAPTER 2: POLYURETHANE FOAM THERMAL INSULATION PANELS

In the 19th century, the processing of organic materials gave rise to the first insulating panels, coinciding with the emergence of various artificial materials such as rock wool, fiberglass, foam glass, hollow bricks, and expanded perlite. However, it was not until 1941 that a monumental revolution in insulation materials began with the introduction of plastic foams, such as polystyrene and polyurethane. This marked a significant shift in the market, as artificial insulation materials, including plastic foams and mineral wool, advanced, gradually displacing natural materials. Until 2010, artificial materials constituted approximately 90-95% of the total production of thermal insulation materials, with plastic foams and mineral wool dominating the landscape [31].

Polyurethanes (PU), in particular, are plastic polymers obtained by combining diisocyanates (toluene diisocyanate, TDI, or methylene diphenyl diisocyanate, MDI) and polyols [32], through a polycondensation reaction [33]. In polycondensation, the reaction develops through a step-growth mechanism, and the polymer does not have the same composition as the monomer or monomers from which it derives. Polymerization occurs between bi- or polyfunctional monomers and involves the formation of both polymer chains and low molecular weight molecules derived from the condensation reaction [33].

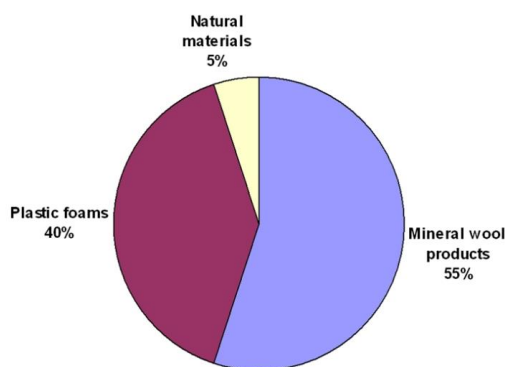


Figure 11: Thermal insulation materials market in 2010, extracted from [31]

The monomers used to produce polymers by polycondensation derive from a succession of petrochemical processes, that is, they are higher-generation petrochemical derivatives [33].

Polyols are oligomers functionalized with hydroxyl groups that have a molecular weight in the range of 300-9000 g/mol and a functionality in the range of 1-8 equivalents per mole [34]. Linear polyols with low functionality ($f = 2-3$ eq/mol) such as glycerin ($f = 3$) or dipropylene glycol ($f = 2$) generate flexible PUs, while branched polyols with high functionality ($f = 3-6$ eq/mol) such as sorbitol ($f = 6$), Mannich bases ($f = 4$), or sucrose ($f = 8$) lead to rigid PU systems. In practice, the molecular weight of the polyols also influences the rigidity of the resulting PUs: low molecular weight polyols are used to manufacture rigid PUs, while flexible PUs are obtained from high molecular weight polyols [34].

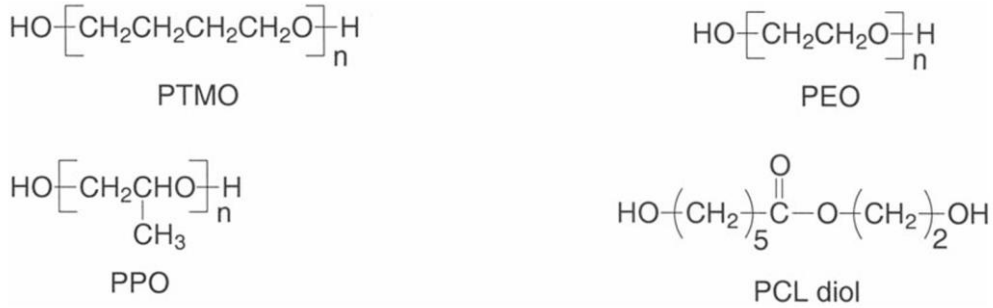


Figure 12: Chemical structures of polyols used for PU synthesis, extracted from [34]

Diisocyanates, on the other hand, are compounds with two isocyanate groups in the molecule. TDI is primarily used for the production of flexible polyurethane foams, while MDI is predominantly used for rigid polyurethane foams [35].

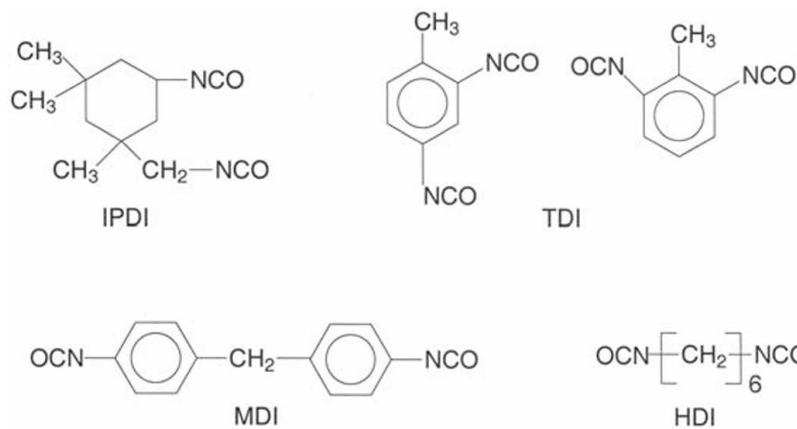
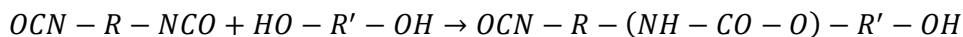


Figure 13: Chemical structures of isocyanates used for PU synthesis, extracted from [34]

Therefore, the elemental reaction for generating the polyurethane functional group, known as the gelation reaction, can be summarized as:



The characteristic group of polyurethanes is, therefore, $\sim\text{O}-\text{CO}-\text{NH}\sim$ and it represents a urethane bond.

Polyurethane resins are widely used in the form of foams, significantly contributing to the consumption of polyurethane in domestic and industrial applications [36]. Rigid polyurethane foam stands out as one of the most cost-effective insulating materials for new constructions regarding building insulation. Its low thermal conductivity is unmatched by any other conventional product, making it an ideal choice for energy-efficient renovation projects.

Installing insulation in existing buildings can reduce average energy consumption by more than 50%, and the simplicity of installation with rigid polyurethane foam streamlines the process. The foam's low thermal conductivity allows for thinner insulation at any specified level, facilitating its insertion into building cavities.

Despite the modest material thicknesses, its insulation performance remains exceptionally high. Additionally, its good mechanical properties and excellent adhesion to other materials expand its applications in various fields [36].



Figure 14: Insulation thickness of different materials with equivalent thermal resistance, extracted from [37]

Due to its low thermal conductivity (or, conversely, high thermal resistance value), polyurethane insulation effectively insulates buildings with thinner layers compared to other types of insulation. This allows builders to achieve the desired levels of insulation while maximizing internal space or reducing the overall footprint of the structure.

2.1. Polyurethane foams

Plastic foams generally consist of at least two phases, a solid polymer matrix and a gaseous phase derived from a blowing agent [38]. Other solid phases can be present in the foams as fillers, either fibrous or other forms.

Foams can be flexible, rigid, or semi-rigid, depending on whether their glass transition temperature is below or above room temperature, which in turn depends on their chemical composition, degree of crystallinity, and degree of cross-linking [38]. The cell geometry can be open-cell or closed-cell, with the latter generally being rigid and the most suitable for thermal insulation, while open-cell foams are better for car seats, furniture, and acoustic insulation, among other uses, and are generally flexible.

The continuous solid phase provides both structural characteristics and, in closed-cell foams, containment for the gaseous phase. The mechanical properties of polymeric foams are essentially those of the structure and can differ widely from those of the corresponding solid. Other properties, such as thermal conductivity, depend on the composition of the gaseous phase. Plastic foams can be produced in a wide range of densities, from approximately 1.6 kg/m³ to over 960 kg/m³ [38]. The applications of these foams generally determine which range of foam densities should be produced, as the mechanical properties are usually proportional to the foam densities. For thermal insulation, low densities are typically used.

Polyurethane foams, along with polyisocyanurate foams that also involve the use of isocyanates in their production processes, comprise the largest and most versatile family of thermoset rigid polymeric foams. Both types are formed by exothermic chemical reactions between low-viscosity liquid starting materials [38]. Rigid polyurethane foams were first developed in Germany during the early 1940s by Otto Bayer and his associates. The first rigid polyurethane foams were based on TDI and hydroxyl- and carboxyl-terminated polyesters. Foam formation occurred by carbon dioxide formed from the reaction of the isocyanate with carboxyl groups and small amounts of water. Today, most PU foams are based on hydroxyl-terminated branched polyether polyols, and MDI has replaced TDI.

Until recently, the most widely used blowing agent was trichlorofluoromethane (CFC-11) [35]. This substance meets many important requirements: low boiling point, liquid at room temperature, low heat of vaporization, low thermal conductivity, non-flammable, non-toxic, and limited solubility in the PU polymer. However, CFC-11 is a long-lasting artificial compound (52-year atmospheric lifetime) that is not only a powerful ozone-depleting substance but also a potent greenhouse gas with a global warming potential of 5160 over 100 years [39]. Therefore, following the Montreal Protocol, which came into force on January 1, 1989, certain national regulations require the complete ban on the use of CFCs. Partially halogenated hydrocarbons, HCFCs, and HFCs, have been used as blowing agents in some rigid PU foam formulations. However, they have a higher global warming potential compared to other alternatives and are being phased out due to their contribution to climate change. Pentane is an important alternative blowing agent that has already been established in rigid PU foam applications, especially in the appliance and construction sectors [35]. These blowing agents, some of which must be added under pressure in liquid form, are known as physical blowing agents. They vaporize when the pressure is released from the reaction mixture, or due to the exothermic heat of the reaction, and are retained in the closed cells of the foam.

In addition to the physical expansion of the foam, chemical expansion also occurs. Chemical blowing agents, unlike physical ones, release the expansion gas through a chemical reaction. Water in the system will react with the isocyanate to form carbon dioxide and polyurea. With ongoing efforts to reduce the use of CFCs, the water/isocyanate reaction is gaining increasing importance [35].

Type	Boiling Point °C	Molecular Weight	Thermal Conductivity [mW/m · K]**
Air	–	29	24.9/10°C
Carbon Dioxide	– 78.5 (subl.)	44	15.3/10°C
n-Pentane*	+ 36	72	13.5/10°C
cyclo-Pentane*	+ 49	70	10.5/10°C
HCFC 22	– 41	86.5	10.7/10°C
HFC 134a	– 26.5	102	13–14/10°C
HCFC 141b*	+ 32	117	8.9/10°C
HCFC 142b*	– 10	100.5	11–13/10°C
HFC 152a*	– 25	66.1	13–14/10°C
HCF 356	+ 24.6	166	9.5/10°C
CFC 11	+ 24	137.4	7.4/10°C
CFC 12	– 30	120.9	9.4/10°C

* flammable

** manufacturer-data

Figure 15: General data on blowing agents, extracted from [35]

In the formation of rigid polyurethane foams, catalysis also plays an important role. The catalysts used in the synthesis of polyurethane foams help precisely control the relative reaction rates of the isocyanate with both the polyol and water. An imbalance between these reactions can cause foam collapse or the formation of inappropriate cells that may close or open prematurely [41]. There are primarily two types of catalysts used in polyurethane technology: amine catalysts, particularly tertiary amines, and organometallic catalysts, particularly organotin compounds. The catalytic activity of amines depends on both their base strength and the steric availability of the nitrogen electron pair [38]. Amine catalysts generally better catalyze the isocyanate-water reaction than the isocyanate-polyol reaction, while organometallic catalysts, on the other hand, are considered isocyanate-polyol reaction catalysts but also additionally influence the expansion reactions [41]. The catalyst requirements for water-blown rigid foams are quite different, as a balance of catalysts is needed for both the isocyanate-hydroxyl and isocyanate-water reactions. Typically, the requirement can be met through a combination of amine and organotin catalysts [35].

The flowability of the foaming reaction mixture, the cell structure, and the closed-cell content also depend on the choice of surfactant. Polyether-polysiloxanes are the surfactants used in the manufacture of rigid polyurethane foams [35].

Rigid polyurethane foam, like all organic materials, is highly flammable and, without suitable additives, can easily ignite and burn rapidly, releasing toxic gases and smoke. Consequently, for safety reasons, fire retardants are commonly added to inhibit foam ignition and retard the dynamic reactions occurring in a fire. The combustion of a solid organic material is a decomposition process to form gaseous products, followed by the oxidation of the combustible gases with the resulting generation of flame and heat. Thermally stable molecular structures form a solid layer that can also oxidize. Fire retardants direct and catalyze these reactions [38]. The most common fire retardants are phosphorus or halogen compounds. These compounds can be reactive, meaning they have hydroxyl groups that allow the molecule to be incorporated into the urethane polymer, or non-reactive [38]. Reactive, hydroxyl-functional additives include polyethers or polyesters containing halogen or

phosphorus. Halogenated compounds act primarily in the gas phase through halogen radicals or hydrohalogenic acids formed during the early stages of combustion. These radicals inhibit gas-phase chain reactions that generate heat and flame. Phosphorus compounds act primarily in the solid phase to catalyze the formation of a solid layer. Many formulations contain both halogenated and phosphorus compounds [38]. On the other hand, most non-reactive additives are liquids and tend to plasticize the polymers to which they are added. These include alkyl and aryl phosphates, phosphonates, and phosphites.

The widespread use of rigid polyurethane foams as thermal insulation is based on their low thermal conductivity. In the normal density range (30-60 kg/m³), their thermal conductivity is primarily determined by:

- the composition of the cell gas;
- the closed-cell content;
- the size and orientation of the cells [38].

For this reason, the blowing agent used in the production of rigid polyurethane foam is preferably one that has the lowest possible thermal conductivity, low solubility in the polymer matrix along with good solubility in the reaction mixture, and a low tendency to diffuse through cell walls so that properties are maintained in the long term [35]. Additionally, it must allow the formation of closed cells during foaming.

As mentioned earlier, the chosen blowing agent is never present in the cells of the rigid PU foam in pure form, as carbon dioxide is almost always formed from the reaction between MDI and water as an additional blowing agent. This produces a cell gas mixture. The gas content in the foam cells attempts to reach equilibrium with the environment by diffusing air in and the blowing agent and CO₂ out of the cells [38]. Air components easily diffuse into the foam cells, but the diffusion of the blowing agent from the cells is slow. When air diffuses into the foam cells, it increases the total gas content within them, and this increase leads to a rise in pressure inside the cells [38]. After reaching a maximum, higher than atmospheric pressure, it gradually decreases. During this process, the thermal conductivity of the foam, calculated from the partial pressures and the thermal conductivity of the individual gases [35], slowly increases.

It follows that a high content of blowing agent in the formulation has a significant effect on the final value of the thermal conductivity, and as explained above, an increase in thermal conductivity over time is of great importance in thermal technology [35].

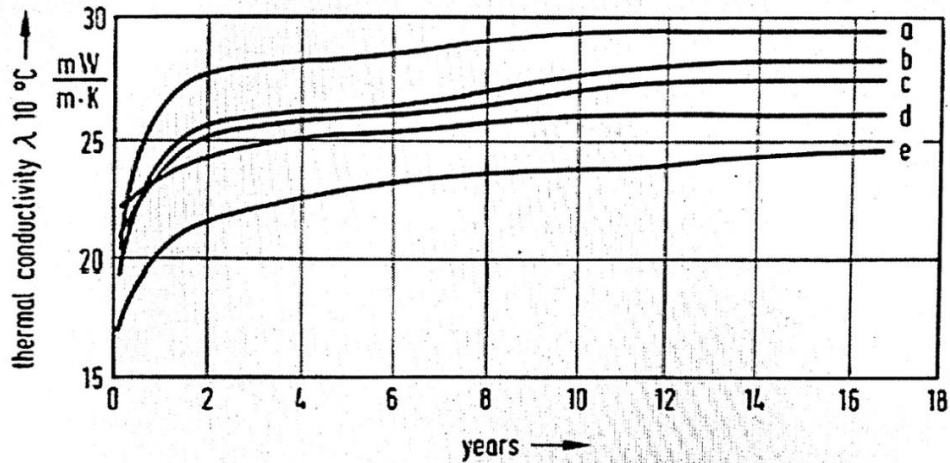


Figure 16: Change in thermal conductivity over time at an average temperature of 10°C for rigid PU foam panels blown with R11, produced by different methods (a, b, c, d, e), extracted from [35]

Additionally, the density of rigid polyurethane foam also affects thermal conductivity. As density increases, the thermal conductivity of the cell walls increases. However, this increase is not directly proportional to the density increase. Nonetheless, within the density range of 30-60 kg/m³, even with more polymer incorporated into the struts and joints, the thermal conductivity barely changes [35].

Regarding temperature, the thermal conductivity of the cell gas (and thus the foam) increases almost linearly as the temperature rises. For example, a 10°C temperature increase between 0°C and 90°C increases the thermal conductivity by approximately 0.001 W/(m·K).

In summary, the thermal conductivity of polyurethane foam is affected by:

- Blowing agent content;
- Foam density;
- Temperature;

CHAPTER 3: LIGNIN-BASED RIGID POLYURETHANE FOAM THERMAL INSULATION PANELS

Polyurethane raises environmental and human health concerns at various points throughout its life cycle. Like other plastics, it is made from fossil fuels derivatives, and its production emits greenhouse gases. It is estimated that the annual GHG emissions from polyurethane production in the United States are 7.8 million metric tons [43].

In Europe, the REACH regulation plays a crucial role in this regard. To enhance the safety and sustainability of polyurethane, biomass-based production pathways and recycling technologies are being developed to increase the amount of renewable raw materials and secondary materials in the polyurethane supply chain [43].

Furthermore, in the context of sustainable development, the use of bio-based materials aligns with the definition of sustainable development provided by the Brundtland Commission, which emphasizes meeting the needs of the present without compromising the ability of future generations to meet their own needs [42]. By using renewable raw materials and reducing the environmental footprint, bio-based polyurethane foams contribute to a more sustainable and resilient future, while addressing several Sustainable Development Goals (SDGs) outlined by the United Nations:

- SDG 7 on Affordable and Clean Energy is supported by the transition to cleaner and more sustainable energy sources by reducing dependence on fossil fuels in insulation applications.
- SDG 9 on Industry, Innovation, and Infrastructure is promoted through the development and adoption of bio-based materials, which encourage sustainable and innovative industrial practices.
- SDG 11 on Sustainable Cities and Communities benefits from better thermal insulation in buildings, achieved through the use of rigid polyurethane foam, contributing to energy efficiency and sustainable urban development.
- SDG 12 on Responsible Consumption and Production is promoted by using renewable raw materials in the production of bio-based foam, encouraging sustainable consumption and production patterns by reducing resource depletion and environmental degradation.
- SDG 13 on Climate Action is also addressed by bio-based polyurethane foam, which helps mitigate climate change by reducing greenhouse gas emissions associated with the production and use of petroleum-based materials.



Figure 17: Sustainable Development Goals related to bio-based polyurethane foams

A vast amount of research has been dedicated to finding bio-based substitutes for traditionally petroleum-derived polyols, especially. Alternative polyols are often developed from various vegetable oils, whose typical structure does not contain the functional groups (epoxy, amine, thiol, hydroxyl)

necessary to react with isocyanate. Most vegetable oils consist of a main structure of glycerol and a chain of oleic, linoleic, and linolenic acids.

To generate hydroxyl groups, these oils must first undergo an epoxidation reaction followed by the opening of the epoxy ring. While this modification has been shown to be successful in many cases, it will not always yield the same results for each type of vegetable oil.

Castor oil is an exception to this rule, as it already contains the functional groups necessary to react with isocyanates without modification [45]. Complicated by the fact that each vegetable oil has different chemical structures to begin with, the type of oil used has a significant impact on the reaction with the isocyanate and the overall foam structure.

While partially bio-based polyurethanes substitute petrochemical polyols, they do not replace isocyanates. Therefore, although partially bio-based PUs synthesized with vegetable oil polyols are the most common and developed form of bio-based PUs, other chemical approaches have been investigated. In recent years, significant research has been dedicated to developing PUs that do not require the use of isocyanates (Non-Isocyanate Polyurethanes, NIPU) [45]. NIPUs offer advantages such as reducing environmental and health concerns associated with isocyanates, as well as improved sustainability by replacing both polyols and isocyanates with bio-based materials. However, their development is still at early stages, and for this reason they won't be the primary focus of the present work.

In this work, the focus will primarily be on lignin, as potential raw material for implementation in polymeric applications. Many lab-scale processes have demonstrated the ability of lignin to partially replace fossil-based polyols in rigid polyurethane foam formulation.

3.1 Lignin as a renewable raw material for biopolyols

Lignin is an organic substance that binds the cells, fibers, and vessels that constitute wood and the lignified elements of plants, such as straw. After cellulose, it is the most abundant renewable carbon source on Earth [46]. Large amounts of lignin are available in pulp mills and paper mills or cellulosic ethanol plants. During the pulping process, lignin is separated from cellulose fibers and considered a byproduct. In cellulosic ethanol production, lignocellulosic biomass is processed to extract sugars, mainly glucose, which are then fermented into ethanol. Lignin is separated from the cellulose and hemicellulose components of the biomass during this process. It is estimated that the pulp and paper industry generated 50 million tons of lignin in 2010, and despite its abundant availability compared to fossil fuels, a significant portion remains underutilized, often used as a low-value fuel in recovery boilers in pulp mills for heat and power generation. However, only about 2% (1 million tons) of this lignin was marketed for other higher value-added industrial applications.

Recently, lignin has gained increasing attention for its potential uses, either directly or after chemical modification, as a renewable raw material for chemicals such as biopolyols in the preparation of polyurethane foams [47].

It is not possible to define the precise structure of lignin as a chemical molecule. All lignins show some variation in their chemical composition. However, the common definition for all is a network dendritic polymer of basic phenylpropane units, which include derivatives of phenylpropanol.

Commercially available lignins comprise two categories:

- Sulfur-free lignins, obtained mainly from biomass conversion technologies focused on biofuel production, organosolv pulping processes, and soda pulping based on alternative resources such as agricultural residues and non-lignocellulosic fibers;
- Sulfur-containing lignins, resulting mainly from Kraft and sulfite pulping processes. This latter category comprises nearly the entire market for commercially available lignins [48].

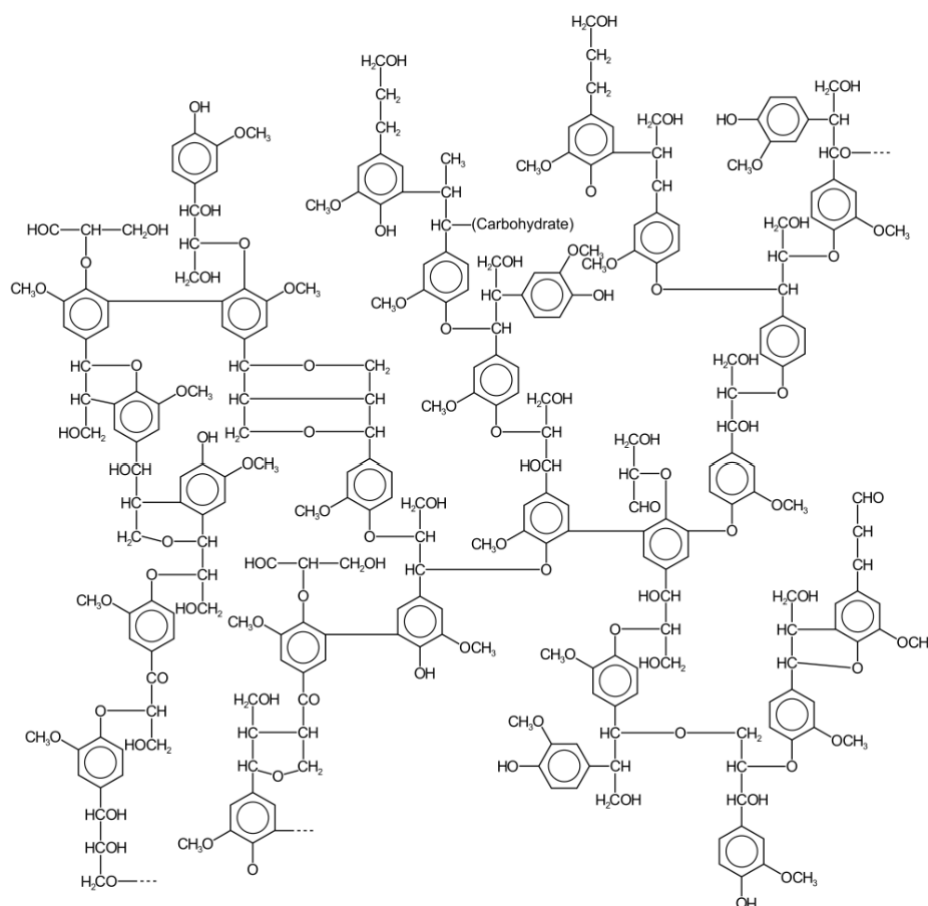


Figure 18: Examples of typical structures in the chemical formula of lignin, extracted from [46]

3.2 Rigid polyurethane foam partially bio-based with lignin

Bio-based polyurethanes are predominantly synthesized using bio-based polyols in combination with petroleum-derived isocyanates. Replacing petroleum-derived isocyanates is challenging due to their availability and reactivity. This specific case falls within the scope of second-generation biorefinery. The biorefinery is a general concept of a promising plant where biomass raw materials are converted and extracted into a spectrum of valuable products [49]. In particular, second-generation biorefineries involve the valorization of waste, which is no longer seen as a problem to be disposed of but as a resource to be used to obtain high value-added products. A second-generation biorefinery, therefore, involves optimizing waste management, valorizing it, and not using land (it does not involve the use of dedicated biomass). In the case of synthesizing polyols from lignin, a non-food renewable raw material, normally considered a waste, is being used to produce a valuable chemical product, thereby contributing

to reducing dependence on fossil and food resources and increasing the overall sustainability of the process.

There are two ways to incorporate lignin-based bio-polyols into rigid polyurethane foam formulations:

- Direct use of lignin without any preliminary chemical modification, alone or in combination with other polyols.
- Use after chemical modification to make the hydroxyl functions more readily available.

3.2.1 Bio-based rigid polyurethane foam using lignin by direct replacement

Numerous studies have examined the integration of lignin directly into polyurethane (PU) formulations by leveraging both aliphatic and aromatic hydroxyl ($-OH$) groups in lignin's structure [47]. However, using crude lignin presents significant challenges, primarily due to its low solubility in the polyol system, which limits the extent of petroleum polyol replacement. Typically, crude lignin achieves only low bio-based replacement ratios in PU foams, thus limiting its potential as a full substitute for petroleum-based polyols.

Ideally, lignin could be incorporated directly from the delignification process without further modification. However, the limited reactivity of lignin's hydroxyl groups often impedes this, as they typically lack the necessary compatibility with isocyanates. As a result, structural modifications are frequently employed to enhance lignin's compatibility. Importantly, such modifications need to be both economically and ecologically feasible to support broader commercial application [76].

Despite these hurdles, directly adding lignin to polyol systems remains the most commercially viable approach for producing lignin-based PU foams. Studies have shown that substituting 20–30 wt.% of the polyol component with lignin can result in foams with suitable properties for rigid thermal insulation. However, in these formulations, the total bio-based content generally remains below 10 wt.%, underscoring the need for further advancements in lignin incorporation. To address this, techniques such as chemical modification and lignin depolymerization have been investigated, showing promise for increasing lignin content in PU foams while maintaining required performance standards [51].

To inform this process, research by Henry et al. was particularly relevant [77]. Henry and colleagues synthesized nineteen rigid polyurethane foams using unmodified lignins from various sources to replace 30 wt.% of fossil-based polyols. The 30% substitution level was chosen based on previous literature, which showed a decline in foam properties when unmodified lignin exceeded this concentration. Unlike the commercial polyol, all lignins used were solid, with no solvents involved in their preparation. When lignin is chemically modified, solvents such as acetone are typically used, especially if the modified lignin is in powder form. However, Henry et al. avoided solvents, observing decreased reactivity relative to commercial polyols, which slowed foam reaction times. This slower reactivity was attributed to steric hindrance from lignin hydroxyl groups and the resulting increase in polyol blend viscosity, which reduces material mobility within the solution.

Nonetheless, lignin-based foams passed all ASTM International C1029-15 standards required for Type 1 rigid insulation foams, with only three exceptions. In the context of this work, rigid PU foams incorporating unmodified softwood kraft lignin are of particular interest. Henry et al.'s findings thus provide a foundational reference for the direct, unmodified implementation of lignin in rigid PU foam formulations. The life cycle inventory of this specific process is presented in the dedicated section and considers a 30wt.% substitution of fossil polyols with crude lignin.

3.2.2 Bio-based rigid polyurethane foam using chemically modified lignin

The depolymerization of lignin is a viable route to unlock its potential and can be carried out by various methods, all sharing the primary goal of producing depolymerized lignin with high yield and a high number of hydroxyl groups/functionality with low molecular weights. This process breaks down the lignin polymer into smaller fragments, increasing the surface area and exposing more functional groups, including hydroxyl groups (-OH) [47].

The high functionality and low molecular weights of the depolymerized products make them suitable for the preparation of rigid PU foams with a higher percentage of bio-based content ($\geq 50\%$) [49]. However, lignin depolymerization is challenging due to the wide distribution of bonding forces in the various C-O and C-C bonds in lignin and the tendency of low-molecular-weight intermediates to undergo recondensation/repolymerization, often into more recalcitrant species [50].

To date, multiple strategies have emerged for lignin depolymerization, including thermochemical treatments, homogeneous and heterogeneous catalysis, and biological depolymerization. In [47], Kraft lignin was successfully depolymerized hydrolytically using only water as a solvent in an alkaline medium (NaOH). The obtained depolymerized KL (DKL) (yield of 77%) was in solid or powder form, soluble in organic solvents, and DKL had acceptable characteristics for use as biopolyols for PU synthesis.

Although no waste streams were generated during this depolymerization process, it can be challenging for industrial applications due to the severity of the reaction conditions (250-300 °C and pressures of 5-10 MPa) [50]. What's more, if a polyol (such as DKL) is in solid powder form, it is crucial to convert it into a liquid form for the preparation of bio-based rigid polyurethane foams. This conversion can be achieved either by oxypropylation or by dissolving DKL in an organic solvent (such as acetone) before adding it to the reaction mixture for foam formation [47]. These processes are studied in detail in the following chapters, where scale-ups from laboratory to industrial setting are proposed.

3.3 Comparative analysis of thermal insulation properties between bio-based and fossil-based rigid polyurethane foams

To ensure that lignin-based rigid polyurethane foams are suitable for use as insulation materials, their physical, mechanical, and chemical properties must match those of fossil-based rigid polyurethane foams as closely as possible. These properties will be compared in this section. The focus is set on the four scenarios presented in the introduction.

The main properties of polyurethane obtained through the traditional route were found using the Ansys Granta EduPack[®] software, version 2023 R2.



GRANTA EDUPACK

Figure 19: Ansys Granta EduPack logo

Granta EduPack supports materials education by providing a comprehensive database of material and process information, material selection tools, and various supporting resources. The software is divided into three levels, allowing users to access the appropriate level of information as they progress in their studies.

The 'Level 3: Polymers' database was selected to locate the rigid polyurethane foam material. Within the program, the polyurethane material was found in the MaterialUniverse, as shown in Figure 20.

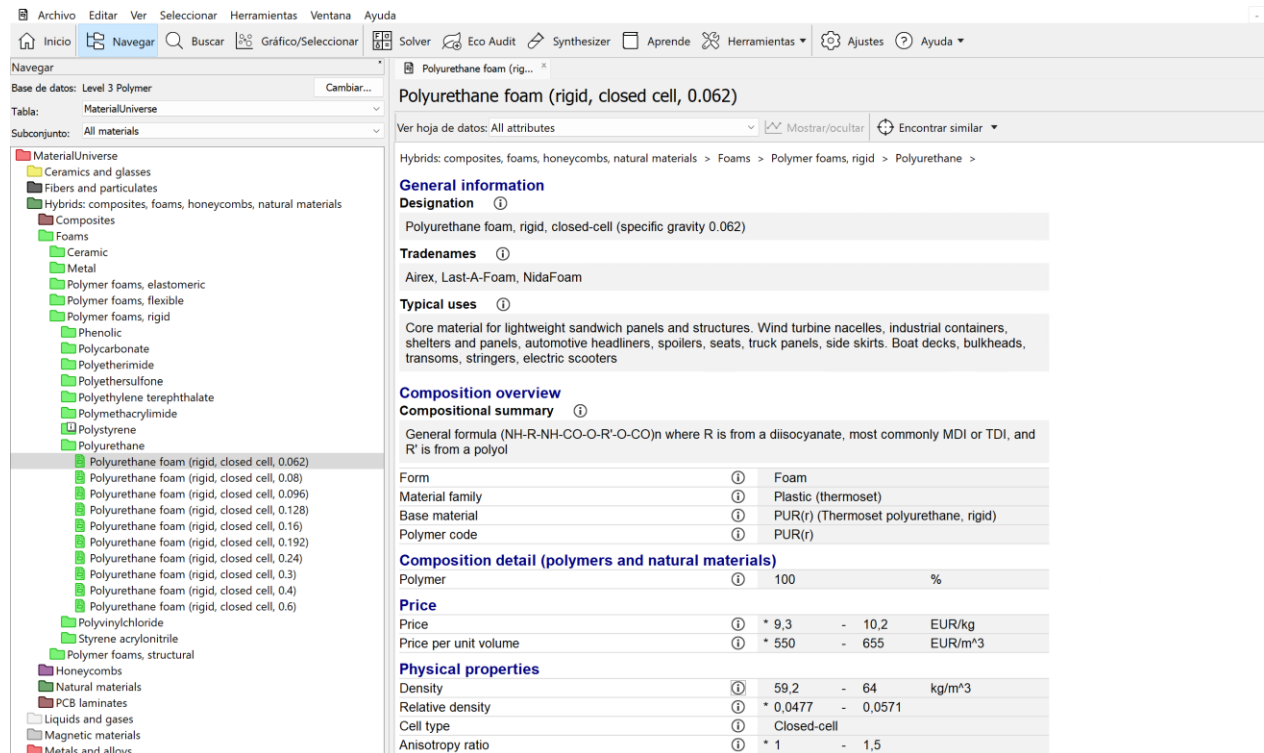


Figure 20: Search for rigid polyurethane foam in Ansys Granta EduPack

As can be seen, the software provides a variety of rigid polyurethane foams with different relative densities. The one with the lowest relative density (and therefore the lowest density) was selected as it effectively represents the most common density range of polyurethane foams for insulation applications.

The following properties were considered, although not all are available for bio-based rigid polyurethane foams in the literature:

- Physical properties: density;
- Absorption and Permeability: water absorption (24h) (A_w);
- Mechanical properties; compressive strength (σ_c) and compressive modulus (E_c);
- Thermal properties: thermal conductivity, specific heat capacity, maximum service temperature and minimum service temperature;

The properties of rigid polyurethane foam based on depolymerized Kraft lignin and oxypropylated depolymerized Kraft lignin are derived from the characterization performed by Mahmood et al. in [47], whereas the ones of untransformed Kraft lignin are taken from the study of Henry et al. [84]. All properties are summarized in the following table, where PUR refers to fossil-based rigid polyurethane foam, KL PUR to rigid polyurethane foam based on untransformed Kraft lignin, DKL PUR to rigid polyurethane foam based on depolymerized kraft lignin, and OxyDKL PUR to rigid polyurethane foam based on oxypropylated depolymerized kraft lignin.

Table 1: physical, mechanical and thermal properties of different rigid polyurethane foams

	ρ [kg/m ³]	A_w [wt.%]	σ_c [MPa]	E_c [MPa]	k [W/(m·°C)]	c_p [J/(kg·°C)]	T_{max} [°C]	T_{min} [°C]
PUR	59.2 – 64	0.15 – 0.19	0.38 – 0.42	5.83 – 8.23	0.0276 – 0.0305	$1.47 \cdot 10^3$ – $1.63 \cdot 10^3$	135 – 177	-205 – -185
KL PUR	46 ± 1	-	$0.170 \pm$ 0.01	-	0.009	-	-	-
DKL PUR	$104.3 \pm$ 1	$4.3 \pm$ 0.5	$0.506 \pm$ 0.07	$5.152 \pm$ 0.08	$0.032 \pm$ 0.001	-	200	-
OxyDKL PUR	55.3 ± 1	$11.8 \pm$ 0,5	$0.578 \pm$ 0.035	10.986 ± 0.055	$0.029 \pm$ 0.001	-	200	-

These values are also consistent with those reported in [36]. Pinto et al. [72] obtained slightly higher values for both density and thermal conductivity for OxyDKL PUR, although the reaction was carried out under different operating conditions compared to the work of Mahmood et al.

As shown in the table, the density of traditional PUR is in the range of 59.2 - 64 kg/m³. However, the DKL PUR foam prepared by directly replacing 50% by weight of fossil-based polyols with DKL has a higher density of 104.3(±1) kg/m³. A possible reason for this significantly increased foam density is the relatively lower reactivity of DKL, which causes a slower gelation reaction rate. A slower gelation reaction rate leads to greater gas release from the foam structure and thus smaller void volumes and higher foam densities. Varying the additional amount of physical blowing agent may be a method to adjust the density value of this foam. Interestingly, the density of polyurethane foam prepared with OxyDKL (55.3 kg/m³) is very similar to that of traditional foams. This result is likely due to the OxyDKL having a molecular structure similar to and thus reactivity similar to that of the reference polyols. KL PUR has a very low density, but the value actually refers to an apparent density, reported by Henry et al.

Water absorption after 24 hours of exposure to water at room temperature was 4.3% by weight when replacing the fossil-based polyols with 50% by weight DKL. The polyurethane foam prepared from oxypropylated DKL absorbed 11.8% by weight of water. Therefore, traditional rigid polyurethane foam remains superior, with much lower water absorption.

Interestingly, Mahmood et al. found that PUR foam prepared with OxyDKL exhibits remarkable mechanical properties, with a compressive modulus of 10.986 MPa and a strength of 0.578 MPa at 20% deformation. These mechanical properties surpass those of all other foams studied, including the fossil-based one. The superior performance of the PUR foam based on OxyDKL can be attributed to the oxypropylation, which converted all phenolic OH groups to aliphatic OH groups, resulting in a highly branched and functionalized polyol.

Regarding thermal properties, all rigid polyurethane foams obtained by Mahmood et al. are stable up to approximately 200°C. Additionally, the thermal conductivities are very similar to those of fossil-based foam, meaning they have comparable insulating properties. Thermal conductivities between 0.02 and 0.03 W/(m·°C) for foams with densities ranging from 30 to 100 kg/m³ are the most common in construction polyurethane foams [73]. The rigid polyurethane foam based on depolymerized lignin has slightly higher density and thermal conductivity, but the properties of the oxypropylated foam fall within these ranges. Thermal conductivity of KL PUR is strangely small, compared to the others. Since these foams were characterized in lab by different groups, with different methods, it's understandable that some values might differ more than expected. This table should just serve as an example of average properties values that can be met by these particular polyurethane foams, rather than exact values.

In conclusion, the good mechanical properties, comparable densities with fossil-based rigid polyurethane foam, and especially the low thermal conductivities show that lignin-based foams are suitable for insulation applications.

CHAPTER 4: SCALE-UP OF LAB-SCALE KRAFT LIGNIN CHEMICAL MODIFICATION PROCESSES

4.1 Hydrolytic depolymerization of Kraft lignin catalyzed by NaOH

The laboratory-scale process conducted by Mahmood et al. [47] served as a reference for modeling a hydrolytic depolymerization plant at a larger scale. They successfully synthesized depolymerized Kraft lignin (DKL) at the laboratory scale by loading a reactor with 25 g of Kraft lignin (KL), 70 g of NaOH (in a 10 wt.% solution in distilled water), and 148 g of distilled water. The reactor was sealed, evacuated, and purged three times with nitrogen to ensure the complete removal of residual air. It was then heated to 250°C with fixed stirring and allowed to react for 2 hours after reaching the required temperature.

At the end of the reaction, the reactor was immediately quenched in an ice-water bath. The gases inside the reactor were vented into a fume hood, and the reactor contents were washed into a beaker using distilled water. The pH of the mixture was adjusted to 2.0 using 1 M sulfuric acid to precipitate the DKL products. The acidified mixture was then filtered, and the solid cake left after filtration was dissolved in acetone. The solid residues (SRs) that remained on the filter paper were separated and dried in an oven at 105°C for 24 hours.

The DKL in the acetone solution was recovered by rotary evaporation at 40–65°C under reduced pressure. The yield of DKL was determined to be 77 wt.% based on the dry weight of KL used in each run. Without additional comments on the pH under these conditions, a value of 10 was assumed. This DKL was then dissolved back in acetone, which is essential for a polyol to be in liquid form for the preparation of rigid polyurethane foams. It was used to directly replace 50% by weight of fossil-based polyols.

For the purposes of this thesis, this process was extensively reimaged to facilitate its implementation at a larger scale, ensuring a fair comparison with standard rigid polyurethane foam synthesis methods. The reaction conditions and yield were considered with the findings of Mahmood et al., that is 2 MPa of pressure and 250°C for the reaction and a 77wt.% yield.

A process flow diagram was drawn with the Microsoft Visio® software to better visualize the new process.

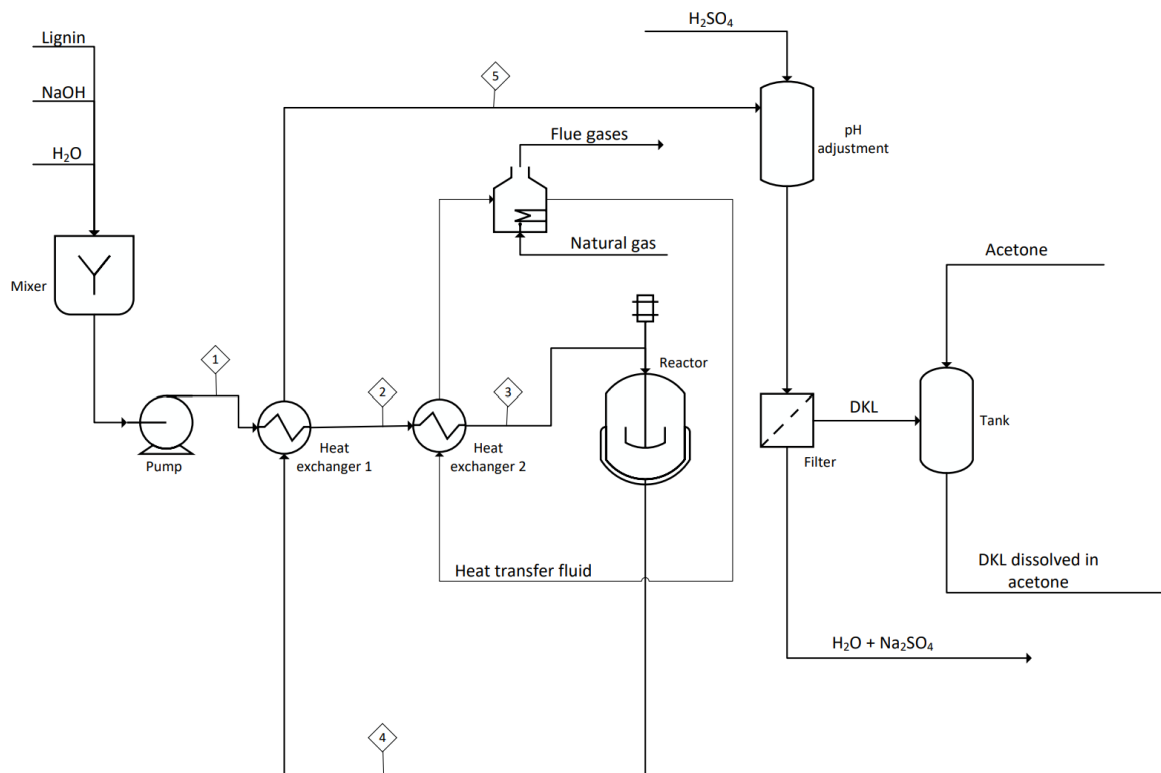


Figure 21: Process flow diagram of the hydrolytic depolymerization of lignin

Below, a list of the enumerated flows is reported, showing the main operating parameters.

Table 2: Main operating parameters of the scaled-up hydrolytic depolymerization process flows

Main operating parameters				
Flow ID	Description	Composition or Material	T [°C]	P [bar]
1	First heat exchanger inlet	Lignin, NaOH, water	25	20
2	Second heat exchanger inlet	Lignin, NaOH, water	220	20
3	Reactor inlet	Lignin, NaOH, water	250	20
4	Reactor output	Depolymerized Lignin (DKL), NaOH, water	250	20
5	Product stream (requiring purification)	Depolymerized Lignin (DKL), NaOH, water	53	20

Just like Mahmood et al.'s process, kraft lignin, a 10wt.% NaOH solution and distilled water are mixed. Then, the process has been largely reimaged, to introduce heat recovery and get rid of typical lab-scale procedures. The mixed flow of kraft lignin, NaOH solution and water is pumped, to increase the pressure to 2MPa, and then is sent to a first heat exchanger, where its temperature rises from room temperature to 220°C. The scaled-up process is designed with a two-stage heating phase, so that after the first heat exchanger the stream flows through a second one, depicted as a furnace in the PFD. This step is the focus of sensitivity analyses in the life cycle assessment of the process, where different energy sources are considered for this second stage. In the PFD, the standard case where natural gas is employed is shown. The second heat exchanger – or furnace – is followed by the reactor, which is imagined to be continuously mixed and heated, in order to be able to provide the energy needed to sustain the endothermic depolymerization reaction. The hydrolytic depolymerization of lignin is known to be an endothermic process, meaning it absorbs heat during the reaction, which requires continuous energy input [70], [78], [79]. Given the complexity of the lignin molecule, and the variety of

depolymerization processes in use, there's a lack of data regarding the reaction enthalpy of lignin depolymerization. This energy needs to be provided by the reactor, in order to sustain the reaction, but its estimation proved to be a real challenge. In an article published by Watkins et al. [80], thermal stability studies on lignin extracted from various fibers, such as pine straw and flax fiber, were carried out through differential scanning calorimetry and the heat of reactions of bond-breaking processes of these lignins were determined. The average of these values was therefore taken as reference value for the energy required. Further comments and considerations on this aspect are to be found in the section dedicated to the life cycle inventories.

In the lab-scale version of the process, Mahmood et al. performed quenching to avoid over-depolymerization at the reactor outlet, which can occur due to the high temperature. Quenching could technically be performed in the scaled-up version too, to bring the reactor outlet from 250°C to 200°C for example. This would allow to partially solve the over-depolymerization problem, but less thermal energy will be available for heat recovery. To enhance heat recovery, quenching can occur inside the heat exchanger for heat recovery, if designed appropriately to do so. This way, the reactor outlet can provide the thermal energy needed to the inlet, to heat it up to 220°C, and cools down to approximately 53°C while doing so. The following steps resemble the ones described in the lab-process, with a pH adjustment with sulphuric acid to precipitate lignin, a filter to collect it and a tank, where acetone can be added to dissolve the powder-form depolymerized lignin. The drying step and the acetone evaporation, performed by Mahmood et al., are here eliminated as such processes are not needed at larger scale. What's more, the product being depolymerized lignin dissolved in acetone is ideal, since depolymerized lignin is normally in powder, solid form and needs to be dissolved in a solvent when added to fossil-based polyols and MDI in the rigid polyurethane foam reacting mixture.

4.2 Oxypropylation of depolymerized Kraft lignin

Oxypropylation is the third, and final process considered. To further improve lignin's reactivity, oxypropylation can occur with already depolymerized lignin, and therefore is seen as a next step of depolymerization. The work performed by Mahmood et al. at lab-scale [47] is again looked upon as the reference for the scale-up here carried out. Mahmood et al. executed oxypropylation in a 100 mL Parr autoclave reactor. In a typical run, 18.9 g of DKL, 21.21 g of propylene oxide (PO), 2.31 g of glycerol and KOH mixture with 16.8 g of acetone were loaded to the reactor, which was sealed under atmospheric pressure (1 atm-g), and heated up to 150°C. Complete consumption of PO by the oxypropylation reactions was observed. After cooling, the oxypropylated depolymerized Kraft lignin (OxyDKL) in the reactor was washed out using acetone and vacuum filtrated. The filtrate was evaporated on a rotary evaporation under reduced pressure to completely remove all acetone and any unused PO if any. The weight of the oxypropylated product was approximately equal to the total weights of DKL, PO and glycerol, implying a complete consumption of the reactants.

Just like with the hydrolytic depolymerization process, oxypropylation was scaled-up to better visualize it at larger scale, making it more adequate for a fair comparison with the fossil-based synthesis of rigid polyurethane foam. Mahmood et al.'s lab-scale work gave the basic theoretical principles, such as conversion of the reactants and reaction conditions. However, pressure was changed to 11.5 bar in the scaled-up version of the process. A process flow diagram, drawn with the Microsoft Visio[®] software, is shown in Figure 2.

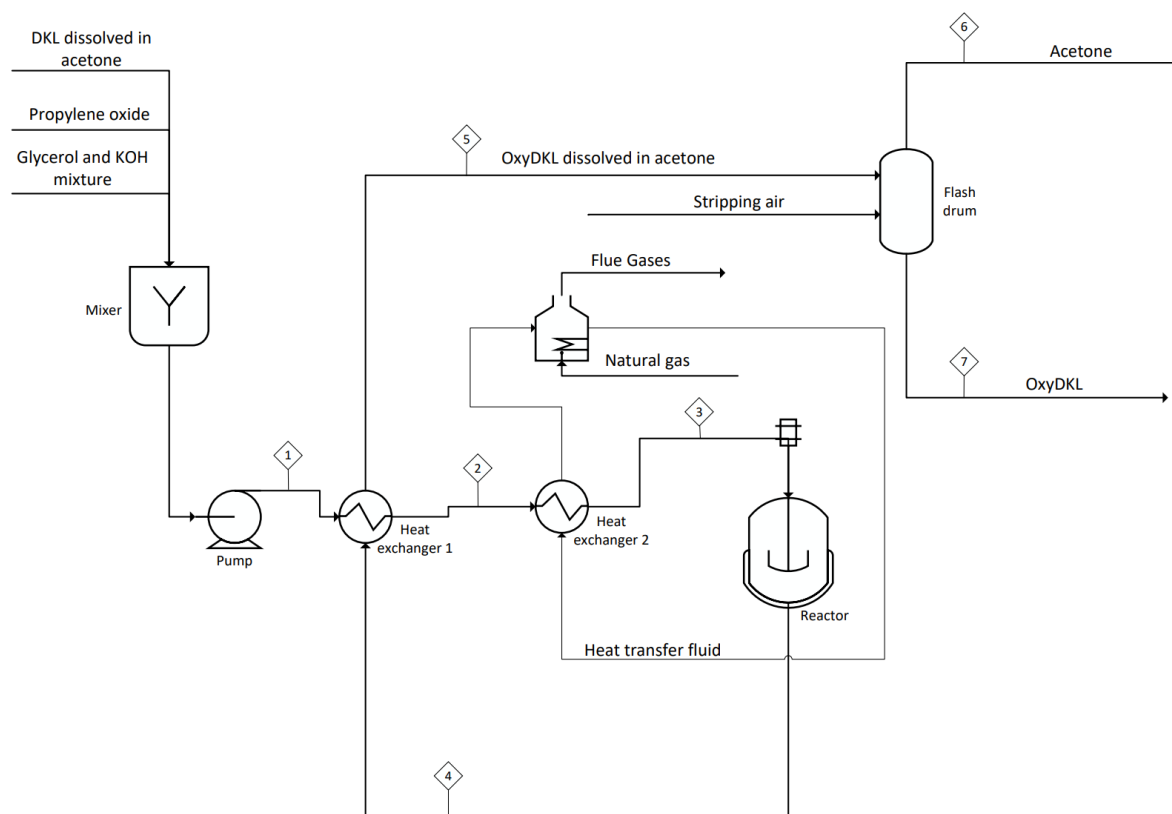


Figure 22: Process flow diagram of the oxypropylation of depolymerized lignin

Below, a list of the enumerated flows is reported, showing the main operating parameters.

Table 3: Main operating parameters of the scaled-up oxypropylation process flows

Main operating parameters				
Flow ID	Description	Composition or Material	T [°C]	P [bar]
1	First heat exchanger inlet	DKL in acetone, PO, glycerol-KOH mixture	25	11.5
2	Second heat exchanger inlet	DKL in acetone, PO, glycerol-KOH mixture	120	11.5
3	Reactor inlet	DKL in acetone, PO, glycerol-KOH mixture	150	11.5
4	Reactor output	OxyDKL in acetone	150	11.5
5	Product stream (requiring purification)	OxyDKL in acetone	42.5	11.5
6	Recovered solvent	Acetone	-	1
7	Final product stream	DKL	-	1

In the scale-up, DKL dissolved in acetone (i.e. the final product stream of hydrolytic depolymerization) is mixed with PO and the glycerol-KOH mixture. Hence, no other acetone is added. Unlike Mahmood et al's process, this stream is then pumped to 11.5 bar. This is because acetone has a boiling point of 56°C at atmospheric pressure, so at the reaction temperature of 150°C, it would evaporate in the reactor, potentially increasing pressure and affecting the reaction. To avoid this issue, the process is conducted at a higher pressure, specifically 11.5 bar, which keeps acetone in the liquid phase throughout, from heating to reaction. This simplifies the process by maintaining a single phase.

Just like the hydrolytic depolymerization process, heating of the reactants is presented in two stages, the first one bringing the stream from room temperature to 120°C, and the second from 120°C to 150°C. Again, the second heating step is shown as powered by burning of natural gas in the PFD, but different options will later be assessed in the life cycle assessment. The reactor output, that is stream 4 consisting of OxyDKL in acetone (which will not have evaporated at this point), is at a temperature of 150°C and holds enough thermal energy to heat up the reactants to 120°C in the first heating step. While doing so it cools down 42.5°C. The oxypropylation reaction is found to be slightly exothermic, with the heat of reaction not available in literature and an estimation being calculated in the section dedicated to the life cycle inventories. In any case, the system is considered to be isothermal, with the reactor output still at 150°C.

Stream 5 consists of OxyDKL dissolved in acetone at 42.5°C and 11.5 bar. At this stage, it's possible to recover the solvent, as OxyDKL remains in liquid phase at other conditions, such as room temperature and atmospheric pressure. Unlike DKL, which is typically in powder form and must be dissolved in acetone before being combined with fossil-based polyols and MDI in rigid polyurethane foam formulation, OxyDKL is already in liquid form. This allows for the recovery of acetone, which can then be reused in the hydrolytic depolymerization process, reducing the need for fresh solvent.

This stage of the scaled-up process was simulated in Aspen Plus® to evaluate solvent recovery. In the software, stream 5 from Figure 2 was modeled, using 2-Methoxy-4-propylphenol to represent OxyDKL, and a flash separation of OxyDKL and acetone was examined. The goal was to evaporate most of the acetone into the vapor-phase outlet while keeping OxyDKL in the liquid phase. The flash unit was set as adiabatic with a pressure of 1 bar. While lower pressures could improve separation, working under vacuum is energy-intensive, so it was preferable to avoid dropping below 1 bar. At 42.5°C and atmospheric pressure, acetone remains in the liquid phase due to its vapor pressure being approximately 0.62 bar. Typically, when a substance's ambient pressure is above its vapor pressure at a certain temperature, it remains in the liquid phase. Thus, the options were to operate below 0.62 bar (which was deemed too energy-intensive), to increase the inlet temperature of the OxyDKL-acetone stream to raise acetone's vapor pressure, or to use air as a stripping agent to facilitate separation. The third option was chosen, using air to strip and carry acetone out of the liquid phase. With air at room temperature and 11.5 bar, 96wt.% of acetone is successfully recovered in the vapor phase outlet of the column.

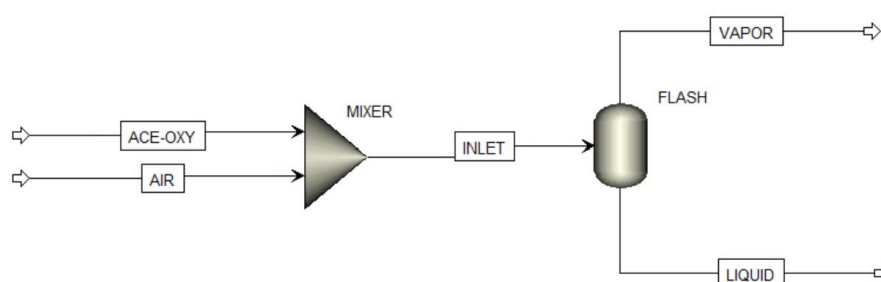


Figure 23: Process flow diagram of the acetone and OxyDKL separation in Aspen Plus®

CHAPTER 5: LIFE CYCLE ASSESSMENT (LCA)

In this work, a comparative Life Cycle Assessment (LCA) is conducted to evaluate the environmental burdens of rigid polyurethane foam production using the SimaPro[®] software. Four different formulations are compared: traditional rigid polyurethane foam insulation panel, partially bio-based rigid polyurethane foam insulation panel obtained by replacing 30% by weight of the polyols with untransformed Kraft lignin, partially bio-based rigid polyurethane foam insulation panel obtained by replacing 50% by weight of the polyols with hydrolytically depolymerized Kraft lignin, and rigid polyurethane foam insulation panel obtained by replacing 100% by weight of the polyols with oxypropylated depolymerized Kraft lignin.

An LCA is defined as a process for assessing the effects a product has on the environment throughout its entire lifecycle, thus increasing resource use efficiency and decreasing liabilities [52].

Before the term "Life Cycle Assessment" was coined, there were several methods and approaches to evaluate the environmental impacts of products and processes. However, these methods lacked standardization, consistency, and transparency, making it difficult to compare results between studies or ensure their reliability. The Society of Environmental Toxicology and Chemistry (SETAC) recognized the need for a standardized approach to LCA and initiated efforts to develop guidelines and frameworks for conducting LCAs. The LCA methodology we rely on today has been extensively shaped and refined by SETAC's leadership and commitment to advancing environmental science and sustainability practices [53].

However, LCA alone cannot be used as the sole decision-support tool in environmental management. To demonstrate complete sustainability, it must be combined with economic and social studies (Life Cycle Costing and Social Life Cycle Assessment). Therefore, in this work, LCA is used as a tool to quantify the impact of the analyzed alternatives, highlight bottlenecks, and set priorities for interventions.

The life cycle assessment framework is described by four phases, also illustrated in Figure 21:

- Definition of goal and scope
- Inventory analysis
- Impact assessment
- Interpretation

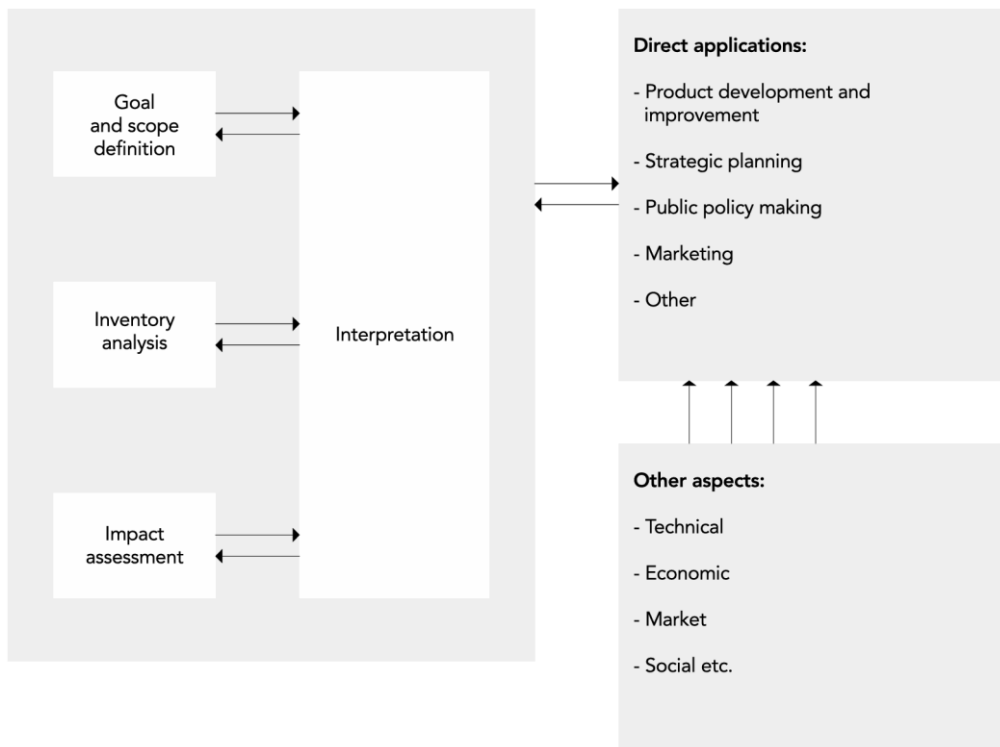


Figure 24: Life Cycle Assessment Framework - Phases of an LCA (ISO, 1997a)

Each phase will be specifically addressed in relation to the particular problem of rigid polyurethane foam insulation panels, starting with an explanation of the Functional Unit chosen in the Goal and Scope, and continuing sequentially through each subsequent phase. First, a brief overview of SimaPro® is presented.

5.1. SimaPro®: software overview

As previously mentioned, the Life Cycle Assessment was carried out using SimaPro® software, version 9.6.0.1. Created in 1990, SimaPro® is now one of the leading LCA programs, trusted by companies, consultancies, and universities in over 80 countries. It is a widely used software tool for conducting LCA studies, providing a comprehensive platform for analyzing the environmental impacts of products and processes throughout their entire life cycle—from raw material extraction to production, use, and final disposal. SimaPro® allows for the modeling of complex systems, data input, and calculations to quantify environmental impacts such as greenhouse gas emissions, energy consumption, water use, and more. It offers a wide range of impact assessment methods and enables the generation of reports and visualizations to effectively communicate LCA results.



Figure 25: SimaPro® text logo

SimaPro® includes a number of life cycle inventory databases, called “libraries” in the software. The available libraries in the 9.6.0.1 version that was used are as follows:

Selección	Nombre	Protección
<input checked="" type="checkbox"/>	Agri-footprint - economic - system	
<input type="checkbox"/>	Agri-footprint - economic - unit	
<input checked="" type="checkbox"/>	Ecoinvent 3 - allocation at point of substitution - system	
<input type="checkbox"/>	Ecoinvent 3 - allocation at point of substitution - unit	
<input checked="" type="checkbox"/>	Ecoinvent 3 - allocation, cut-off by classification - system	
<input type="checkbox"/>	Ecoinvent 3 - allocation, cut-off by classification - unit	
<input checked="" type="checkbox"/>	Ecoinvent 3 - consequential - system	
<input type="checkbox"/>	Ecoinvent 3 - consequential - unit	
<input checked="" type="checkbox"/>	EU & DK Input Output Database	
<input checked="" type="checkbox"/>	Industry data 2.0	
<input checked="" type="checkbox"/>	Methods	
<input checked="" type="checkbox"/>	USLCI	

Figure 26: SimaPro 9.6.0.1 version libraries

Here is a brief explanation of the selected libraries:

- **Agri-footprint:** *Agri-footprint* is a comprehensive LCI (Life Cycle Inventory) database containing approximately 4,800 products and processes specific to agricultural LCA: crops, products and intermediates, feed compounds, food products, animal production systems, and background processes such as transport, auxiliary processing inputs, energy, pesticides, and fertilizers. Three allocation options can be applied: mass, energy, and economic allocation, but only the economic allocation is included in SimaPro by default. It was developed by Mérieux NutriSciences | Blonk, an international leader in food sustainability specializing in the complexities of agricultural LCA [54].

- **Ecoinvent 3:** With over 15,000 LCI datasets in areas such as energy supply, agriculture, transport, biofuels and biomaterials, bulk and specialty chemicals, construction materials, packaging materials, textiles, basic and precious metals, metal processing, ICT and electronics, dairy, wood, and waste treatment, *Ecoinvent* is one of the most extensive international LCI databases. In this case, the *Ecoinvent 3.1* version was installed in the software. In SimaPro®, three *Ecoinvent* databases are available: allocation at the point of substitution (system and unit), cut-off by classification (system and unit), and consequential (system and unit) [55].

The "Allocation at point of substitution" system model follows an attributional approach where responsibility for waste (burdens) is shared between producers and subsequent users who benefit from treatment processes by using valuable products generated within these processes [56].

The "Allocation, cut-off by classification" system model is based on the recycled content or cut-off approach. In this system model, waste is the responsibility of the producer, and there is an incentive to use recyclable products that are available without burden (cut-off) [56].

The consequential system model uses different baseline assumptions to assess the consequences of a change in an existing system. It applies substitution to credit processes with the avoided burdens of supply chains replaced by co-products generated within them [56]. This is the preferred system model of the three in LCA as it provides a more comprehensive and dynamic understanding of environmental impacts associated with changes in systems.

- EU & DK Input Output Database: this database allows modelling the environmental impacts of products imported to Denmark and produced in the 27 EU countries.
- Industry Data 2.0: it includes over 300 datasets from the plastics, surfactants, detergents, and steel industries. Data are collected by various industry associations: Plastics Europe, ERASM, World Steel, International Molybdenum Association, and the Alliance for Beverage Cartons and the Environment. These five industry databases contain data from each specific industry, which are also relevant for many other downstream sectors. The data are at the system level, meaning only Life Cycle Inventory (LCI) rather than unit processes are available [57].
- Methods: The methods library contains various impact assessment methods used to characterize and quantify the environmental impacts of products and processes. These methods provide a framework for assessing different environmental impact categories, such as climate change, acidification, eutrophication, and human toxicity, among others. It includes a variety of impact assessment methods, each with its own set of characterization factors and calculation procedures. Some commonly used methods include *ReCiPe*, *CML*, *IMPACT 2002+*, and *Eco-Indicator 99* [58].
- USLCI: The *USLCI* database provides individual tracking from gate to gate, cradle to gate, and cradle to grave of energy and material flows to and from the environment associated with the production of a material, component, or assembly in the United States. It was created by NREL and its collaborators [59].

As shown in Figure 23, the *Agri-footprint* and *Ecoinvent 3.1* libraries are available in two versions: unit and system.

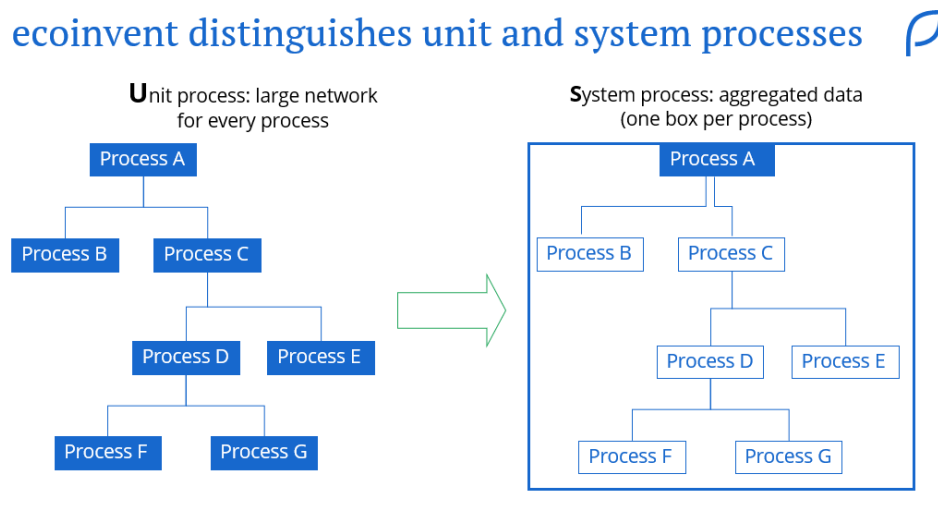


Figure 27: *Ecoinvent* (and *Agri-footprint*) distinguishes unit and system processes, extracted from [60]

A unit process is the smallest element in the life cycle inventory analysis for which input and output data are quantified (ISO 14040). Unit processes describe a distinct part of a life cycle, not a complete life cycle themselves. The scope of a unit process can vary, and there are often several possible approaches to defining the scope and level of detail of life cycle elements [60]. On the other hand, system processes result from compiling and quantifying input and output data for a product throughout its life cycle (ISO 14040:2006). In other words, a system process is a single aggregation from cradle to gate of all environmental flows caused by the provision of the reference product. For this reason, they are also known as an aggregated life cycle inventory [60].

In this study, the system option was chosen and among all the database options, *Ecoinvent* was used for the modelling of every single LCI.

Regarding the method chosen to evaluate the environmental impact, *ReCiPe 2016 Midpoint (H)* was selected. *ReCiPe* is a method for life cycle impact assessment (LCIA), first developed in 2008 through cooperation between RIVM, Radboud University Nijmegen, Leiden University, and PRé Sustainability.

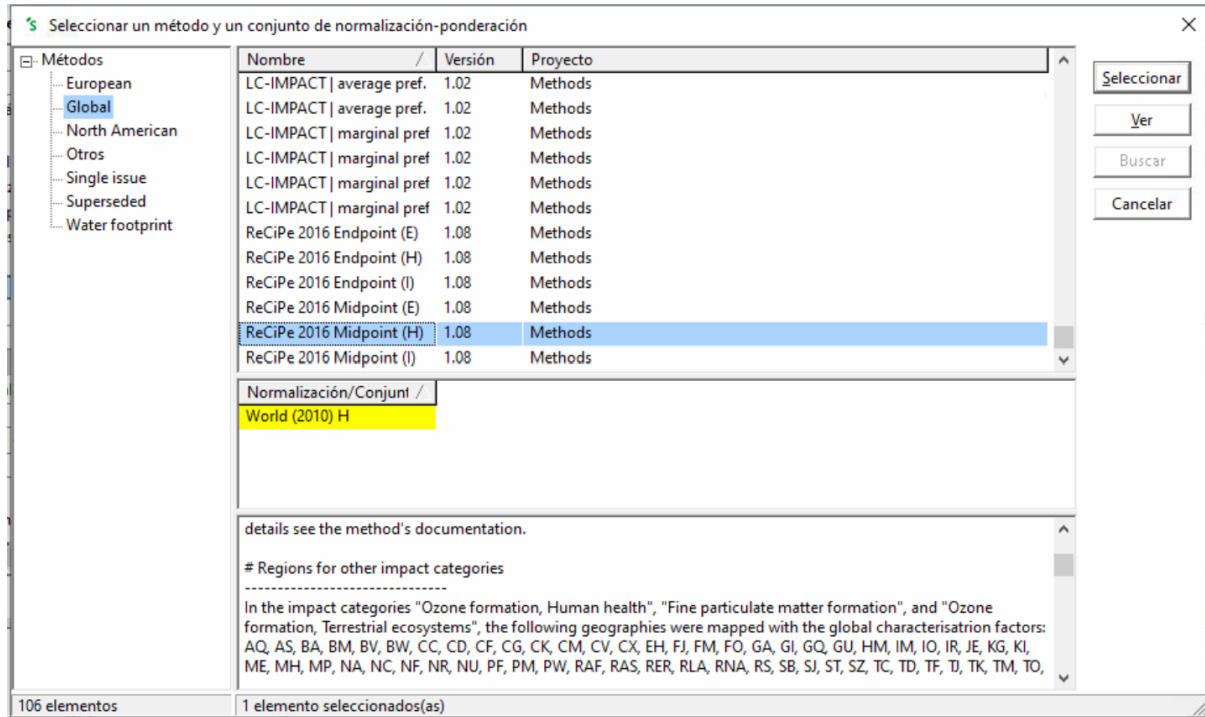


Figure 28: Life cycle impact assessment methods

The life cycle of a product is associated with a large number of emissions of substances and resource extractions, which can vary significantly in their environmental relevance. Life cycle impact assessment aids in interpreting LCA studies by translating these emissions and resource extractions into a limited number of environmental impact scores. This is done using characterization factors. Characterization factors (CF_m) indicate the environmental impact per unit of a stressor (e.g., per kg of resource used or emission released). There are two main ways to derive characterization factors: at the midpoint or endpoint level.

Midpoint characterization factors are found somewhere along the impact pathway, typically at the point after which the environmental mechanism is identical for all environmental flows assigned to that impact category. Endpoint characterization factors correspond to three areas of protection: human health, ecosystem quality, and resource scarcity. The two approaches are complementary in that midpoint characterization has a stronger relationship with environmental flows and relatively low uncertainty, while endpoint characterization provides better information on the environmental relevance of environmental flows but is also more uncertain than midpoint characterization factors. For this reason, the midpoint approach was considered more appropriate for this work.

The impact categories of *ReCiPe2016* (midpoint) and areas of protection (endpoint) are shown in the figure below.

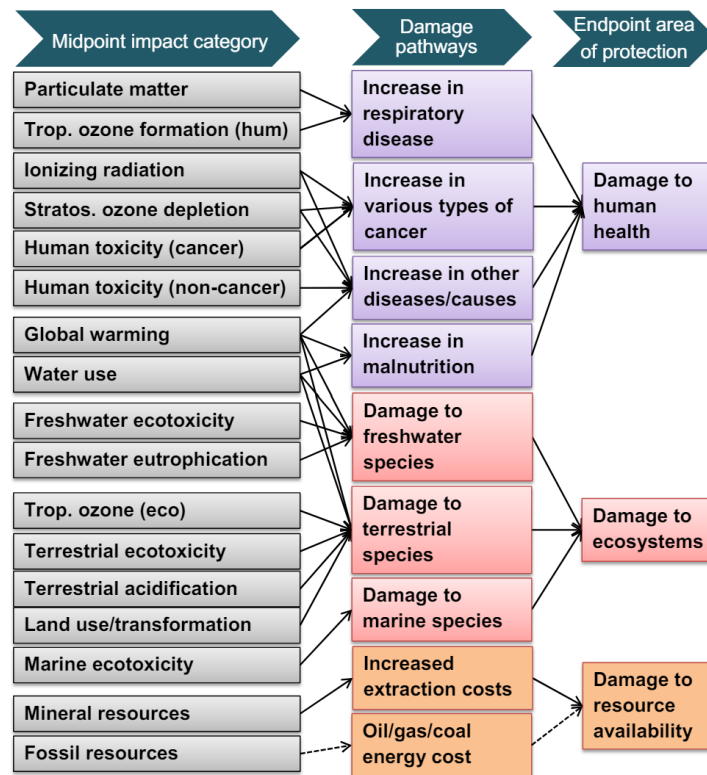


Figure 29: Overview of the impact categories that are covered in the ReCiPe2016 methodology and their relation to the areas of protection, extracted from [61]

Categories and indicators at the midpoint level are presented in the following table [61].

Table 4: ReCiPe2016 Categories and indicators at the midpoint level

Impact category	Indicator	Unit	CF _m	Abbr.	Unit
Climate change	Infra-red radiative forcing increase	W·yr/m ²	Global warming potential	GWP	kg CO ₂ to air
Ozone depletion	stratospheric ozone decrease	ppt·yr	Ozone depletion potential	ODP	kg CFC-11 to air
Ionizing radiation	absorbed dose increase	man·Sv	Ionizing radiation potential	IRP	kBq Co-60 to air
Fine particulate matter formation	PM2.5 population intake increase	kg	Particulate matter formation potential	PMFP	kg PM2.5 to air
Photochemical oxidant formation: ecosystem quality	tropospheric ozone increase (AOT40)	ppb·yr	Photochemical oxidant formation potential: ecosystems	EOFP	kg NO _x to air
Photochemical oxidant formation: human health	tropospheric ozone population intake increase (M6M)	kg	Photochemical oxidant formation potential: humans	HOFP	kg NO _x to air
Terrestrial acidification	proton increase in natural soils	yr·m ² ·mol/l	Terrestrial acidification potential	TAP	kg SO ₂ to air

Impact category	Indicator	Unit	CF _m	Abbr.	Unit
Freshwater eutrophication	phosphorus increase in fresh water	yr·m ³	Freshwater eutrophication potential	FEP	kg P to freshwater
Human toxicity: cancer	risk increase of cancer disease incidence	-	Human toxicity potential	HTP _c	kg 1,4-DCB to urban air
Human toxicity: non-cancer	risk increase of noncancer disease incidence	-	Human toxicity potential	HTP _{nc}	kg 1,4-DCB to urban air
Terrestrial ecotoxicity	Hazard-weighted increase in natural soils	yr·m ²	Terrestrial ecotoxicity potential	TETP	kg 1,4-DCB to industrial soil
Freshwater ecotoxicity	hazardweighted increase in fresh waters	yr·m ³	Freshwater ecotoxicity potential	FETP	kg 1,4-DCB to freshwater
Marine ecotoxicity	hazardweighted increase in marine water	yr·m ³	Marine ecotoxicity potential	METP	kg 1,4-DCB to marine water
Land use	occupation and time-integrated transformation	yr·m ²	Agricultural land occupation potential	LOP	m ² ·yr annual crop land
Water use	increase of water consumed	m ³	Water consumption potential	WCP	m ³ water consumed
Mineral resource scarcity	ore grade decrease	kg	Surplus ore potential	SOP	kg Cu
Fossil resource scarcity	upper heating value	MJ	Fossil fuel potential	FFP	kg oil

SimaPro[®] uses the selected impact assessment method and associated characterization factors to calculate environmental impacts. There is a difference in the unit of the indicator for each category and the unit of the midpoint characterization factor (CF_m). This is because a reference substance has been introduced, so the characterization factor is a dimensionless number that expresses the strength of an amount of substance relative to that of the reference substance. For all emission-based and resource scarcity impact categories, this is a reference substance of kg for a specific environmental compartment, while for land use it is the area and time integrated for a type of land use. For example, for the impact category "climate change," the CF_m is the "global warming potential" (GWP). If a certain production process emits carbon dioxide, methane, and nitrous oxide, the *ReCiPe* method will use the characterization factors for these emissions in the impact category to convert each emission into its CO₂ equivalent.

The characterization factors depend on the method's perspective. In fact, in the *ReCiPe2016* method, different sources of uncertainty and different choices have been grouped into a limited number of perspectives [61]. These perspectives are used to group similar types of assumptions and choices. The perspectives included in *ReCiPe2016* are:

- Individualist perspective (I): based on short-term interest, undisputed impact types, and technological optimism regarding human adaptation.

- Hierarchist perspective (H): based on scientific consensus regarding the time frame and plausibility of impact mechanisms.
- Egalitarian perspective (E): the most precautionary, taking into account the longest time frame and all impact pathways for which data are available.

The approach that best reflects our society is the hierarchist perspective, so it was chosen option. This is why the letter H is in *ReCiPe 2016 Midpoint (H)*.

In this work, not all impact categories were studied, but only those considered most relevant to the impacts caused by the production of rigid polyurethane foam, and ultimately focusing on climate change in particular. These will be discussed in more detail later.

Next, a more detailed analysis of the LCA is presented, with particular reference to the specific problem of this work and the help of SimaPro[®] visualization tools.

5.2. Goal and Scope definition

The goal and scope definition is the first phase in a life cycle assessment, encompassing the following main topics. Each definition is derived from [62].

- Goal: The goal of an LCA study must unambiguously state the intended application, including the reasons for carrying out the study and the target audience, i.e., who the results of the study are intended to be communicated to.
- Scope: The scope refers to the boundaries and constraints of the study. It defines what is included and excluded from the analysis, helping to establish the context within which the environmental impacts of a product or process will be evaluated.
- Functional Unit: The functional unit serves as a reference parameter to which the LCA results are attributed; therefore, its definition is the foundation of an LCA. For carrying out comparative LCAs, it is important to use the same functional unit for all products or processes being analyzed. This ensures that comparisons are meaningful and accurate, allowing for a fair evaluation of the environmental impacts of different options.
- System Boundaries: System boundaries define the process units to be included in the analysis model, constituting the interface between a product system and the environment or another product system. They define the processes (e.g., manufacturing processes, transportation, and waste management) and the inputs and outputs that should be considered in the LCA. The definition of system boundaries includes the following limits: geographical boundaries, life cycle boundaries (i.e., limitations in the life cycle), and boundaries between the technosphere and the biosphere.
- Data Quality and Category: Data quality refers to the reliability, precision, and completeness of the data used in the analysis. On the other hand, the data category typically refers to the type of data used in the analysis and may also encompass how the data were obtained, such as primary or secondary sources.
- Critical Review Process: The purpose of the critical review process is to ensure the quality of the life cycle analysis. The review can be internal, external, or involve stakeholders.

This is a critical phase as it lays the foundation for the entire LCA study and has a significant influence on its outcome.

5.2.1. Goal

The objective of this LCA study is to compare the environmental impacts of traditional and partially biobased processes in the production of rigid polyurethane foam, destined to thermal insulation panels. The study aims to provide information on the environmental performance of each process variant, intending to inform decision-making processes related to product marketing and regulation. Ultimately, the study seeks to understand which of the four different processes had the least impact during their production. Interest is given to lignin's extraction, which is studied by comparing two different allocation methods.

5.2.2. Scope

The study considers all stages of the life cycle up to the point where the rigid polyurethane foam leaves the factory gate, therefore using a cradle-to-gate approach. The analysis includes inputs such as energy, water, and raw materials, as well as outputs such as emissions, waste, and by-products. The study aims to provide a comprehensive and transparent assessment of the environmental performance of each process variant. However, it should be noted again that the scope of this study does not extend to evaluating the economic or social aspects of the production processes, nor does it consider other potential environmental impacts beyond those directly related to the production of rigid polyurethane foam. The production processes involving lignin are relatively new and their Technological Readiness Levels (TRL) differ from the traditional fossil fuel-based route. Rigid polyurethane foam panels made from polyols and MDI have been widely used in various applications for many years, and the production processes are well-established, standardized, and commercially available. The materials, production techniques, and end-use performance characteristics are well understood and documented. This means that a TRL of 9 can be assigned to the traditional route, as it describes a real system proven in an operational environment, as defined by the European Commission. Despite almost 30 years since the development of lignin oxypropylation and significant progress at the laboratory scale, this technology has not yet been brought to commercial scale. Consequently, it would be assigned a TRL of only 4 (technology validated in the laboratory). The same can be said for lignin depolymerization and its subsequent substitution for polyols in the formulation of rigid polyurethane foam. This would allow for a fair comparison between the three biobased solutions. However, comparing a technology that has a well-established production process (TRL 9) with technologies that have demonstrated basic functionality but are still far from being fully developed and deployable systems can be challenging. To explore the sustainability potential of the lignin-based formulations and allow for a fair comparison with the fossil-based one, three lab-scale processes have been adapted to envision an industrial-scale scenario.

Thus, three bio-based processes have been analysed, with two of them adapted to a hypothetical industrial scale, as presented in Chapter 4. The only process not scaled up involves directly incorporating lignin, as extracted from the pulp and paper industry, into rigid polyurethane formulations without chemical modification.

5.2.3. Functional Unit

To allow for a precise comparison between the different production processes analysed, a functional unit of 1 kg of rigid polyurethane foam has been chosen. This choice is based on the simplicity and availability of inventory data, as well as the importance of using a consistent unit to ensure comparability between processes. However, it is important to recognize that polyurethane foam produced through different processes may have variable densities, affecting the amount of polyurethane contained in each panel.

5.2.4. Allocation methods

Two allocation methods for lignin extraction were analysed in this study. The reference for this analysis is a scientific article by Hermansson et al. [89], which presents a comprehensive comparison of 12 allocation approaches and their impact on results. As noted in the article, there is no consensus on how allocation should be addressed in lignin-generating processes, with methodologies varying significantly across studies.

Out of the 12 approaches discussed, two were chosen for this work: the *marginal approach*, proposed by Bernier et al., and the *main product bears all burden* approach, introduced by Sandin et al. [90].

The *marginal approach* focuses on the change in system-wide impacts before and after lignin extraction, making it particularly suited for consequential LCA studies that assess global impact shifts. Lignin is extracted from black liquor, which reduces the need for its combustion in pulp mill recovery boilers. Emissions from substitute fuels like natural gas are attributed to lignin but are offset by the reduced emissions from black liquor combustion [69].

In contrast, the *main product bears all burden* approach assigns the entire environmental burden to a single main product. According to Hermansson et al., in current systems where pulp is considered the main product, lignin is essentially impact-free. However, if future demand shifts and lignin becomes the main product, it would bear the full system burden, resulting in significantly higher impacts.

These two contrasting methods were chosen to evaluate how allocation decisions influence the results, providing insight into their potential variability.

5.2.5. System Boundaries

Based on the chosen cradle-to-gate approach, the system boundaries encompass all processes involved in the product's life cycle from raw material extraction (cradle) to the point where it leaves the factory (gate). This includes the extraction of raw materials, such as petroleum-derived chemicals and their subsequent processing into polyols and MDI, and the extraction and processing of Kraft lignin. Additionally, the manufacturing processes involved in producing the insulation panels, such as mixing, foaming, and curing, are considered within the system boundaries. The transportation of raw materials, including kraft lignin, and finished products, along with associated emissions and energy consumption, up to the point where the foam panels are ready for distribution at the factory gate, are also included.

Geographic boundaries are defined to specify the locations of raw material extraction, manufacturing facilities, transportation routes, and waste management processes, with a focus on Europe. Within these boundaries, the analysis will consider inputs such as energy, water, and raw materials, as well as outputs such as emissions, waste, and by-products.

To fully study the environmental impacts and their allocation among the materials involved, the production of polyols and MDI is analyzed first, using a cradle-to-gate approach from the *Ecoinvent* data library. These products then serve as raw materials for producing non-bio-based rigid polyurethane foam. Below are the flow diagrams that reference the system boundaries for polyols and MDI. Both are derived from [63], which once again serves as the followed model.

- **System Boundaries: MDI**

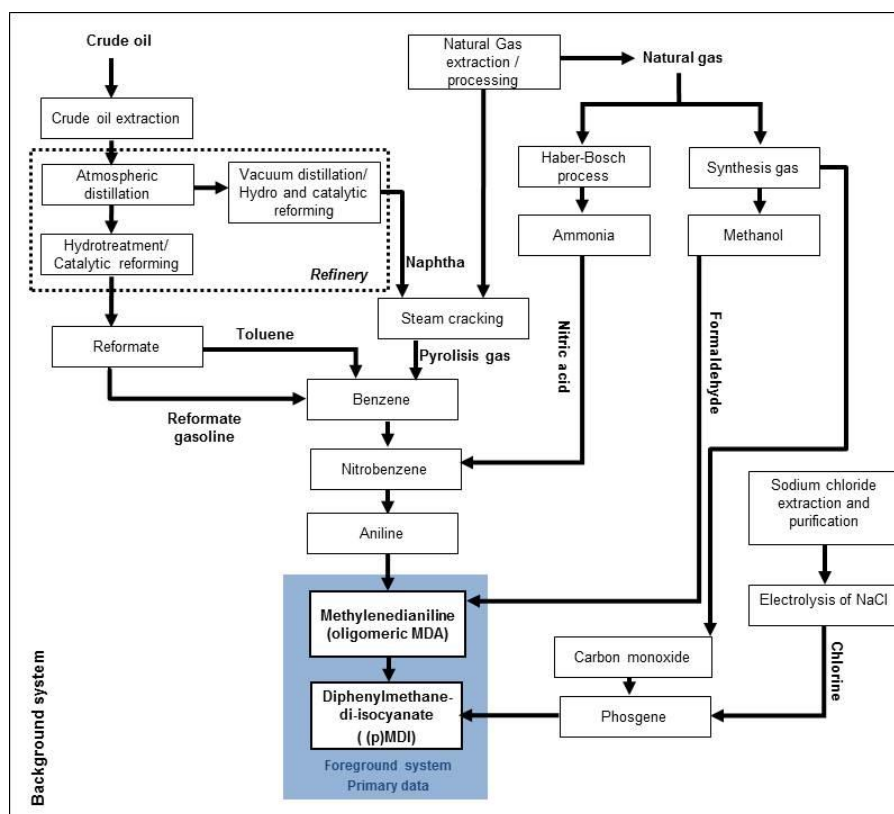


Figure 30: Cradle-to-gate system boundaries (MDI), extracted from [64]

The synthesis of methylene diphenyl diisocyanate (MDI) from crude oil is a complex process involving several intricate steps aimed at refining and transforming various hydrocarbon compounds. It begins with the extraction of crude oil from natural deposits, followed by atmospheric distillation to separate hydrocarbons based on their boiling points. Vacuum distillation further refines the oil, enhancing its purity, while hydrodesulfurization removes sulfur compounds, improving its quality. Catalytic reforming converts naphthenes and paraffins into aromatics such as benzene and toluene. Steam cracking breaks down heavy fractions into lighter ones, producing pyrolysis gas. Benzene is then separated from reformat gasoline and converted into nitrobenzene through a nitration process. Nitrobenzene is reduced to aniline by hydrogenation using catalysts like palladium on carbon or nickel.

Simultaneously, the extraction and processing of natural gas produce ammonia through the Haber-Bosch process, which is then converted into aniline via an amination process. Natural gas is also used to produce methanol through synthesis gas. Aniline is then combined with formaldehyde in an acid-catalyzed reaction to produce methylenedianiline (MDA). At this step, the aniline-to-formaldehyde

ratio, acid concentration, and reaction conditions determine the percentage distribution of MDA isomers [64]. After neutralization with caustic soda, the crude MDA is washed, with excess aniline distilled for recycling. The aqueous phase is purified from residual organics. Subsequently, phosgene reacts with MDA in an inert solvent to produce crude MDI and hydrogen chloride. Once the hydrogen chloride evolution is complete and a homogeneous solution is obtained, the solvent is recovered by distillation. Purified MDI is then obtained through fractional distillation, crystallization, or sublimation [64].

- **System boundaries: polyols**

Reference [65] discusses both long-chain and short-chain polyether polyols. However, since short-chain polyether polyols are predominantly used in the production of rigid polyurethane foams, the focus here is exclusively on them.

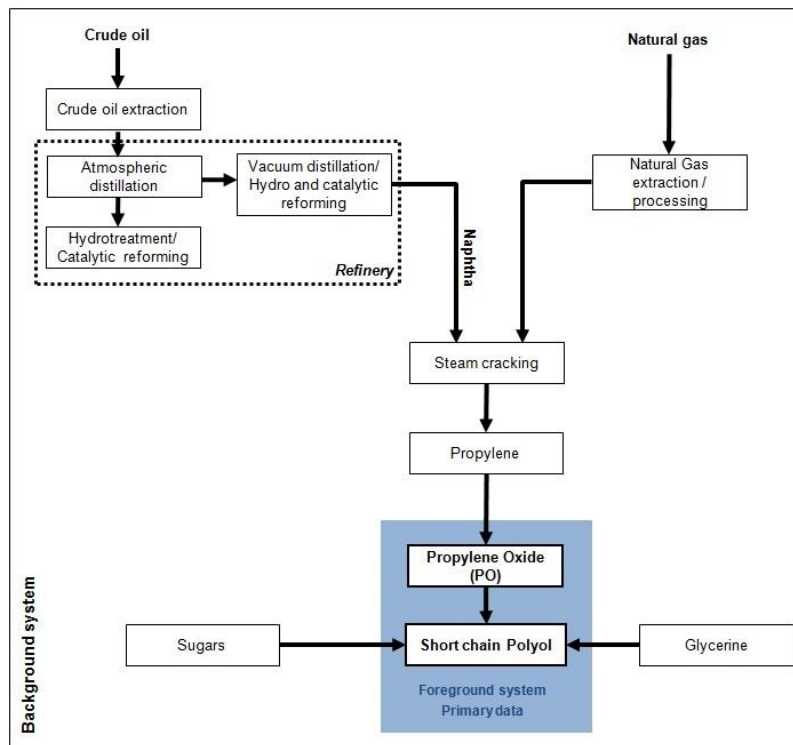


Figure 31: Cradle-to-gate system boundaries (short chain polyols), extracted from [65]

The process for obtaining short-chain polyether polyols begins with naphtha, a product derived from the refining of crude oil, which serves as the raw material for the production of propylene. The propylene is then converted into propylene oxide (PO) through a series of chemical reactions. Simultaneously, an initiator containing OH- groups, such as glycerin or sugars, is prepared. Next, the process of alkoxylation takes place, where the initiator reacts with the propylene oxide in the presence of a catalyst. This reaction, occurring at elevated temperature and pressure, is highly exothermic. As the reaction progresses, the propylene oxide continues to react with the initiator, leading to the formation of polyether polyols. The chain length of the polyol and their molecular weights can be controlled by adjusting the amount of propylene oxide used in the reaction [65]. Once the reaction is complete, the polyether polyol products are separated from any byproducts and water, if necessary. The resulting polyether polyols can then be used in a variety of applications, including the production of polyurethane products.

- **System Boundaries: traditional rigid polyurethane foam**

Figure 29 represents the system boundaries for the production of rigid polyurethane foam via the traditional route, with MDI and polyols as raw materials. The blowing agent used for foam formation considered is pentane, and it is found in the "production of other materials inputs" box.

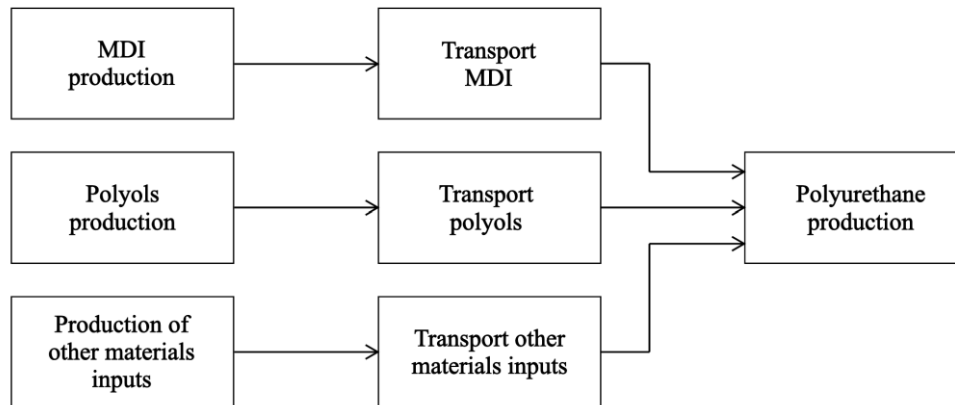


Figura 32: Traditional rigid polyurethane foam system boundaries

It is also assumed that the co-location of the MDI and polyols production facilities in a single location, situated 500 km from the polyurethane production site, optimizes logistics and minimizes transportation impacts. On the other hand, pentane occurs naturally as one of the components of crude oil and is extracted and purified during oil refining. It is also produced in smaller quantities in various hydrocarbon reactions, such as isobutane production [66]. Additionally, it typically involves specialized equipment and processes due to its flammable nature. Because of this, it is assumed to be produced at another site, but its transportation has not been considered, since it's negligible due to the much lower amount of pentane needed compared to the other raw materials. The extraction and chemical modifications of Kraft lignin also fall within the "Production of other material inputs" box.

- **System Boundaries: Kraft lignin**

As already mentioned, Kraft lignin is considered as the natural resource for three rigid polyurethane foam formulations.

For the system boundaries of KL, a cradle-to-gate approach has been adopted. Figure 30 is from the study carried out by Bernier et al. [69], which serves as the model followed for the life cycle analysis of 1 kg of untransformed dry Kraft lignin powder with the *marginal approach* method. It shows the main steps of lignin recovery in a Kraft pulp mill and the corresponding life cycle inventory system boundaries.

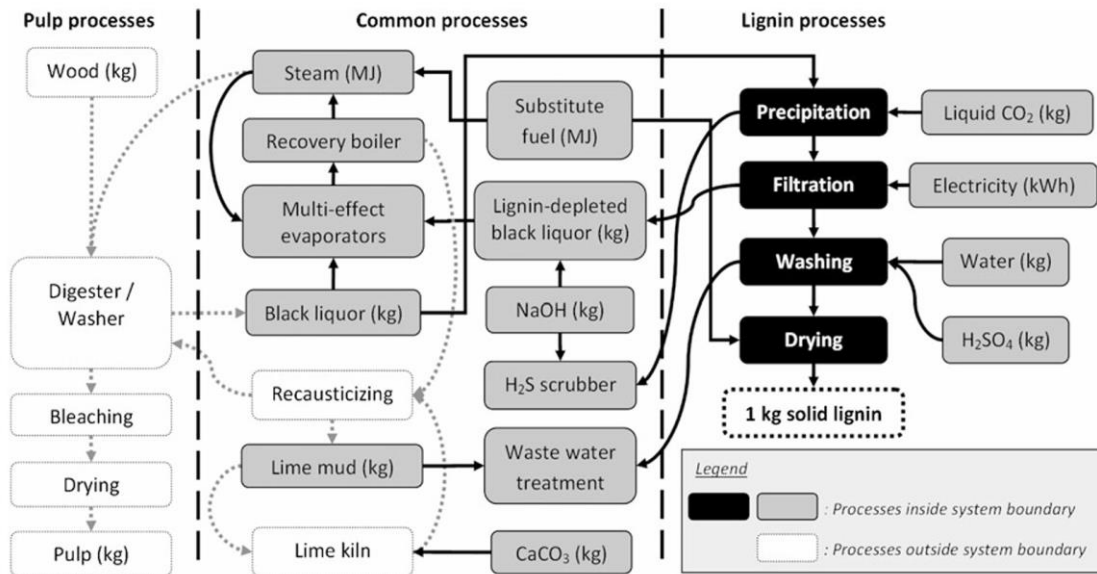


Figure 33: System boundaries for the life cycle inventory of kraft lignin, extracted from [69]

Black liquor is a byproduct of the Kraft process, the predominant method for producing paper pulp. It consists of a complex mixture of water, lignin, hemicellulose, and inorganic chemicals used during pulping. Lignin can be extracted from black liquor, making it a valuable source for further processing. In Figure 30, under lignin processes, the main steps for lignin extraction are shown.

Lignin is first precipitated by acidifying the concentrated black liquor. According to the work of Bernier et al. [69], industrial-grade CO_2 is injected into the black liquor to lower its pH. Then, the lignin partially precipitates in decreasing order of molecular weight. A small amount of H_2S is also emitted, which is neutralized in the existing non-condensable gas scrubber, consuming NaOH in an additional amount assumed to be stoichiometric. The remaining black liquor is recycled to multi-effect evaporators and the recovery boiler, where it is burned as it normally would be, despite its calorific value being partially depleted.

The precipitated and wet lignin is separated from the liquid phase by filtration. The filtrate from the filtration step, which consists of black liquor depleted of lignin, is recycled back to the multiple-effect evaporators.

The lignin is then washed to remove residual inorganic chemicals and other impurities. Washing is performed with water and H_2SO_4 , part of which is neutralized by the remaining traces of black liquor. The wash effluent, which is more diluted than the filtrate and contains excess H_2SO_4 , is neutralized at the wastewater treatment plant by increasing the bleed rate of lime sludge, indirectly increasing compensatory CaCO_3 purchases. In Figure 30, this is shown as a CaCO_3 input between recausticizing and the lime kiln, which are two processes outside the system boundary because their operation (and CO_2 emissions) is independent of lignin production. As a worst-case scenario, Bernier et al. assume that additional CaCO_3 is required in the same amount as H_2SO_4 .

Finally, the washed lignin is dried to obtain it in solid form.

As for the *main product bears all burden* approach, Kraft lignin is considered to be an impact-free byproduct, with all the environmental impacts attributable to pulp.

- **System Boundaries: depolymerized Kraft lignin**

The system boundaries for the synthesis of DKL are developed based on the scale-up proposed in Chapter 4. Figure 34 can also be seen as the visualization of the system boundaries of the hydrolytic depolymerization process. However, the dissolution of DKL in acetone is considered outside of the system boundaries in this case, as the final product is considered to be DKL in powder state.

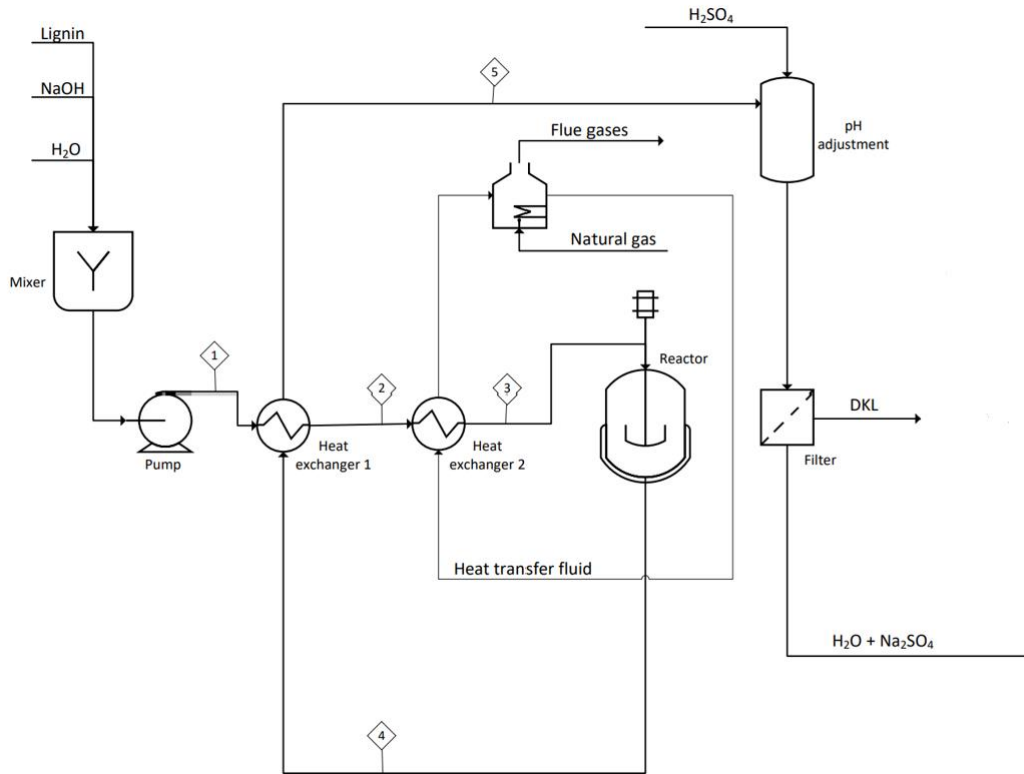


Figure 34: System boundaries for the life cycle inventory of DKL

- **System Boundaries: oxypropylated depolymerized Kraft lignin**

The same applies to the oxypropylation process, where the PFD of the scale-up provides a clear visualization of the system boundaries considered. Acetone recovery is included within the system boundaries, as it is recycled within the process, requiring only minimal make-up. The following scheme illustrates the system boundaries for the chemical modification processes.

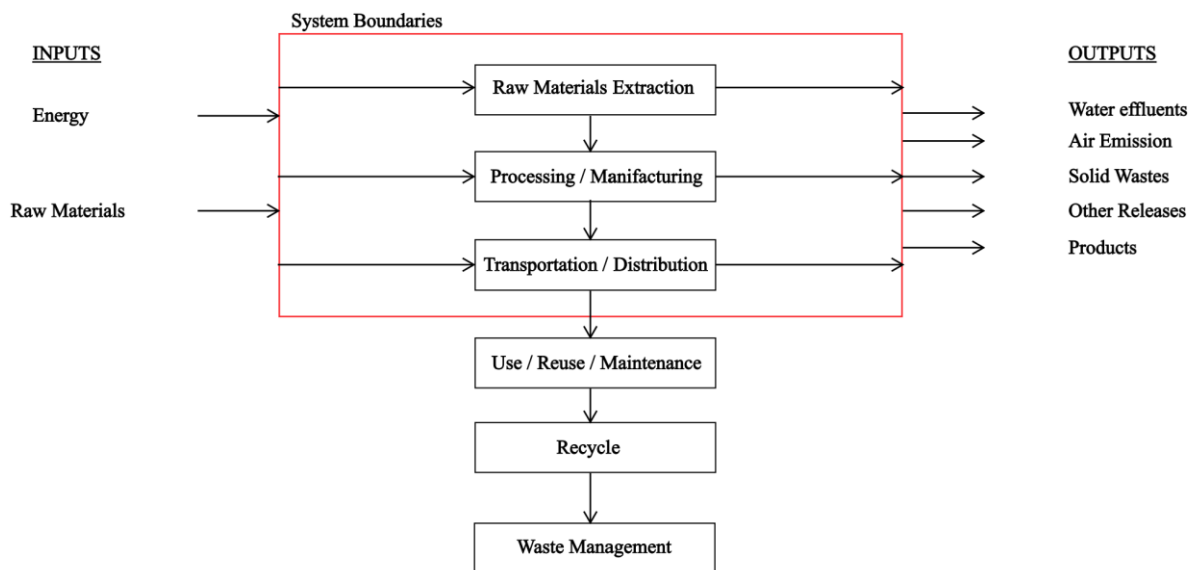


Figure 35: System boundaries for the life cycle inventories of chemical modification processes

5.2.6. Data Quality and Categories

For the traditional rigid polyurethane foam synthesis route, data was collected from the Eco-profiles set of Plastics Europe, known for their accuracy, completeness, and transparency in representing the environmental impacts of European plastic production and continuously updated since 1993. These profiles, representative of average industrial practices, gather data from member companies and cover the cradle-to-gate life cycle stage, providing a comprehensive perspective on production processes [67]. In the case of rigid polyurethane foam, calculations were performed in 2005, with data processed in 1996 and considering only one site. The MDI calculations were carried out in 2020, using data processed in 2018, examining six sites. Similarly, polyols calculations conducted in 2020 incorporated 2018 data, distinguishing between long-chain polyols (six sites) and short-chain polyols (four sites) [63]. Regarding pentane, data was last calculated in 2005, with no information on the number of companies [66]. All these data are already included and available in the *Ecoinvent* library of SimaPro®.

Since the data used comes from the Eco-profiles set on the PlasticsEurope website, they would be classified as secondary data.

Regarding partially bio-based rigid polyurethane foam incorporating chemically modified kraft lignin, since kraft lignin is a residue from another process rather than a primary product produced directly, its production and related data are not included in the life cycle inventory. Instead, the focus is on accounting for the environmental impacts associated with the extraction and transportation of kraft lignin to the facility where it is used in polyol synthesis.

5.2.7. Critical Review Process

A critical review process is not included in this work.

5.3. Life cycle inventory (LCI)

Inventory analysis involves data collection and calculation procedures to quantify the relevant inputs and outputs of a product system. These inputs and outputs may include resource usage and emissions to air, water, and soil associated with the system. Data can be site-specific, such as from specific companies, areas, and countries, but also more general, from sources like trade organizations, public surveys, and studies. Data must be collected from all individual processes in the life cycle. Additionally, this data can be quantitative or qualitative [62]. Quantitative data is important in process or material comparisons, as in the present work. However, in some cases, quantitative data may be missing or of poor quality (too old or not technologically representative). In that case, more descriptive qualitative data can be used for environmental aspects or individual life cycle steps that cannot be quantified, or if the goal and scope definition allows for a non-quantitative description of conditions.

As data is collected and more is learned about the system, new data requirements or limitations may be identified, necessitating a change in data collection procedures to ensure the study objectives continue to be met.

Data collection is often the most labor-intensive part of a life cycle assessment, especially if site-specific data is needed for all individual processes in the life cycle. In many cases, average data from the literature or data from trade organizations are used. PlasticsEurope is, in fact, a trade organization, representing the plastics industry in Europe and serving the interests of its member companies.

In the following paragraphs, the life cycle inventories of the processes studied in SimaPro[®] are described and performed. Before explaining in detail the life cycle inventories modelled for each process, other inventories personally created are explained first.

- Electricity generation mix

Original inventories were constructed in SimaPro to represent the EU electricity mix. Electricity is used as an energy source in various processes, but the software accounts for the EU energy shares only in the market entries of electricity, specifically, the electricity purchased from the grid. To ensure consistency with the cradle-to-gate approach, the environmental footprint of electricity is considered from its production at high voltage, through its transformation to medium voltage, and its distribution via the grid. A custom entry was created in SimaPro to accurately reflect the EU grid electricity mix, labeled as “Electricity, medium voltage {EU}.” Details of this entry are reported below.

Table 5: Life cycle inventory of the Electricity, medium voltage {EU} dataset

Input	Unit	Quantity	ecoinvent process name
Electricity from coal	kWh	17.1	Electricity, high voltage {DE} electricity production, hard coal
Electricity from natural gas	kWh	20.9	Electricity, high voltage {DE} electricity production, natural gas
Electricity from oil	kWh	1.5	Electricity, high voltage {DE} electricity production, oil
Electricity from hydropower	kWh	18.7	Electricity, high voltage {DE} electricity production, hydro, reservoir, non-alpine region
Electricity from nuclear	kWh	14.8	Electricity, high voltage {DE} electricity production, nuclear, boiling water reactor
Electricity from wind	kWh	13.8	Electricity, high voltage {DE} electricity production, wind, >3MW turbine, onshore
Electricity from solar power	kWh	6.2	Electricity, high voltage {DE} electricity production, solar thermal parabolic trough, 50 MW
Electricity from biogas	kWh	4.6	Electricity, high voltage {DE} electricity production, heat and power co-generation, gas engine
Voltage transformation	kWh	97.6	Electricity, medium voltage {DE} electricity voltage transformation from high to medium voltage
Product			
Electricity, medium voltage {EU}	kWh	97.6	

The electricity generation mix is the one reported by the International Energy Agency [83], which refers to 2022. As an approximation, all the high voltage electricity entries are considered as based in Germany, except for the solar one, which refers to Spain. The electricity produced is then transformed to medium voltage, adding more environmental impact to the output. This inventory wants to consider the overall impact of the electricity that will be used in the processes, from the one based on fossil-resources to the modification of lignin, starting directly from the electricity production.

In terms of impact assessment, the result obtained is reasonable and coherent with the EU energy mix. The Sankey diagram, as obtained in SimaPro, is shown in Figure 4.

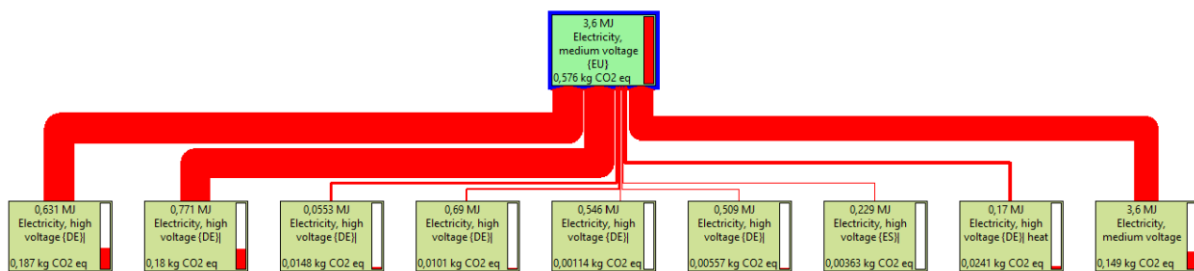


Figure 36: Sankey diagram, global warming potential of electricity production and voltage transformation

Producing 1 kWh of electricity and transforming it to medium voltage results in 576 g CO₂ eq, with 427 g attributed to electricity generation and 149 g to voltage transformation. Medium voltage was chosen as it is the standard in medium-scale industries.

A similar approach was followed for other two custom data sets, referring to electricity generated from wind power alone, and hydro power alone.

Table 6: Life cycle inventory of the Electricity, medium voltage {RER} | from wind dataset

Input	Unit	Quantity	ecoinvent process name
Electricity from wind	kWh	1	Electricity, high voltage {DE} electricity production, wind, >3MW turbine, onshore
Voltage transformation	kWh	1	Electricity, medium voltage {DE} electricity voltage transformation from high to medium voltage
Product			
Electricity, medium voltage {RER} from wind	kWh	1	

Table 7: Life cycle inventory of the Electricity, medium voltage {RER} | from hydropower dataset

Input	Unit	Quantity	ecoinvent process name
Electricity from hydropower	kWh	1	Electricity, high voltage {DE} electricity production, hydro, reservoir, non-alpine region
Voltage transformation	kWh	1	Electricity, medium voltage {DE} electricity voltage transformation from high to medium voltage
Product			
Electricity, medium voltage {RER} from hydropower	kWh	1	

Electricity generated from wind at high voltage results in an impact of only 40 g CO₂ eq per kWh. This estimate is relatively conservative, as the U.S. Department of Energy [86] reports emissions of approximately 11 g CO₂ per kWh for wind energy. However, it is unclear whether their data accounts solely for CO₂ or for CO₂ eq, which include other greenhouse gases. An additional 149 g CO₂ eq per kWh is added for transformation to medium voltage.

Hydropower electricity has a total global warming impact of 202 g CO₂ eq per kWh.

These custom datasets correctly consider electricity production, voltage transformation, and the operation and maintenance of wind and hydro power plants. However, they exclude the impacts of raw material extraction, plant decommissioning, and waste treatment, as these activities are already covered by other infrastructure datasets. Consequently, the datasets focus on electricity production from existing plants rather than modeling custom-built facilities.

The 40 g CO₂ eq per kWh for wind electricity likely accounts for operational and maintenance activities, as no CO₂ is emitted during the actual generation of wind-powered electricity.

When compared to the EU energy mix, wind and hydropower electricity represent a 67% and 65% reduction in impact, respectively.

- **Polyether polyols, short chain**

For the polyols used in rigid polyurethane foam production, a slight adjustment to the process in *ecoinvent* was made, to include a generic transportation of 500 km.

Table 8: Life cycle inventory of the Polyether polyols, short chain dataset

Input	Unit	Quantity	<i>ecoinvent</i> process name
Polyols	kg	1	Polyether polyols, short chain {RER} polyether polyols production, short chain
Trucking	tkm	0.5	Transport, freight, lorry 16-32 metric ton, EURO4 {RER} market
Product			
Polyether polyols, short chain	kg	1	

The dataset relative to polyols production represents the average production of 1 kg of short chain polyether polyol (MW < 1000 g/mol), as per SimaPro, and it's directly modelled based on the Plastics Europe Public LCI database [65]. As said by the eco-profile [65], this dataset provides environmental performance data representative of the average European production of polyether polyols, from cradle to gate (from crude oil extraction to granulates or resin at plant). Production data is from three suppliers. Fuel and energy inputs in the system reflect average European conditions and whenever applicable, site specific conditions were applied, to reflect representative situations. Therefore, the study results are intended to be applicable within EU boundaries [65]. This is perfectly in line with the geographical reference of the present study, so just the transportation to a generic polyurethane plant in Europe was added.

- **Methylene diphenyl diisocyanate (MDI)**

An identical approach was followed for the life cycle inventory of MDI, where once again the program and methodology of SimaPro are as according to Plastics Europe [64], among others.

Table 9: Life cycle inventory of the Methylene diphenyl diisocyanate (MDI) dataset

Input	Unit	Quantity	<i>ecoinvent</i> process name
MDI	kg	1	Methylene diphenyl diisocyanate {RER} methylene diphenyl diisocyanate production
Trucking	tkm	0.5	Transport, freight, lorry 16-32 metric ton, EURO4 {RER} market
Product			
Methylene diphenyl diisocyanate (MDI)	kg	1	

The dataset is based on industry data from five different MDI producers with six plants in five European countries, who participated in the primary data collection.

- **Kraft Lignin extraction process**

For this process, the work of Bernier et al. [69] was used as a reference, modeling a 1 kg inventory of unprocessed dry Kraft lignin powder produced using natural gas. Bernier et al.'s work dates to 2012 and makes use of an old version of the *ecoinvent* database (i.e. *ecoinvent* v2.2). In the case of the present

work, the life cycle inventory was updated with *ecoinvent* v3.10. For the *main product bears all burden* approach, a custom dataset of untransformed dry Kraft lignin with a 0 kg CO₂ eq impact was created.

The life cycle inventory for the extraction of Kraft lignin is therefore as follows:

Table 10: Life cycle inventory of 1 kg of untransformed dry Kraft Lignin, based on Bernier et al.'s work

Input	Unit	Quantity	<i>ecoinvent</i> process name
Natural gas	MJ	31.500	Heat, district or industrial, natural gas {Europe without Switzerland} heat production, natural gas, at industrial furnace >100kW
CO ₂	kg	0.300	Carbone dioxide, liquid {RER} carbon dioxide production, liquid
H ₂ SO ₄	kg	0.230	Sulfuric acid {RER} sulfuric acid production
NaOH	kg	0.107	Sodium hydroxide, chlor-alkali production mix, at plant/RER
CaCO ₃	kg	0.230	Lime, packed {CH} lime production, milled, packed
Water	kg	4.850	Tap water {RER} , market
Electricity	kWh	0.010	Electricity, medium voltage {EU}
Trucking	tkm	0.934	Transport, freight, lorry 16-32 metric ton, EURO 4 {RER} market
Product			
Untransformed dry Kraft Lignin (KL)	kg	1	
Output			
Emissions to air			
Carbon dioxide	kg	-2.534	
Nitrogen, atmospheric	kg	-8.385	
Oxygen	kg	-0.326	
Water	kg	-1.356	

Bernier et al. have modelled this life cycle inventory assuming that lignin, normally burned as black liquor for energy in pulp mills, is instead diverted to other uses (polymers production). This creates an energy deficit in the Kraft process, and to compensate for it, natural gas is used as a substitute fuel for on-site energy needs, as well as for drying lignin after precipitation and washing.

Bernier et al. do not state explicitly the process outputs (air emissions), and therefore have been modelled with a personal approach. In the outputs section of SimaPro, a carbon dioxide emission of -2.30 kg was entered to account for lignin's carbon sequestration potential. As Bernier et al. state, 1 kg of lignin can sequester up to 2.30 kg of CO₂, corresponding to a composition of 62% carbon, based on the average of four samples provided to them by FPInnovations [69].

In this life cycle inventory, the negative CO₂ value represents the biogenic carbon content stored within lignin. Lignin, often a byproduct of the paper and pulp industry as already mentioned, retains a large amount of carbon originally absorbed by biomass (e.g., trees). This stored CO₂ reduces emissions by locking carbon within lignin's structure, rather than releasing it back into the atmosphere.

While Bernier et al. do not list this value explicitly in their life cycle inventory, it has been added here to fully reflect their results. What's more, natural gas combustion is generally considered to be cleaner compared to black liquor and, as a result, substituting natural gas creates a credit in emissions compared to the baseline. The article says that it is fair to assume that 1 MJ of lignin removed corresponds to 1 MJ of substitute fuel energy, leading to a credit of 2.1 kg of black liquor per kg of Kraft lignin removed. This means that 2.1 kg of black liquor that would have been burned, don't. Bernier et al. do not explicitly

state this credit (accounted as negative emissions) in their inventory, so it has been developed in an original way. Assuming an air to fuel ratio of 0.2 in the recovery boiler, typical of a 40% carbon mole fraction of the fuel [81], 10.5 kg of air are needed to burn 2.1 kg of black liquor. For simplicity, this would lead to 12.6 kg of flue gases, whose mole composition has been taken from another study [82]. The combustion of 2.1 kg of black liquor would therefore release to the atmosphere 2.534 kg of CO₂, 8.385 kg of N₂, 0.326 kg of O₂ and 1.356 kg of water. However, since black liquor is essentially bio-based, its combustion is almost neutral when accounting for lignin's carbon uptake, which actually leads to a net emission of 0.234 kg of CO₂ to the atmosphere. All of these values are accounted as credits in the output section, as negative entries.

A comparison of the results is shown in the life cycle impact assessment section.

- Hydrolytic depolymerization process

Here, the inventory is built thanks to the general information of hydrolytic depolymerization on Kraft lignin found in Mahmood et al.'s studies. These data were personally scaled-up to account for the production of 0.193 kg of DKL, therefore using a scaling factor of 10. The process considered is thus the scaled-up version already discussed.

Table 11: Life cycle inventory of 0.193 kg of depolymerized Kraft Lignin

Input	Unit	Quantity	ecoinvent process name
KL	kg	0.251	Untransformed dry Kraft lignin
Distilled water	L	2.19	Water, unspecified natural origin, Europe, without Russia and Turkey
NaOH	kg	0.0702	Sodium hydroxide, chlor-alkali production mix, at plant/RER
N ₂	kg	0.075	Nitrogen, liquid {RER} , market
H ₂ SO ₄	kg	0.086	Sulfuric acid {RER} sulfuric acid production
Cooling water	L	2.334	Water, cooling, unspecified natural origin, Europe, without Russia and Turkey
Energy (N ₂ pressurization)	kJ	40.846	Electricity, medium voltage {EU}
Energy (required by the pump)	kJ	6.800	Electricity, medium voltage {EU}
Energy (for heating up the reactants from 220°C to 250°C)	kJ	285.200	Electricity, medium voltage {RER} from wind
Steam (to sustain the endothermic reaction)	kJ	40.300	Heat, from steam, in chemical industry {RER} steam production, as energy carrier, in chemical industry
Products			
DKL	kg	0.193	
Output			
<i>Emissions to air</i>			
Gaseous residues	kg	0.020	VOC, volatile organic compounds, unspecified origin
<i>Emissions to water</i>			
Aqueous residues	kg	0.020	Organic carbon
Water	kg	1.586	Water, Europe, without Russia and Turkey
<i>Solid residues</i>			
Solid residues	kg	0.017	Biowaste {CH}
Na ₂ SO ₄	kg	0.125	Sodium sulphate (wfr)/RER

The first heating step of the reacting mixture is excluded from the inventory because the required thermal energy can be entirely supplied by the hot products exiting the reactor. In contrast, the second heating step represents the most significant energy demand of the process and is analyzed through a sensitivity analysis, considering various energy inputs:

- Heat transfer fluid (HTF): Fluids like Therminol66® are commonly used in chemical plants. Since the HTF operates in a closed loop and requires regeneration, its contribution is represented as the thermal energy from natural gas combustion in a boiler.
- Electricity from wind: Electric heaters with high precision are increasingly prevalent in chemical plants. Electricity generated from wind has minimal GHG emissions, making it a worthwhile option.
- Electricity from hydropower: Like wind power, hydropower offers a sustainable alternative as it does not rely on fossil fuels.
- Electricity from the EU mix: This serves as the baseline for comparison.

The other energy inputs for the process include pressurizing reactants, providing nitrogen for reactor venting, and sustaining the endothermic reaction. The hydrolytic depolymerization of lignin is inherently endothermic, requiring continuous energy input [79]. This is due to the highly stable and complex structure of lignin, where breaking ether and carbon-carbon bonds demands significant energy. A study using differential scanning calorimetry reports the heat of reaction for four types of lignin [80]. Since no specific data is available for the hydrolytic depolymerization of softwood Kraft lignin, an average of the reported values was used. This calculation estimates that 40.3 kJ is required to sustain the reaction of 0.251 kg of lignin. For this energy need, steam was chosen as the energy carrier and is accounted for in the inventory.

In the pH adjustment step, sulfuric acid reacts with sodium hydroxide (used as a catalyst) to precipitate lignin. This exothermic reaction releases energy and produces water and sodium sulfate. Cooling water is included for temperature control, and sodium sulfate is considered as waste requiring disposal.

- **Oxypropylation process**

Oxypropylation can occur between propylene oxide and already depolymerized lignin, when dissolved in a solvent. As already discussed, acetone is the solvent considered, however only a small amount of it figures in the inventory, since its recovery is considered and only a small makeup is needed. What's more, the solvent recovery is performed in a stripping column thanks to compressed air as stripping agent, which is the main impact of such an operation. In the proposed scale-up, air at 11.5 bar was used in Aspen Plus®, and is considered in the inventory as the production of compressed air at 1000 kPa gauge (approximately 11 bar). The inventory is shown below, with scaled-up values considering Mahmood et al.'s work and the proposed scale-up.

Table 12: Life cycle inventory of 0.43 kg of oxypropylated depolymerized Kraft Lignin

Input	Unit	Quantity	ecoinvent process name
DKL	kg	0.193	Depolymerized Kraft lignin
Propylene oxide	kg	0.217	Propylene oxide, liquid {RER} propylene oxide production, liquid
Acetone	kg	0.017	Acetone, liquid {RER} acetone production, from isopropanol
Glycerol and KOH mixture	kg	0.024	Glycerine {RER} glycerine production, from epichlorohydrin
Energy (required by the pump)	kJ	1.30	Electricity, medium voltage {EU}
Energy (for heating up the reactants from 120°C to 150°C)	kJ	46.26	Heat, from steam, in chemical industry {RER} steam production, as energy carrier, in chemical industry
Stripping air	m ³	0.941	Compressed air, 1000 kPa gauge {RER} compressed air production, 1000 kPa gauge
Product			
OxyDKL	kg	0.43	

A major difference between hydrolytic depolymerization and oxypropylation lies in the fact that the latter is exothermic. No information could be found in literature regarding the heat of reaction, so a calculation had to be made.

In the scaled-up process, oxypropylation between DKL and propylene oxide takes place at 150°C and 11.5 bar to improve DKL's reactivity and its potential to substitute fossil-based polyols in polyurethane formulations.

The reaction scheme for oxypropylation is as follows [84]:

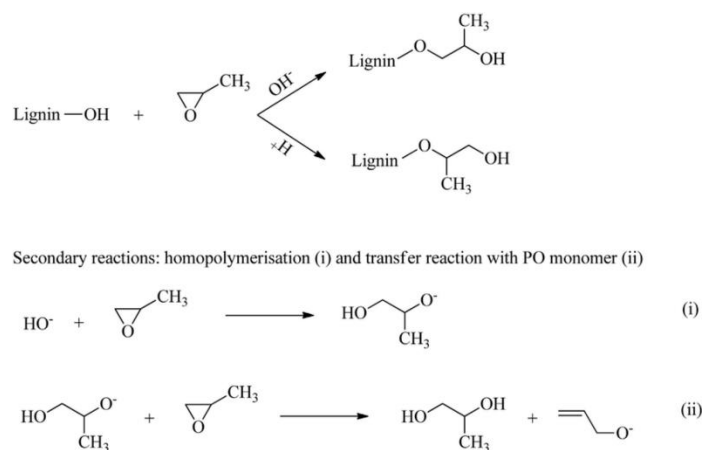


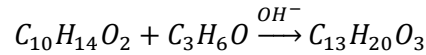
Figure 37: oxypropylation reaction schemes, extracted from [84]

Due to the complex and variable structure of lignin, and considering that this process involves already depolymerized lignin, the reaction was modeled using one of lignin's core monomers, 2-Methoxy-4-propylphenol (also known as 4-Propylguaiacol). This approach is commonly adopted in scientific studies for similar purposes.

In scaling up the process, it's crucial to determine whether additional energy input is required to maintain the reaction, which depends on the heat of reaction for DKL oxypropylation, a value not readily available in the literature.

For simplicity, the main reaction is considered without accounting for secondary reactions. Additionally, it's worth noting that in practice, multiple propylene oxide molecules may react with a single lignin unit, resulting in a product mixture with different substitution levels.

Thus, the oxypropylation reaction is represented as follows:



The oxypropylation process involves attaching a propylene glycol group (derived from propylene oxide) to the depolymerized lignin structure. The chemical structure of the oxypropylated depolymerized lignin (OxyDKL) would therefore resemble the following:

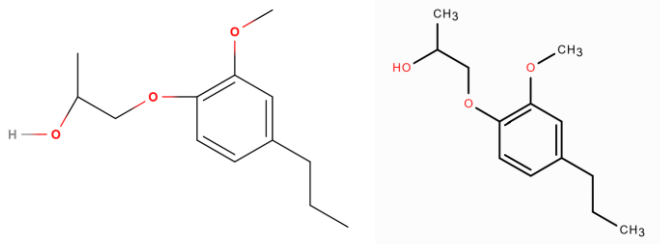


Figure 38: oxypropylated depolymerized lignin

The heats of formation for DKL and OxyDKL were determined using the Joback group-contribution method, while the heat of formation for propylene oxide was sourced from NIST. These values are listed in [85].

$$\Delta H_{f,DKL}^0 = -390.42 \frac{kJ}{mol}$$

$$\Delta H_{f,PO}^0 = -122.60 \frac{kJ}{mol}$$

$$\Delta H_{f,OxyDKL}^0 = -538.63 \frac{kJ}{mol}$$

Since the specific OxyDKL compound shown in Figure 2 could not be found in any chemical database, a structurally similar compound with comparable functional groups, 3-(3,4-Dimethoxyphenyl)-1-propanol, was chosen as a reference, despite its slightly lower molecular weight. This compound's heat of formation was used as an approximation.

For specific heat capacities, the values are reported below:

$$c_{p,DKL} = 0.23 \frac{kJ}{mol \cdot ^\circ C}$$

$$c_{p,OxyDKL} = 0.27 \frac{kJ}{mol \cdot ^\circ C}$$

$$c_{p,PO} = 0.08 \frac{kJ}{mol \cdot ^\circ C}$$

The heat of reaction was first calculated at 25°C, indicating that the reaction is slightly exothermic. The effect of pressure is considered negligible compared to that of temperature.

$$\Delta H_r(25^\circ C) = \sum (\Delta H_{f,products}^0) - \sum (\Delta H_{f,reactants}^0)$$

$$\Delta H_r(25^\circ\text{C}) = -538.63 \frac{\text{kJ}}{\text{mol}} - \left(-390.42 \frac{\text{kJ}}{\text{mol}} - 122.60 \frac{\text{kJ}}{\text{mol}} \right) = -25.61 \frac{\text{kJ}}{\text{mol}}$$

Finally, by assuming constant heat capacities over temperature, the heat of reaction was estimated at 150°C.

$$\Delta H_r(150^\circ\text{C}) = \Delta H_r(25^\circ\text{C}) + \sum(\Delta H_{temp,products}) - \sum(\Delta H_{temp,reactants})$$

With:

$$\begin{aligned} \sum(\Delta H_{temp,products}) - \sum(\Delta H_{temp,reactants}) &= (c_{p,OxyDKL} - c_{p,DKL} - c_{p,PO}) \cdot (150 - 25) \\ &= -5 \frac{\text{kJ}}{\text{mol}} \end{aligned}$$

Finally:

$$\Delta H_r(150^\circ\text{C}) = -25.61 \frac{\text{kJ}}{\text{mol}} - 5 \frac{\text{kJ}}{\text{mol}} = -30.61 \frac{\text{kJ}}{\text{mol}}$$

At 150°C, the oxypropylation reaction is exothermic, releasing approximately 30.61 kJ per mole of product. Given that the scaled-up process yields 433.18 g of OxyDKL—about 0.12 moles—the reaction releases roughly 3.67 kJ of heat. This analysis confirms that, unlike the endothermic hydrolytic depolymerization, no additional heat from the reactor is required to drive the oxypropylation reaction. Furthermore, since the heat released is minimal relative to other energy inputs in the process, it is reasonable to approximate the reaction and reactor as adiabatic.

This limited heat release implies only a modest temperature rise within the system, suggesting that any energy released is either absorbed by the system or dissipated slowly enough to maintain near-adiabatic conditions. In industrial-scale settings, reactors are typically equipped with heat sinks or controls to manage minor exothermicity, keeping temperatures stable around 150°C. Thus, treating the system as adiabatic is a realistic simplification, as the reactor's thermal inertia would prevent significant temperature fluctuations from this limited reaction heat.

It's important to note that numerous simplifications were made due to limited data on these specific lignin compounds in the literature. While the results may lack precise accuracy, the data and reference compounds were selected to approximate the actual reaction as closely as possible, providing a rough estimate of the reactor's energy requirements to ensure a comprehensive view of the process's energy needs.

The biggest energy requirement is therefore found to be the heating up of reactants. Again, a sensitivity analysis is performed, considering HTF, steam and electricity from the EU mix.

PUR foams
- Fossil-based

Table 13: Life cycle inventory of 1 kg of fossil based rigid polyurethane foam

Input	Unit	Quantity	ecoinvent process name
Polyol	kg	0.386	Polyether polyols, short chain
MDI	kg	0.616	Methylene diphenyl diisocyanate (MDI)
Pentane	kg	0.054	Pentane {RER} pentane production
Electricity	MJ	1.5	Electricity, medium voltage {EU}
Product			
Rigid polyurethane foam	kg	1	
Outputs			
<i>Air emissions</i>			
Pentane	kg	0.003	Pentane
<i>Outputs to technosphere</i>			
Waste polyurethane foam	kg	0.02	Waste polyurethane foam {CH}

The entries of this life cycle inventory come directly from the data found in the PlasticsEurope public database [75].

- Direct implementation of Kraft lignin

Table 14: Life cycle inventory of 1 kg of KL PUR

Input	Unit	Quantity	ecoinvent process name
Polyol	kg	0.270	Polyether polyols, short chain
KL	kg	0.116	Untransformed dry Kraft lignin
MDI	kg	0.616	Methylene diphenyl diisocyanate (MDI)
Pentane	kg	0.054	Pentane {GLO}
Electricity	MJ	2.3	Electricity, medium voltage {EU}
Product			
Rigid polyurethane foam	kg	1	
Outputs			
<i>Air emissions</i>			
Pentane	kg	0.003	Pentane
<i>Outputs to technosphere</i>			
Waste polyurethane foam	kg	0.02	Waste polyurethane foam {CH}

This life cycle inventory is partially based on the work performed by Henry et al. [77], who synthesized nineteen rigid polyurethane foams at lab-scale, employing unmodified lignins from different sources to substitute 30wt.% of fossil-based polyols. As they state in their publication, 30wt.% polyol substitution was chosen based on previous works in the literature that reported a decline in foam properties with higher than 30wt.% loading of unmodified lignin. A notable thing is that, unlike the commercial polyol, all lignins they used were in a solid state, and no solvent was used. This caused a decreased reactivity of the mixture, as well as an increase in viscosity which also affects foam reactivity by reducing the mobility of raw materials in the solution. Normally, polyols and MDI are in liquid state for rigid polyurethane foam synthesis. So, a modification of the process studied by Henry et al. is applied, in order for it to be coherent with the inventory provided by PlasticsEurope. This means that acetone would be used to dissolve Kraft lignin (0.918 kg are needed to dissolve 0.116 kg of powdered Kraft lignin). To maintain a correct mass balance, this amount of acetone is not shown

in the inventory, but it's supposed to be recovered completely during the process, which allows for a complete makeup. The acetone contribution is therefore considered as an increase in energy need for this process, compared to the fossil-based one, with the difference in energy being the one needed to recover acetone.

- **Depolymerized Kraft lignin implementation**

Table 15: Life cycle inventory of 1 kg of DKL PUR

Input	Unit	Quantity	ecoinvent process name
Polyol	kg	0.193	Polyether polyols, short chain
DKL	kg	0.193	Depolymerized Kraft lignin
MDI	kg	0.616	Methylene diphenyl diisocyanate (MDI)
Pentane	kg	0.054	Pentane {GLO}
Electricity	MJ	1.8	Electricity, medium voltage {EU}
Product			
Rigid polyurethane foam	kg	1	
Outputs			
<i>Air emissions</i>			
Pentane	kg	0.003	Pentane
<i>Outputs to technosphere</i>			
Waste polyurethane foam	kg	0.02	Waste polyurethane foam {CH}

It has been shown that depolymerized kraft lignin can be used in the formulation of rigid polyurethane foam as a substitute for fossil-based polyols up to 50% by weight, while maintaining acceptable physical, mechanical, and thermal properties for insulation applications [47], [71]. As it was seen in the scale-up section, depolymerized Kraft lignin is obtained in powder form and is then dissolved in acetone for its incorporation in the polyurethane foam reacting mixture. Again, acetone is taken account of by considering an increase in energy consumption of the whole process, which is less than before because, although fossil-based polyols substitution is higher, the solubility of depolymerized Kraft lignin is also higher (i.e. less solvent is required).

- **Oxypropylated depolymerized Kraft lignin implementation**

Table 16: Life cycle inventory of 1 kg of OxyDKL PUR

Input	Unit	Quantity	ecoinvent process name
OxyDKL	kg	0.386	Oxypropylated depolymerized Kraft lignin
MDI	kg	0.616	Methylene diphenyl diisocyanate
Pentane	kg	0.054	Pentane {GLO}
Electricity	MJ	1.5	Electricity, medium voltage {EU}
Product			
Rigid polyurethane foam	Kg	1	
Outputs			
<i>Air emissions</i>			
Pentane	kg	0.003	Pentane
<i>Outputs to technosphere</i>			
Waste polyurethane foam	kg	0.02	Waste polyurethane foam {CH}

Mahmood et al. state in [47] that it is possible to obtain rigid polyurethane foam with a 100wt.% substitution of fossil-based polyols with OxyDKL. However, OxyDKL is not fully bio-based, as hydrolytically depolymerized Kraft lignin reacts with propylene oxide, a fossil raw material.

5.4. Life Cycle Impact Assessment (LCIA)

Life cycle impact assessment is a quantitative and/or qualitative process intended to characterize and evaluate the magnitude and significance of potential environmental impacts of a product system, based on the environmental interventions identified in the inventory table [62].

This stage of the comparative LCA evaluates the impacts of the modelled processes across the four scenarios considered, with comparisons to literature data where available. The climate change impact category is the primary focus due to limited data availability for other categories, particularly regarding lignin extraction. As a consequence, the final results using the two allocation methods are compared solely within this category.

Where literature data permits, additional checks on other impact categories are conducted. However, climate change remains the most frequently studied category in existing research. A brief explanation is provided on how SimaPro® and the *ReCiPe* impact assessment method calculate climate change impacts, according to the *ReCiPe 2016* characterization report [61].

For this impact category, the damage modeling is subdivided into several steps (Figure 43). An emission of a greenhouse gas (kg) leads to an increased atmospheric concentration of greenhouse gases (ppb), which, in turn, increases the radiative forcing capacity (W/m^2), resulting in a rise in the global mean temperature ($^{\circ}C$). Increased temperature ultimately causes damage to human health and ecosystems. The *ReCiPe* method estimates the damage to human health, terrestrial ecosystems, and freshwater ecosystems.

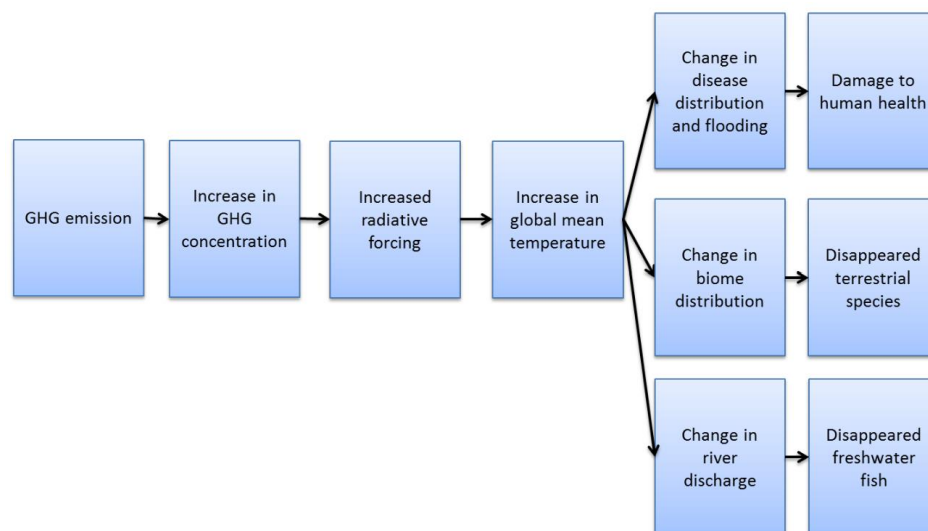


Figure 39: Causal chain from greenhouse gas emissions to human health damage and relative loss of species in terrestrial and freshwater ecosystems [61]

The midpoint characterization factor for climate change is the widely used Global Warming Potential (GWP). GWP expresses the amount of additional radiative forcing integrated over time (20, 100, or 1,000 years in the *ReCiPe* method, depending on the perspective) caused by the emission of 1 kg of a greenhouse gas, relative to the additional radiative forcing over the same time horizon caused by the

release of 1 kg of CO₂. The amount of radiative forcing integrated over time caused by the emission of 1 kg of a GHG is called the Absolute Global Warming Potential (AGWP) and is expressed in the unit W m⁻² yr kg⁻¹. The midpoint characterization factor for any GHG (x) and any time horizon (TH) can then be calculated as follows:

$$GWP_{x,TH} = \frac{AGWP_{x,TH}}{AGWP_{CO_2,TH}}$$

This calculation yields a time-horizon-specific GWP, expressed in kg CO₂ eq/kg GHG. In the hierarchist perspective, the reference time horizon is 100 years.

Polyurethane foams indeed contribute to greenhouse gas emissions during their production and lifecycle. Comparing the global warming potential of fossil-based foam with lignin-based alternatives can highlight the environmental benefits of one or the other in reducing carbon footprints.

5.4.1. Kraft lignin extraction process

First off, a check on the Kraft lignin extraction process impact assessment is essential. For the *marginal approach* allocation method, this step was modelled based on the work performed by Bernier et al., so the results here obtained should look similar, if not identical, to their work. For the *main product bears all burden* method, a value of 0 kg CO₂ eq was considered. Bernier et al.'s work, however, is quite outdated (the article was published in 2012). It is based on the SimaPro[®] 7.3.2 software, using the *Ecoinvent v2.2* database. This work, on the other hand, made use of the latest SimaPro[®] version, 9.6.0.1, as well as the latest *Ecoinvent v3.1*. The updated database can imply some minor changes on the results obtained. What's more, in the LCIA step they used the *IMPACT 2002+ v2.10* method, which is obsolete and not present in SimaPro[®] anymore. This work is based on the *ReCiPe 2016 MidPoint (H) V1.08*, that shares only two impact categories with *IMPACT 2002+ v2.10* with the same unit of measurement. Said categories are "Ozone layer depletion" and "Global warming". Therefore, only those two categories can serve as comparison of the results.

Table 17: Comparison of the results obtained for 1 kg untransformed dry Kraft lignin powder

	Present work	Bernier et al.
Global warming [kg CO ₂ eq]	0.541	0.570
Stratospheric ozone depletion [kg CFC11 eq]	3.74E-7	3.6E-7

With the *consequential* system model, very similar results have been obtained in the comparable impact categories. A possible reason for the slight variation is the difference in life cycle inventory entries, mainly due to the outdated database version used by Bernier et al. Their electricity entry was "Electricity, medium voltage, production UCTE, at grid/UCTE", while SimaPro now reveals that UCTE is an outdated geography identity. Furthermore, the entry for natural gas differs between the two analyses. Credit of the avoided black liquor combustion in the recovery boiler has been modelled in the present work. Bernier et al. have modelled it as well, but have not reported the results, meaning that the assumptions made here might be another reason for the slight dissimilarity.

Apart from these slight dissimilarities, the results are similar, implying a correct modelling of the Kraft lignin extraction process.

5.4.2. Hydrolytic depolymerization of kraft lignin catalyzed by NaOH

As for DKL, the production of 0.193 kg was modelled, since it's the amount that can be included in rigid polyurethane foams formulations. No literature data was found for this specific process. As it was mentioned, a sensitivity analysis regarding the biggest energy requirement of the process is conducted in order to find the least impactful option, especially in terms of climate change. It's the one that has the lowest impact that is then implemented in rigid polyurethane foam formulation. The results obtained are shown in the table below:

Table 18: Comparison of the results obtained for 0.193 kg DKL

<i>Marginal approach</i>	DKL HTF	DKL Electricity from wind	DKL Electricity from hydropower	DKL Electricity EU mix
Global warming [kg CO ₂ eq]	0.205	0.197	0.198	0.228

The differences between the studied options are minimal. However, as expected, using wind-generated electricity for heating the reactants from 220°C to 250°C is the most efficient solution, followed closely by hydropower-generated electricity.

To better illustrate the results, the Figure below presents a normalization of the global energy requirements of the process. This normalization is independent of the allocation method chosen for Kraft lignin extraction. Energy provision using a heat transfer fluid is selected as the reference method, and the other methods are compared based on their performance relative to this reference. The diagram reads like: using wind-generated electricity to cover for the largest energy demand of the process, compared to using natural gas (and a HTF), results in 25% less CO₂ eq emissions.

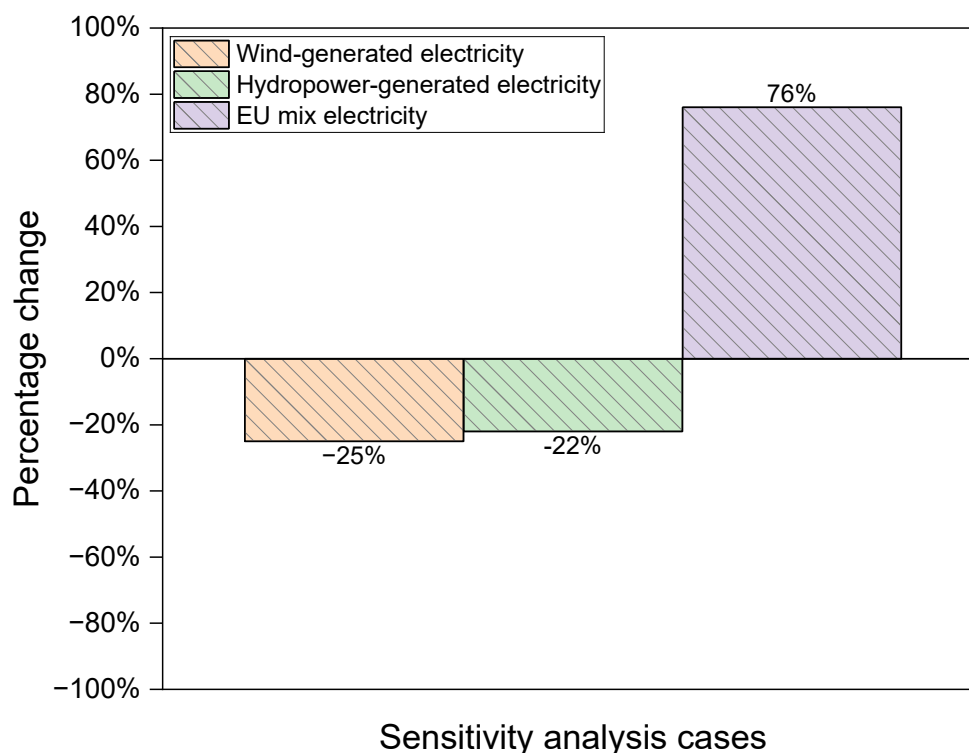


Figure 40: hydrolytic depolymerization sensitivity analysis results, as CO₂ eq percentage change

Interestingly, when natural gas is burned to reheat the heat transfer fluid, this option results in lower greenhouse gas emissions compared to the EU electricity mix, which accounts for an increase of 76%. Even though the EU mix includes renewables, fossil fuels (mainly coal and natural gas) still account for a significant share. Coal and oil, which is also used even if with a lower share, are much more carbon-intensive and push the average GHG impact of the grid electricity higher than what might result from directly burning natural gas for heat. Another key point is that natural gas, when burned on-site for heating, avoids the losses associated with grid electricity, such as transmission inefficiencies and energy losses during conversion at power plants. This direct use of energy increases efficiency. This is also confirmed by a second analysis performed, where electricity is supposed to be used at high voltage, avoiding the voltage transformation, which lead to an increase of GHG emissions of 37%. Thus, also in this case the use of the EU electricity mix results in the highest emissions.

High-voltage electricity is typically used in large-scale chemical plants, while medium-voltage electricity is more common in medium-scale facilities. Given that the amount of processed lignin will always be significantly lower than that of fossil-based polyols, due to the foam's properties when lignin is included, a medium-scale plant for lignin chemical modifications is a more realistic and appropriate choice.

For this reason, it was decided to stick with the medium voltage option, in particular with the energy requirement covered by electricity from wind, which turned out to be the less impactful in terms of climate change.

5.4.3. Oxypropylation of depolymerized Kraft lignin

Although 0.386 kg of OxyDKL is used in the production of 1 kg of rigid polyurethane foam, life cycle inventory inputs were based on 0.43 kg, as this approach aligned better with the available literature data. When calculating the impact assessments, SimaPro[®] automatically adjusts and scales down all inputs accordingly.

Since the heating of reactants from 25°C to 120°C is entirely covered through heat integration provided by the hot products, and acetone recovery requires no additional energy input, the most significant energy demand comes from heating the reactants from 120°C to 150°C, which requires approximately 46 kJ.

Once again, a sensitivity analysis is conducted on this step, whose results are reported in the table below in terms of CO₂ eq emissions.

Table 19: Comparison of the results obtained for 0.193 kg DKL

<i>Marginal approach</i>	OxyDKL HTF	OxyDKL Steam	DKL Electricity EU mix
Global warming [kg CO ₂ eq]	1.06	1.06	1.07

These results are not comparable with the ones obtained for the production of 0.193 kg of DKL, since the amount of OxyDKL is double the one of DKL. This only serves to visualize which of the three energy options is the less impactful in terms of GHG emissions. A graphical representation is shown in Figure, once again normalized on the energy requirements of the process to better visualize the differences. The use of natural gas to regenerate the HTF is still considered the reference method.

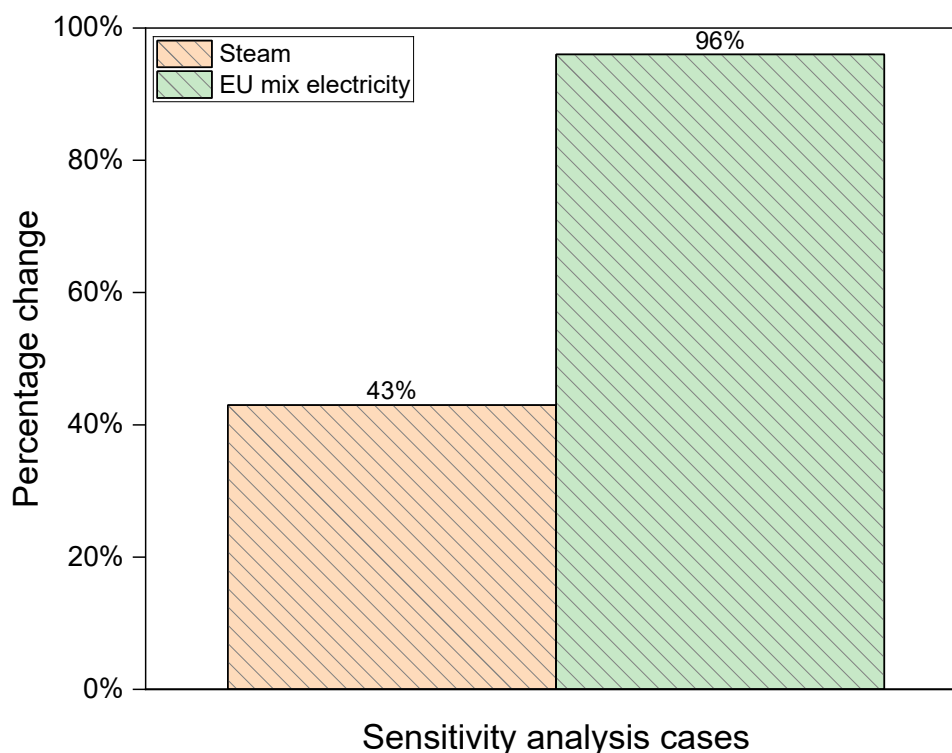


Figure 41: oxypropylation sensitivity analysis results, as CO₂ eq percentage change

The data indicate no significant difference between the three options. However, when normalized for energy inputs, both steam and electricity from the EU mix result in higher CO₂ eq emissions, at 43% and 96% higher than the reference, respectively. Despite this, steam is retained as the energy carrier for this process and in subsequent analyses, as it is the most common option for temperatures in the range of 120°C–150°C in the chemical industry. Furthermore, the selected inventory data assumes steam production from water, which is more representative of the process start-up phase. Once the plant reaches steady-state operation, steam will no longer need to be generated from water but rather regenerated from depleted steam or condensate, likely resulting in lower emissions than those shown in the figure, and being very close if not identical to the ones related to a HTF.

5.4.4. Comparative impact assessment of the four rigid polyurethane foam scenarios

The final four scenarios considered are summarized here. The only variable among the cases is the source of polyols, as MDI is consistently assumed to be derived from fossil sources, and the allocation method of Kraft lignin's extraction.

1. Rigid polyurethane foam synthesis with 100wt.% fossil-based polyols (PUR);
2. Rigid polyurethane foam synthesis with 30wt.% replacement of fossil-based polyols with untransformed Kraft lignin (KL PUR);

3. Rigid polyurethane foam synthesis with 50wt.% replacement of fossil-based polyols with hydrolytically depolymerized Kraft lignin (DKL PUR), where the biggest energy demand of lignin's chemical modification is covered by wind-generated electricity;
4. Rigid polyurethane foam synthesis with 100wt.% replacement of fossil-based polyols with oxypropylated hydrolytically depolymerized Kraft lignin (OxyDKL PUR), where the biggest energy demand of lignin's oxypropylation is covered by steam;

Global warming is no longer be the sole impact category assessed; the comparison will be expanded to include additional categories for a more comprehensive analysis. However, many reports and reviews focus mainly on global warming and climate change, so this will still be the easiest way to compare the results obtained with literature data. Results are summarized in the table below. For the *main product bears all burden* allocation approach, only climate change impact has been considered due to a lack of additional data.

Table 20: Comparison of the results obtained for 1 kg of rigid polyurethane foam in four scenarios

<i>Marginal approach</i>	PUR	KL PUR	DKL PUR	OxyDKL PUR
Climate change [kg CO ₂ eq]	4.56	4.36	4.15	4.31
Stratospheric ozone depletion [kg CFC-11 eq]	4.97E-06	4.93E-06	4.76E-06	4.22E-06
Terrestrial acidification [kg SO ₂ eq]	9.40E-03	9.08E-03	9.60E-03	9.49E-03
Freshwater eutrophication [kg P eq]	6.78E-04	5.21E-04	4.20E-04	5.38E-04
Marine eutrophication [kg N eq]	4.16E-04	3.44E-04	2.97E-04	1.73E-04
<i>Main product bears all burden</i>	PUR	KL PUR	DKL PUR	OxyDKL PUR
Climate change [kg CO ₂ eq]	4.56	4.30	4.01	4.13

The analysed impact categories are the ones that are more commonly reported in literature with the *ReCiPe* impact method. Overall, the obtained values are according to literature data, even if comparisons are difficult to make given the wide range of different approaches (cradle to gate, cradle to grave etc.) and system boundaries of literature work.

The next section is dedicated to the interpretation of the results.

5.5. Interpretation

A useful tool provided by SimaPro[®] for fully understanding the impact of each input is the Sankey diagram. A Sankey diagram is a specific type of flow diagram where the width of the arrows is proportional to the flow rate of the quantity represented. These diagrams are particularly useful for visualizing energy and material flows in various systems. In the context of an LCA study, a Sankey diagram can be extremely helpful for many reasons, as proportional widths of the arrows make it easy to see immediately which processes or materials have the most significant impact. Sankey diagrams can highlight hot spots in the life cycle where the most significant environmental impacts occur. The Sankey diagram relative to the climate change impact of the production of 1 kg of fossil-based rigid polyurethane foam is shown in the Figure below.

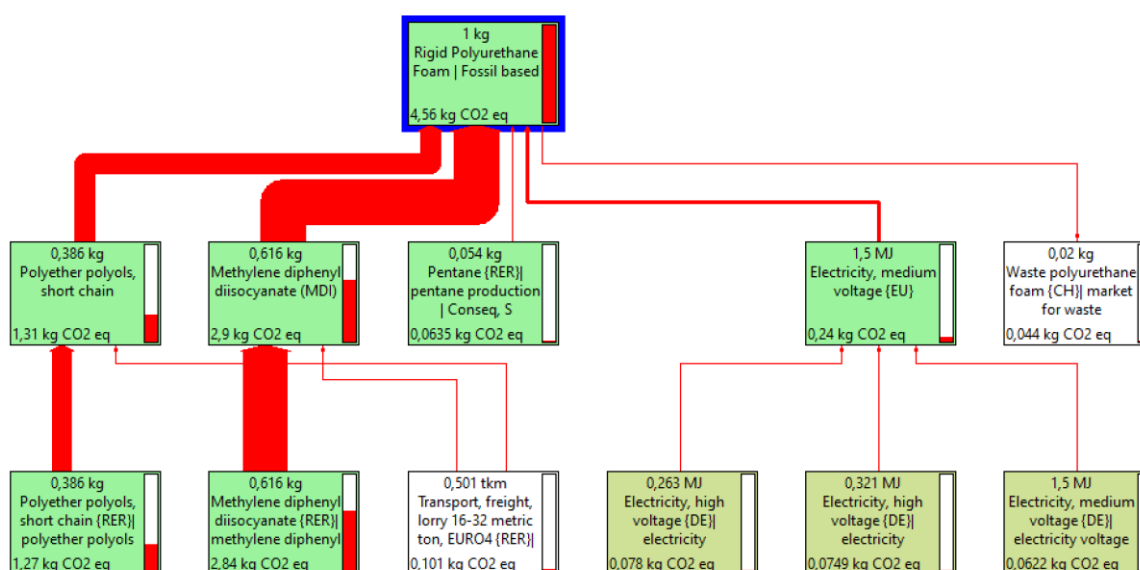


Figure 42: Sankey diagram of climate change impact relative to 1 kg fossil PUR

From the diagram, it is evident that most of the climate change impact arises from MDI, which is also used in a larger quantity in the production of 1 kg of rigid polyurethane foam. Research is increasingly focused on replacing this raw material, with significant efforts directed toward developing non-isocyanate rigid polyurethane foams. However, most current studies primarily concentrate on sourcing bio-based polyols, while effective alternatives to isocyanates remain in developmental stages.

In terms of greenhouse gas emissions, 63.6% of the climate change impact from producing 1 kg of fossil-based PUR is attributable to MDI, 28.7% to polyols, and the remaining 7.7% to raw material transportation and energy requirements. Given this breakdown, the present work focuses on the 28.7% impact from polyols. To the best of the author's knowledge, most life cycle assessments of polyurethane foams are conducted on lab-scale processes, with limited exploration of industrial-scale settings. This study aims to bridge that gap by providing an LCA that considers a larger scale for bio-based polyol synthesis.

Bio-based polyols are typically derived from vegetable oils, with limited research exploring lignin as a source. As previously discussed, the LCA results for Kraft lignin vary significantly depending on the allocation method used, with no consensus on the best approach due to differences in the intended application of lignin. The two allocation methods selected for this work, *marginal approach* and *main product bears all burden*, are well-documented in the literature and represent opposing extremes: one attributes all impacts to lignin, while the other assigns all impacts to the main products of pulp mills.

The results presented earlier reveal only a small difference between the allocation methods. This is because MDI dominates the overall impact, and the contributions from lignin extraction and chemical modification are relatively minor. Additionally, as the substitution ratio of fossil-based polyols with lignin-based polyols increases, the energy required for solvent recovery also rises, creating a counterbalancing effect.

The focus now shifts exclusively to polyols and their synthesis, based on the quantity used in 1 kg of rigid PUR. With this focus, the functional unit effectively transitions to the polyols alone: 0.386 kg per 1 kg of PUR.

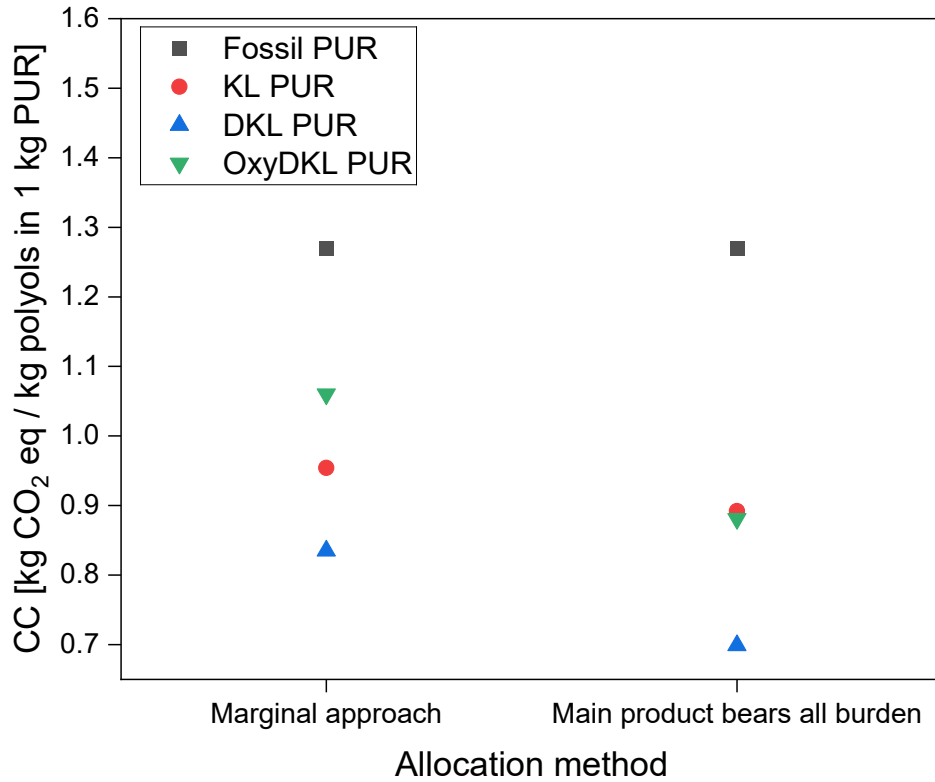


Figure 43: climate change per kg of polyols in 1 kg of PUR, with the studied allocation methods

This Figure illustrates the climate change impact of all polyols, considering the two different allocation approaches applied to Kraft lignin’s extraction. As expected, there is no difference for fossil-based PUR polyols, as they do not contain any bio-based polyols.

The results align with expectations, showing that polyol formulations using the *main product bears all burden* approach are less impactful. However, the difference is relatively small, primarily because lignin-based polyols constitute only a portion of the total polyols used.

Results are also summarized in the following table:

Table 21: Climate change impact per amount of polyols in 1 kg of PUR

Climate change [kg CO ₂ eq]	Allocation method	
	<i>Marginal approach</i>	<i>Main product bears all burden</i>
Fossil-based polyols	1.27	1.27
Lignin-based polyols (30wt.% KL)	0.954	0.892
Lignin-based polyols (50wt.% DKL)	0.835	0.699
Lignin-based polyols (100wt.% OxyDKL)	1.06	0.881

If the impact of fossil-based polyols is taken as reference, it is possible to calculate the percentage of impact reduction of all the different scenarios studied, and these are reported in the Figure below.

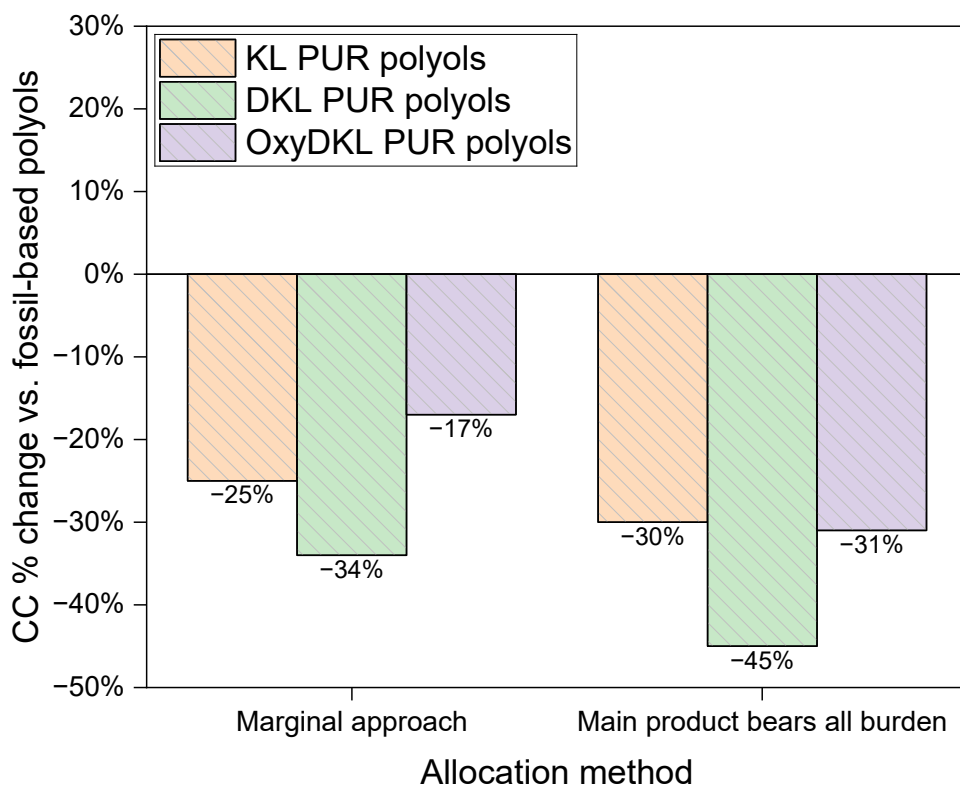


Figure 44: climate change % of bio-based polyols vs. fossil-based polyols

In all cases, lignin-based polyols with 50 wt.% DKL achieve the best balance between substitution ratio and energy consumption for the chemical modification process at the proposed scale-up level.

Interestingly, when the *main product bears all burden* allocation approach is applied, OxyDKL-based polyols exhibit a lower environmental impact compared to KL PUR polyols. This is likely due to the substitution ratio relative to fossil-based polyols: 30 wt.% for OxyDKL versus 100 wt.% for KL polyols. While it is true that in oxypropylation, depolymerized Kraft lignin reacts with propylene oxide, a fossil-based raw material essential for fossil polyols synthesis, the allocation method and proposed scale-up make OxyDKL polyols a more sustainable option than KL polyols under this approach.

Once again, the choice of allocation method proves to be a decisive factor. The observed differences between KL polyols and OxyDKL polyols are not evident when the marginal approach allocation method is used, under which KL polyols appear less impactful.

Currently, even though the marginal approach is particularly suited for consequential analyses like the one in this study, the *main product bears all burden* method seems more accurate for reflecting the typical present-day situation, where pulp is the main product and lignin is treated as a byproduct.

CHAPTER 6: CONCLUSIONS

Out of the four scenarios studied, the results obtained showed that, in terms of environmental impact and specifically climate change, substituting 50wt.% of fossil-based polyols with polyols obtained from the hydrolytic depolymerization of Kraft lignin results in an improvement compared to current rigid polyurethane foam formulations. What's more, mechanical and thermal properties of such foam are suitable for thermal insulation applications, resulting in a viable commercial foam. A scale-up of the lignin's modification process was proposed, as initial step to implement this technology at larger scale. The sensitivity analyses showed ways to minimize the impact also in terms of energy carriers.

It's difficult to find in literature some comparable life cycle assessments, due to the very different ways in which LCA can be approached. Nevertheless, a review of different LCAs of rigid polyurethane foam was published by Silva et al. [87]. Although they all differ in terms of approach and system boundaries, the ones that resemble the most the present work were analysed. The results obtained are consistent with literature, as shown in the Figure below, although hydrolytic depolymerization and oxypropylation are not considered in any of the literature studies.

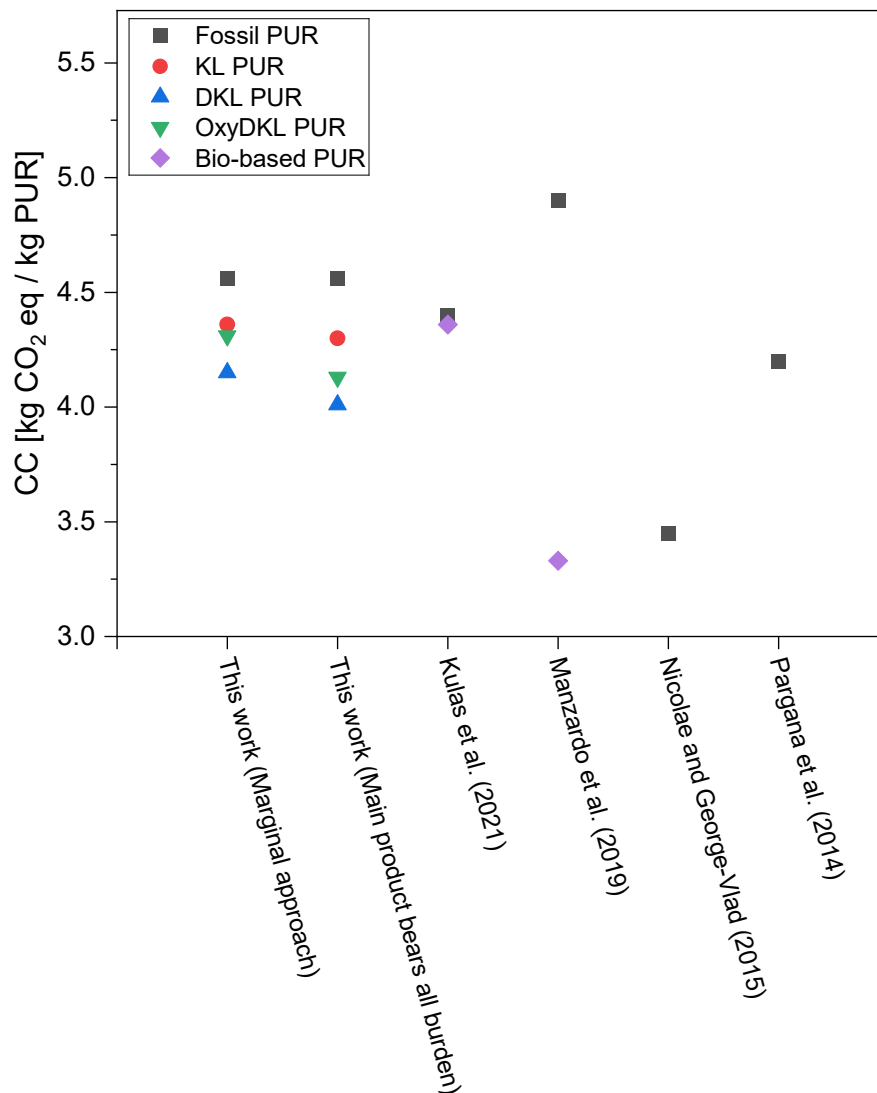


Figure 45: Results of the present work, compared with literature data

The key factor lies in the allocation method chosen for Kraft lignin's extraction process, as the scope of the LCA can significantly influence this decision. In the present work, a consequential approach was adopted, reflecting a forward-looking perspective on the future of polyurethane foam production. Modeling future systems is often critical in applications like consequential LCAs, where the impacts of potential future decisions are assessed.

One straightforward way to model the future is to assume it mirrors the present and base the system design on current operations [88]. In some cases, this assumption is valid, such as with the *main product bears all burden* approach, where all impacts are attributed to pulp, the primary product of pulp mills today. However, for other scenarios, it may be more appropriate to consider alternative future contexts or technological shifts.

Currently, pulp mills are driven primarily by pulp production. However, in future contexts or with advancements in technology, lignin may emerge as the key driver, thereby becoming the main product that bears the entire burden. This suggests that while the *main product bears all burden* approach is a reasonable approximation of current realities, and likely for the next decade, the *marginal approach* could become the more appropriate choice as we transition to a lignin-centered system.

Bibliography

- [1] Bardan, R. (2024, January 12). "NASA Analysis Confirms 2023 as Warmest Year on Record". National Aeronautics and Space Administration. Retrieved from [\[URL\]](#).
- [2] National Centers for Environmental Information, "Annual 2023 Global Climate Report". Retrieved from [\[URL\]](#).
- [3] European Environment Agency Glossary (2000). Retrieved from [\[URL\]](#).
- [4] European Parliament (23, March 2023). "Climate change: the greenhouse gases causing global warming". Retrieved from [\[URL\]](#).
- [5] British Geological Survey. "The greenhouse effect". Retrieved from [\[URL\]](#).
- [6] EDGAR - Emissions Database for Global Atmospheric Research. "GHG emissions of all world countries", 2023 report. Retrieved from [\[URL\]](#)
- [7] Eurostat. "EU economy emissions in 2022: down 22% since 2008". Retrieved from [\[URL\]](#).
- [8] The European Green Deal, first presented on 2019, December 12. Retrieved from [\[URL\]](#).
- [9] Close, P. D. (1951). *Building Insulation: Principles and Application of Heat and Sound Insulation for Buildings* (4th ed.). American Technical Society.
- [10] Bynum, R. T., Jr. (2001). *Insulation Handbook*. McGraw-Hill.
- [11] Repsol. "An efficient measure for the home". Retrieved from [\[URL\]](#).
- [12] Tomasz Kisilewicz, Małgorzata Fedorczyk-Cisak, Tamas Barkanyi. Energy and Buildings, Volume 205, 2019. "Active thermal insulation as an element limiting heat loss through external walls". Retrieved from [\[URL\]](#).
- [13] Tec-Science. "Thermal conduction in solids and ideal gases". Retrieved from [\[URL\]](#).
- [14] Ingersoll, L. R., Zobel, O. J., & Ingersoll, A. C. (1948). *Heat conduction with engineering and geological applications (1st ed.)*. New York, NY: McGraw-Hill Book Company, Inc.
- [15] Kern, D. Q. (1965). *Process Heat Transfer*. International student edition. McGraw-Hill International Book Company.
- [16] Bozsaky, David. (2012). New thermal insulation material from agricultural waste product. Retrieved from [\[URL\]](#).
- [17] Manohar, Krishpersad & Adeyanju, Anthony A.. (2016). A Comparison of Banana Fiber Thermal Insulation with Conventional Building Thermal Insulation. *British Journal of Applied Science & Technology*. 17. 1-9. 10.9734/BJAST/2016/29070. Retrieved from [\[URL\]](#).
- [18] Camila S. Carriço, Thaís Fraga, Vagner E. Carvalho, and Vânia M. D. Pasa. "Polyurethane Foams for Thermal Insulation Uses Produced from Castor Oil and Crude Glycerol Biopolyols". National library of medicine. Retrieved from [\[URL\]](#).
- [19] Incropera, F. P., & DeWitt, D. P. (2002). *Fundamentals of heat and mass transfer (5th ed.)*. Hoboken, NJ: John Wiley & Sons.
- [20] McQuiston, F. C., Parker, J. D., & Spitler, J. D. (2001). *Heating, ventilating, and air conditioning analysis and design (5th ed.)*. Hoboken, NJ: John Wiley & Sons, Inc.
- [21] Modest, M. F. (2013). *Radiative heat transfer (3rd ed.)*. Elsevier.

- [22] Baudouy, Bertrand. (2015). Heat Transfer and Cooling Techniques at Low Temperature. CAS-CERN Accelerator School: Superconductivity for Accelerators - Proceedings. 10.5170/CERN-2014-005.329. Retrieved from [\[URL\]](#).
- [23] Bird, R. B., Stewart, W. E., & Lightfoot, E. N. (1960). *Transport phenomena*. Hoboken, NJ: John Wiley & Sons, Inc.
- [24] Zirin, Harold. "Solar constant". Encyclopedia Britannica, 24 Aug. 2012. Retrieved from [\[URL\]](#).
- [25] Repsol. "Benefits of energy efficiency". Retrieved from [\[URL\]](#).
- [26] International Energy Agency (IEA). "Energy efficiency". Retrieved from [\[URL\]](#).
- [27] European Commission. "Energy Performance of Buildings Directive". Retrieved from [\[URL\]](#).
- [28] Pitts, G. Y. (1941). *The thermal insulation of structures*. London: Charles Griffin and Company Limited.
- [29] National Mineral Wool Association. (1946). *Insulation and your home (2nd ed.)*. New York, NY: National Mineral Wool Association.
- [30] Roberts, Tobias. "Rigid Board Insulation: The Ultimate Guide", 16 Apr. 2020. Retrieved from [\[URL\]](#).
- [31] Bozsaky, David. (2010). The historical development of thermal insulation materials. *Periodica Polytechnica Architecture*. 41. 49. 10.3311/pp.ar.2010-2.02. Retrieved from [\[URL\]](#).
- [32] Polyurethanes.org, "What is polyurethane?". Retrieved from [\[URL\]](#).
- [33] Gozzelino, Giuseppe. *Industrial Chemistry for Oils and Polymers*, Industrial Polymers pag.8. Politecnico di Torino.
- [34] Ratna, D. (2022). *Recent advances and applications of thermoset resins (2nd ed.)*. Amsterdam, Netherlands: Elsevier.
- [35] Oertel, G. (Ed.). (1994). *Polyurethane handbook: Chemistry, raw materials, processing, application, properties* (2nd ed.). Munich, Germany; New York, NY: Hanser; Hanser/Gardner.
- [36] BING. Federation of European Rigid Polyurethane Foam Associations, Report N°1, October 2006. "Thermal insulation materials made of rigid polyurethane foam (PUR/PIR) | Properties – Manufacture". Retrieved from [\[URL\]](#).
- [37] Australian Modern Building Alliance, "Physical properties of polyurethane insulation". Retrieved from [\[URL\]](#).
- [38] Klempner, D., & Frisch, K. C. (Eds.). (1991). *Handbook of polymeric foam and technology*. Munich, Vienna, New York, Barcelona: Hanser Publishers.
- [39] Harris, N.R., Montzka, S.A., & Newman, P.A. (2019). Report on the International Symposium on the Unexpected Increase in Emissions of Ozone-Depleting CFC-11.
- [40] Código Técnico de la Edificación (CTE). Retrieved from [\[URL\]](#).
- [41] Sylwia Dworakowska, Dariusz Bogdał, Federica Zaccheria, Nicoletta Ravasio, The role of catalysis in the synthesis of polyurethane foams based on renewable raw materials, *Catalysis Today*, Volume 223, 2014, Pages 148-156, ISSN 0920-5861, <https://doi.org/10.1016/j.cattod.2013.11.054>. Retrieved from [\[URL\]](#).

- [42] World Commission on Environment and Development. (1987). "Our common future: Report of the World Commission on Environment and Development". Oxford University Press.
- [43] Liang, C., Gracida-Alvarez, U. R., Gallant, E. T., Gillis, P. A., Marques, Y. A., Abramo, G. P., Hawkins, T. R., & Dunn, J. B. (2021). Material flows of polyurethane in the United States. *Environmental Science & Technology*, 55(20), 14215-14224. <https://doi.org/10.1021/acs.est.1c03654>.
- [44] Cornille, A., Auvergne, R., Figovsky, O., Boutevin, B., & Caillol, S. (2017). A perspective approach to sustainable routes for non-isocyanate polyurethanes. *European Polymer Journal*, 87, 535-552. <https://doi.org/10.1016/j.eurpolymj.2016.11.027>.
- [45] Mort, R., Vorst, K., Curtzwiler, G., & Jiang, S. (2021). Biobased foams for thermal insulation: material selection, processing, modelling, and performance. *RSC Advances*, 11(8), 4375-4394. <https://doi.org/10.1039/D0RA09287H>.
- [46] International Lignin Institute. (2021). What's lignin? ILI LIGNIN. Retrieved from [URL].
- [47] Mahmood, N., Yuan, Z., Schmidt, J., & Xu, C. (2015). Preparation of bio-based rigid polyurethane foam using hydrolytically depolymerized Kraft lignin via direct replacement or oxypropylation. *European Polymer Journal*, 68, 1-9. <https://doi.org/10.1016/j.eurpolymj.2015.04.030>.
- [48] Borges da Silva, E.A., Zabkova, M., Araújo, J.D., Cateto, C.A., Barreiro, M.F., Belgacem, M.N., & Rodrigues, A.E. (2009). An integrated process to produce vanillin and lignin-based polyurethanes from Kraft lignin. *Chemical Engineering Research and Design*, 87(9), 1276-1292. <https://doi.org/10.1016/j.cherd.2009.05.008>.
- [49] DeMichelis, F. (2023). *What is a biorefinery system?* Politecnico di Torino.
- [50] Mahmood, N., Yuan, Z., Schmidt, J., & Xu, C. (2016). Depolymerization of lignins and their applications for the preparation of polyols and rigid polyurethane foams: A review. *Renewable and Sustainable Energy Reviews*, 60, 317-329. <https://doi.org/10.1016/j.rser.2016.01.037>
- [51] Sternberg, J., Sequerth, O., & Pilla, S. (2024). Structure-property relationships in flexible and rigid lignin-derived polyurethane foams: A review. *Materials Today Sustainability*, 25*, 100643. <https://doi.org/10.1016/j.mtsust.2023.100643>
- [52] European Environment Agency. *Life Cycle Assessment (LCA)*. Retrieved from [URL].
- [53] Klöpffer, W. *The Role of SETAC in the Development of LCA*. *Int J Life Cycle Assessment* 11 (Suppl 1), 116–122 (2006). <https://doi.org/10.1065/lca2006.04.019>
- [54] SimaPro. (n.d.). *Agri-footprint database*. Retrieved from [URL].
- [55] SimaPro. (n.d.). *Ecoinvent LCI database*. Retrieved from [URL].
- [56] Ecoinvent support. (14, February 2024). *System models*. Retrieved from [URL].
- [57] SimaPro. (n.d.). *Industry data LCA library*. Retrieved from [URL].
- [58] Database & Support team at PRé Sustainability. (2022). *SimaPro database manual: Methods library*. Retrieved from [URL].
- [59] NREL. (n.d.). *Energy analysis: U.S. Life Cycle Inventory Database*. Retrieved from [URL].
- [60] SimaPro Help Center. (n.d.). *What are unit and system processes?* Retrieved from [URL].

- [61] Huijbregts, M. A. J., Steinmann, Z. J. N., Elshout, P. M. F., Stam, G., Verones, F., Vieira, M. D. M., Hollander, A., Zijp, M., & van Zelm, R. (2016). *ReCiPe 2016: A harmonized life cycle impact assessment method at midpoint and endpoint level: Report I: Characterization (RIVM Report 2016-0104)*. National Institute for Public Health and the Environment.
- [62] Jensen, A. A., Hoffman, L., Møller, B. T., Schmidt, A., Christiansen, K., Elkington, J., & van Dijk, F. (1997). *Environmental Issues Series no. 6: Life Cycle Assessment: A guide to approaches, experiences and information sources*. dk-TEKNIK Energy & Environment; Sophus Berendsen A/S; SustainAbility.
- [63] PlasticsEurope. (n.d.). *Eco-profiles set*. Retrieved from [\[URL\]](#).
- [64] PlasticsEurope. (2021, April). *Eco-profile of toluene diisocyanate (TDI) and methylene diphenyl diisocyanate (MDI)*. Retrieved from [\[URL\]](#).
- [65] PlasticsEurope. (2021, April). *Eco-profile of long and short chain polyether polyols for polyurethane products*. Retrieved from [\[URL\]](#).
- [66] Boustead, I. (2005, March). *Eco-profiles of the European plastics industry: Pentane*. PlasticsEurope. Retrieved from [\[URL\]](#).
- [67] PlasticsEurope. (2022). *Eco-profiles program and methodology (Version 3.1)*. Retrieved from [\[URL\]](#).
- [68] Plastics Europe Public LCI Database. (n.d.). *Short Chain Polyether Polyols (rigid)*. Retrieved from [\[URL\]](#).
- [69] Bernier, E., Lavigne, C., & Robidoux, P. Y. (2013). *Life cycle assessment of kraft lignin for polymer applications*. The International Journal of Life Cycle Assessment, 18(3), 520-528. <https://doi.org/10.1007/s11367-012-0503-y>
- [70] Mahmood, N., Yuan, Z., Schmidt, J., & Xu, C. (2013). *Production of polyols via direct hydrolysis of kraft lignin: Effect of process parameters*. Bioresource Technology, 133, 218-226. <https://doi.org/10.1016/j.biortech.2013.03.029>
- [71] Saffar, T., Bouafif, H., Braghiroli, F.L. et al. *Production of Bio-based Polyol from Oxypropylated Pyrolytic Lignin for Rigid Polyurethane Foam Application*. Waste Biomass Valor 11, 6411–6427 (2020). <https://doi.org/10.1007/s12649-019-00876-7>
- [72] Pinto, J. A., Fernandes, I. P., Pinto, V. D., Gomes, E., Oliveira, C. F., Pinto, P. C. R., Mesquita, L. M. R., Piloto, P. A. G., Rodrigues, A. E., & Barreiro, M. F. (2021). *Valorization of lignin side-streams into polyols and rigid polyurethane foams—a contribution to the pulp and paper industry biorefinery*. Energies, 14(13), 3825. <https://doi.org/10.3390/en14133825>
- [73] Ribeiro da Silva, V., Mosiewicki, M. A., Yoshida, M. I., Coelho da Silva, M., Stefani, P. M., & Marcovich, N. E. (2013). *Polyurethane foams based on modified tung oil and reinforced with rice husk ash I: Synthesis and physical chemical characterization*. Polymer Testing, 32, 438-445. <http://dx.doi.org/10.1016/j.polymertesting.2013.01.002>
- [74] Plastics Europe Public LCI Database. (n.d.). *Methylenediphenyl diisocyanate ((p)MDI)*. Retrieved from [\[URL\]](#).
- [75] Boustead, I. (2005, March). *Eco-profiles of the European plastics industry: Polyurethane rigid foam*. PlasticsEurope. Retrieved from [\[URL\]](#).
- [76] Belgacem, M. N., & Gandini, A. (Eds.). (2008). *Monomers, polymers and composites from renewable resources*. Elsevier.

- [77] Henry, C., Gondaliya, A., Thies, M., & Nejad, M. (2022). *Studying the suitability of nineteen lignins as partial polyol replacement in rigid polyurethane/polyisocyanurate foam*. *Molecules*, 27(8), 2535. <https://doi.org/10.3390/molecules27082535>
- [78] Zhou, N., Thilakarathna, W. P. D. W., He, Q. S., & Rupasinghe, H. P. V. (2022). *A review: Depolymerization of lignin to generate high-value bio-products: Opportunities, challenges, and prospects*. *Frontiers in Energy Research*, 9, Article 758744. <https://doi.org/10.3389/fenrg.2021.758744>
- [79] Xue, B.-L., Huang, P.-L., Sun, Y.-C., Li, X.-P., & Sun, R.-C. (2017). *Hydrolytic depolymerization of corncob lignin in the view of a bio-based rigid polyurethane foam synthesis*. *RSC Advances*, 7(12), 7411-7420. <https://doi.org/10.1039/C6RA26318F>
- [80] Watkins, D., Nuruddin, M., Hosur, M., Tcherbi-Narteh, A., & Jeelani, S. (2014). *Extraction and characterization of lignin from different biomass resources*. *Journal of Materials Research and Technology*, 4(1), 26-32. <https://doi.org/10.1016/j.jmrt.2014.10.009>
- [81] Hupa, M. (2007). *Recovery boiler chemical principles*. TAPPI Kraft Recovery Course 2007.
- [82] Onarheim, K., Santos, S., Kangas, P., & Hankalin, V. (2017). *Performance and costs of CCS in the pulp and paper industry part 1: Performance of amine-based post-combustion CO₂ capture*. *International Journal of Greenhouse Gas Control*, 62, 186-195. <https://doi.org/10.1016/j.ijggc.2017.02.008>
- [83] International Energy Agency. (n.d.). *Europe, sources of electricity generation*. IEA. Retrieved from [\[URL\]](#)
- [84] Laurichesse, S., & Avérous, L. (2014). *Chemical modification of lignins: Towards biobased polymers*. *Progress in Polymer Science*, 39(6), 1266–1290. <https://doi.org/10.1016/j.progpolymsci.2013.11.004>
- [85] Céondo GmbH. (2010–2023). *Cheméo: Predict chemical & physical properties*. Retrieved from [\[URL\]](#).
- [86] U.S. Department of Energy. (2021, August). *How wind can help us breathe easier*. Retrieved from [\[URL\]](#).
- [87] Silva, R., Barros-Timmons, A., & Quinteiro, P. (2023). *Life cycle assessment of fossil- and bio-based polyurethane foams: A review*. *Journal of Cleaner Production*. <https://doi.org/10.1016/j.jclepro.2023.139697>
- [88] Finnveden, G., Hauschild, M. Z., Ekvall, T., Guinée, J., Heijungs, R., Hellweg, S., Koehler, A., Pennington, D., & Suh, S. (2009). *Recent developments in Life Cycle Assessment*. *Journal of Environmental Management*, 91(1), 1–21. <https://doi.org/10.1016/j.jenvman.2009.06.018>
- [89] Hermansson, F., Janssen, M., & Svanström, M. (2020). *Allocation in life cycle assessment of lignin*. *The International Journal of Life Cycle Assessment*, 25(9), 1620–1632. <https://doi.org/10.1007/s11367-020-01770-4>
- [90] Sandin, G., Røyne, F., Berlin, J., Peters, G. M., & Svanström, M. (2015). *Allocation in LCAs of biorefinery products: Implications for results and decision-making*. *Journal of Cleaner Production*, 93, 213–221. <https://doi.org/10.1016/j.jclepro.2015.01.013>

Ringraziamenti

Ringrazio la mia famiglia per il costante supporto, sia morale che economico, che mi ha permesso di raggiungere questo importante traguardo.

Ringrazio gli amici e compagni di corso, soprattutto coloro che mi sono stati vicini nei momenti più difficili, offrendomi il loro sostegno e la loro amicizia.

Un ringraziamento speciale, infine, va a mio fratello, per essere sempre il mio migliore amico.

Grazie di cuore a tutti voi!